ANL-5668
Chemistry-Separation Processes
for Plutonium and Uranium
M-3679 (19th Ed., Suppl. 1)
This document consists of 111 pages.
No. 128 of 242 copies. Series A.

ARGONNE NATIONAL LABORATORY
P. O. Box 299
Lemont, Illinois

CHEMICAL ENGINEERING DIVISION SUMMARY REPORT

October, November, and December, 1956

Stephen Lawroski, Division Director

W. A. Rodger, Associate Division Director
R. C. Vogel, Associate Division Director
V. H. Munnecke, Assistant Division Director

March, 1957

Preceding Quarterly Reports:

ANL-5560 January, February, March, 1956
ANL-5602 April, May, June, 1956
ANL-5633 July, August, September, 1956

Operated by The University of Chicago
under
Contract W-31-109-eng-38

TABLE OF CONTENTS

CHEMICAL ENGINEERING DIVISION

SUMMARY REPORT

October, November, and December, 1956

SUMMARY

I. Solvent Extraction - Study of Mass Transfer in a Continuous-Flow Mixing Chamber (pages 9 to 10).

A final series of runs was made in a four-inch continuous-flow mixing chamber to study the transfer of isobutanol into water and of nitrobenzene into ethylene glycol. Satisfactory techniques were developed to provide for the rapid analysis of these systems. In addition, a light-scattering correlation was prepared to provide a measure of the interfacial area of the yellow-colored nitrobenzene-ethylene glycol mixtures.

II. Fluoride Volatilization Separations Process (pages 11 to 39).

The development of a scheme for processing zirconium-matrix fuel alloys containing enriched uranium has continued. Additional corrosion tests show graphite has good resistance to chemical attack during the dissolution process.

The behavior of plutonium in the fused salt process was examined in the laboratory to explore the possibility of a fluoride volatility process capable of handling both uranium and plutonium.

Additional investigations on the fluorination of crude uranium tetrafluoride produced from ore concentrates by reduction and hydrofluorination in fluidized bed reactors indicated that uranium tetrafluoride of suitable particle size could be fluidized and fluorinated satisfactorily in a 1-inch fluidized bed reactor.

Preliminary experiments have been performed in order to elucidate the behavior of vanadium in ore-processing schemes involving fluorination reactions.

Iodine pentafluoride and iodine heptafluoride have been examined with particular emphasis on their role in fluoride methods of fuel processing in which iodine is present as a fission product. The kinetics of the reaction between iodine pentafluoride and fluorine to form iodine heptafluoride was investigated.

Shakedown tests of the fused salt equipment were made. Fractionations of bromine pentafluoride-uranium hexafluoride mixtures were carried out to a high degree of uranium hexafluoride purity in the pilot plant columns.

III. Fluidization (pages 40 to 50).

Primary emphasis during the quarter was on the installation and shakedown of new fluidized-bed equipment.

The green salt pilot plant, consisting of two multistage fluidized-bed reactors with associated equipment, was completed and several shakedown runs were made with refined uranium oxide feed. Operation was generally satisfactory, though some minor modifications are necessary. No caking was observed and green salt of good appearance was produced. Some difficulty was encountered in maintaining downcomer seals in the hydrofluorination reactor, but this condition is believed capable of correction.

Installation of the shielded calciner for converting radioactive waste solutions to solid oxides was about 90 per cent completed, and initial runs are planned for the next quarter.

The fundamental study of particle size distribution in fluidized beds was concluded.

IV. Reactor Chemistry (pages 51 to 63).

The study of the oxidation characteristics of uranium, thorium, zirconium and plutonium has been continued. It is likely that conditions which accelerate the oxidation will lower the ignition temperature and increase the possibility of spontaneous ignition. An understanding of the kinetics of oxidation and the mechanism of the reaction should help predict when these metals will be unusually sensitive to spontaneous ignition. Data have been obtained for the oxidation of uranium which show it to be a two-stage process. Experimental work on zirconium has just started.

Work has been completed on the determination of the yield of cesium-137 for fast fission for uranium-235 and plutonium-239. The EBR alpha determination for uranium-235 and plutonium-239 has been completed and the EBR alpha determination for uranium-238 is in progress.

V. Chemical-Metallurgical Separation Processes (pages 64 to 107).

A study of the kinetics of uranium-ceramic oxide reactions is being carried out with high purity uranium and uranium alloys. Studies have been made of beryllia-uranium and zirconia-uranium systems. The reaction of beryllia with uranium shows that the rate of pickup of beryllium increases

with exposure time. Pickup of zirconium in uranium is too small to permit kinetic studies. Additional tests of the effects of alloying agents on the corrosion of alumina, beryllia and thoria by uranium have been made.

Experiments to determine the removal of cerium from "fissium" alloys by melt refining have been made in ceramic oxide crucibles. The "fissium" alloys contained cerium, ruthenium, molybdenum, palladium and zirconium in various combinations. Magnesia removes cerium effectively and shows the best resistance to cracking by thermal shock or chemical reaction.

A sessile drop method is being used to measure the physical properties of liquid uranium, including density and surface tension. The surface tension of uranium at about 1250 C is 825 ± 83 dynes/cm and its work of adhesion to five stable ceramic materials having close-packed oxygen anion surfaces is 240 ± 50 ergs/sq cm.

The preparation of the compound $2CaO \cdot 3BeO$ in the lime-beryllia system was studied.

The variables affecting extraction of plutonium from uranium powder produced by hydriding were studied further.

Data on the partition of various fission product elements between liquid magnesium and uranium-chromium eutectic alloy (five per cent chromium) have been obtained. Zirconium, molybdenum and ruthenium strongly favor the uranium phase, while rhodium, palladium, silver and cadmium favor the magnesium phase.

A full-scale uranium melting furnace, a prototype of the one to be used in the EBR-II pyrometallurgical pilot plant for fuel purification, was received and installed in the last quarter.

Uranium ingots, purified by melt refining, will have equilibrium temperatures of the order of 600 C as a result of fission product heating. It was shown that at this temperature essentially no attack of the uranium by the nitrogen in the argon cell gas (five volume per cent nitrogen) will occur.

A large number of materials have been screened with regard to their efficacy in trapping metals volatilized at high temperatures during the melt refining process. Surface active materials have been found to be effective. Three materials: activated alumina, an activated charcoal, and "Molecular Sieves," have been selected for further study.

Work on purification of uranium by fractional crystallization from zinc was continued. Individual solubilities of uranium and a number of fission products elements in zinc have been determined as a function of temperature.

The five-kilogram scale batch extraction unit of the magnesium extraction process for plutonium has operated satisfactorily in inactive runs using magnesium and a 5 w/o chromium-uranium alloy. A magnesium distillation unit has operated very well with a sodium-cooled condenser. A magnesium "freeze" valve has been developed.

VI. Analytical Research (page 108).

Work during the past quarter has been directed toward the use of paper chromatographic methods which, coupled with pulse analysis, make a more sensitive and versatile approach to the varied target and fission product analysis problems.

VII. Routine Operations (pages 109 to 111).

The operation of the radioactive waste facility and the gamma-irradiation facility continued without incident. A new gamma rack for the accommodation of larger samples has been completed and installed.

I. SOLVENT EXTRACTION - A STUDY OF MASS TRANSFER IN A CONTINUOUS-FLOW MIXING CHAMBER

(W. A. Rodger, V. G. Trice, L. F. Dorsey)

This program is being terminated because of shortages of space and manpower. A final series of runs was made in a four-inch continuous-flow mixing chamber to study the transfer of isobutanol into water and of nitrobenzene into ethylene glycol. Satisfactory techniques were developed to provide for the rapid analysis of these systems. In addition, a light-scattering correlation was prepared to provide a measure of the interfacial area of the yellow-colored nitrobenzene-ethylene glycol mixtures.

The overall aim of this program, to provide a more fundamental basis for the design of mixer-settler types of solvent extraction equipment, has been realized with a fair degree of success. The first phase, the development of a rapid method for estimating the interfacial area of liquid-liquid dispersions, was reported in ANL-5512. The second step, relating the interfacial area formed to fluid motion and to the physical properties of the liquid pair, was reported in ANL-5575. Unfortunately, the final phase, the study of mass transfer in terms of coefficients based on areas, was terminated before many of the more interesting avenues of study could be fully explored; however, the two systems studied represent opposite extremes with respect to transfer rates and will provide a good test of the applicability of contemporary film theories to continuous flow equipment.

The rate of transfer of isobutanol from water-saturated isobutanol drops to pure water was studied at influent rates of 0.5 to 2.2 gallons per minute. The equipment used included a six-inch chamber, described in ANL-5560, page 17, and a four-inch chamber. These were of similar construction with the exception that, in the smaller unit, brass cylinder walls were used to give improved structural strength.

At all flowrates employed, the aqueous effluent from the six-inch chamber was isobutanol-saturated and it was impossible to calculate mass transfer coefficients. In order to reduce the contact time, further studies were carried out in a four-inch diameter chamber. In this unit partial saturation, 90 per cent or better, was effected at the lower flow rates. At higher flowrates, the effluent water was saturated with the organic liquid.

The phenomena of saturation at high flowrates and of partial saturation at lower flowrates were not expected. It is conceivable that the rate of mass transfer in this system is a sensitive function of fluid motion and is relatively insensitive to the magnitude of interfacial area present.

Mass transfer from glycol-saturated nitrobenzene drops to pure ethylene glycol was studied in the four-inch, continuous-flow, mixing chamber at influent rates of 0.5 to 2.0 gallons per minute. The rates of

mass transfer were much lower than those found in the isobutanol-water system; this might be expected because of the lower Schmidt number of the isobutanol-water system. However, as in the case of the isobutanol-water system, the per cent saturation of the effluent glycol increased with flow-rate, reaching a maximum of 80 per cent saturation.

It was necessary to develop a new light scattering-interfacial area correlation for the nitrobenzene-ethylene glycol system. The previously published correlations are valid only for colorless liquids and were unsatisfactory for use with the yellow-colored nitrobenzene system. Accordingly, light-scattering data were obtained for 50, 25 and 10 per cent dispersions. Satisfactory correlations were obtained for the 25 and 10 per cent dispersions. Photographs of the 50 per cent system showed a mixed dispersion (O/W and W/O) and the interfacial area could not be defined.

Satisfactory analytical techniques were developed for both systems studied. The isobutanol content of water was determined from a refractive index-composition plot. The nitrobenzene content of ethylene glycol was determined colorimetrically. The required absorbency-composition plot was determined at 260 millimicrons, using samples diluted 1000-fold with ethyl alcohol.

A complete evaluation of experimental results will be possible after all analytical data have been obtained. The overall results, together with detailed descriptions of sampling and analytical techniques, will be published subsequently in a summary report.

II. FLUORIDE VOLATILIZATION SEPARATIONS PROCESS

The development of a scheme for processing zirconium-matrix fuel alloys containing enriched uranium has continued. This method consists of dissolution of the alloy by hydrogen fluoride in a sodium fluoride-zirconium fluoride melt at 600 C. The uranium is then removed from the melt by a fluorine or bromine pentafluoride sparge, which converts it to the hexafluoride. The final decontamination and purification are accomplished by fractional distillation.

Additional corrosion tests have been made on graphite, which shows good resistance to chemical attack during the dissolution procedure. Further tests have also been made on metals which may serve as backing materials for graphite vessels, or as primary materials themselves. Carburization experiments have been performed to determine whether various metals would suffer from exposure to the graphite in this type of application.

Further work was done on the behavior of plutonium in the fused fluoride process. Experiments were carried out on the volatilization of plutonium (fluorination to the hexafluoride) in which fluorine and bromine pentafluoride were used to fluorinate the melt. Studies have been continued on the possibility of a fluoride volatilization process capable of handling both uranium and plutonium. Specific experiments were performed to establish the degree of fluorination required by nickel equipment for the transfer of plutonium hexafluoride without excessive reduction on the walls of the equipment.

More investigations were made on the fluorination of crude uranium tetrafluoride produced from ore concentrates by reduction and hydrofluorination in fluidized-bed reactors. It was found that uranium tetrafluoride of suitable particle size could be fluidized and fluorinated satisfactorily in a 1-inch fluidized-bed reactor.

Preliminary experiments have been performed in order to elucidate the behavior of vanadium in ore-processing schemes involving fluorination reactions.

Iodine pentafluoride and iodine heptafluoride have also been investigated, with particular emphasis placed on their role in fluoride methods of fuel processing in which iodine is present as a fission product. The kinetics of the reaction between iodine pentafluoride and fluorine to form iodine heptafluoride was determined. Several observations were made on the reactions of the iodine fluorides with iodine, bromine, bromine trifluoride and bromine pentafluoride.

During this quarter shakedown tests of the fused salt equipment were made. Fractionations of bromine pentafluoride-uranium hexafluoride mixtures were carried out to a high degree of uranium hexafluoride purity in the pilot plant columns. Small-scale tests made of the ignition of 1020 steel in fluorinating atmospheres showed it to be unsuitable as a construction material for the fluorinator.

Mr. A. Florin of Los Alamos Scientific Laboratory visited Argonne on November 20 to discuss fluoride volatility. On November 30 Mr. O. Roth of AEC visited Argonne to discuss fluidization and volatility processing.

A. Laboratory Investigations
(R. K. Steunenberg)

1. Fused Salt Processing of Enriched Reactor Fuels

a. Corrosion Investigations
(W. B. Seefeldt, S. Vogler, R. L. Breyne, L. Hays)

Corrosion testing of several materials in fused fluoride systems sparged with hydrogen fluoride and with bromine pentafluoride has been continued. Unless otherwise noted, all the tests reported were conducted at 600 C in equimolar sodium fluoride-zirconium fluoride melts sparged with hydrogen fluoride.

During the quarter the emphasis in the program of testing metals was placed on the exposure of nickel to hydrogen fluoride-saturated melt. Previously, the exposure had been to the more severe alternate contacting of gaseous hydrogen fluoride and liquid-phase melt. Presumably a dissolver could be designed so as to isolate the gaseous hydrogen fluoride from the metallic vessel wall, possibly using graphite. The information reported can be placed in the following four categories:

(1) The potential use of graphite as a material of construction.

(2) Additional information on the life tests of metals reported previously (ANL-5633, page 18). The exposure in these tests was alternate gas-liquid (two-phase exposure).

(3) Information on the corrosion of metal by hydrogen fluoride-saturated melt in the absence of a gaseous phase (one-phase exposure).

(4) Data from tests that were conducted to determine the degree of carburization of metals in contact with graphite in the absence of melt. These tests were directed to the possible use of these metals as back-up materials for graphite liners.

1. Graphite

The corrosion investigations of graphite in the two-inch furnace have been completed. The data indicate that in molten equimolar sodium fluoride-zirconium fluoride at 600 C with hydrogen fluoride passed through the melt, graphite displays very good corrosion resistance. There is, however, some variation in the permeability of the graphite by the melt. For example, a highly dense graphite (National Carbon Type CCN, apparent density 1.90 g/cc) allowed large amounts of melt to pass through the wall, whereas a less dense variety (National Carbon Type CS, apparent density 1.68 g/cc) contained the molten salt.

Two additional runs are reported to complete the data reported in ANL-5633, page 16. In the first run, Type CCN graphite was the crucible material. After three days of operation, it was noticed that the hydrogen fluoride was no longer passing through the melt, so the experiment was terminated. Examination revealed that sufficient melt had penetrated the graphite to fill the space between the graphite and the supporting nickel container. The resultant lowering of the melt level had exposed the sparge tube, so that the gas was no longer passing through the melt. An examination of the graphite crucible and sparge tube showed no dimensional changes.

The second run was made to determine the effects of thermally cycling Type CS graphite with hydrogen fluoride passing through the melt. Each six-hour cycle was equally divided between heating the system to 600 C and cooling it to 75 C. The flow of hydrogen fluoride was 36 g/hr, and the test continued for two weeks. The impingement plate holes showed a diameter increase of one mil, slightly greater than the precision of the measurement. Channelling of the gas through the melt was suspected because the impingement plate holes showed uneven attack.

The complete series of corrosion tests indicate that, chemically, graphite is a suitable material for containing the fused fluoride melts sparged with hydrogen fluoride. The principal limitations on the use of graphite which might exist are the mechanical effects of thermal cycling and the penetration of melt through the graphite. An effort is being made to clarify these effects.

2. Metals: Two-Phase Exposure

Run 73; Monel - A 32-mil Monel liner was used in the liner-impingement plate configuration described in ANL-5494, pages 33 and 34. The test was terminated after 1188 hours. The average hydrogen fluoride sparge rate was 46 g/hr. Three sparge assemblies were used. The first plugged after 300 hours; the second fractured above the impingement plate after 768 hours; the third was used for the remaining 120 hours. The liner suffered severe copper depletion through its entire cross section. A representative cross section of the liner is shown in Figure 1. The Monel apparently was not weakened by intergranular effects.

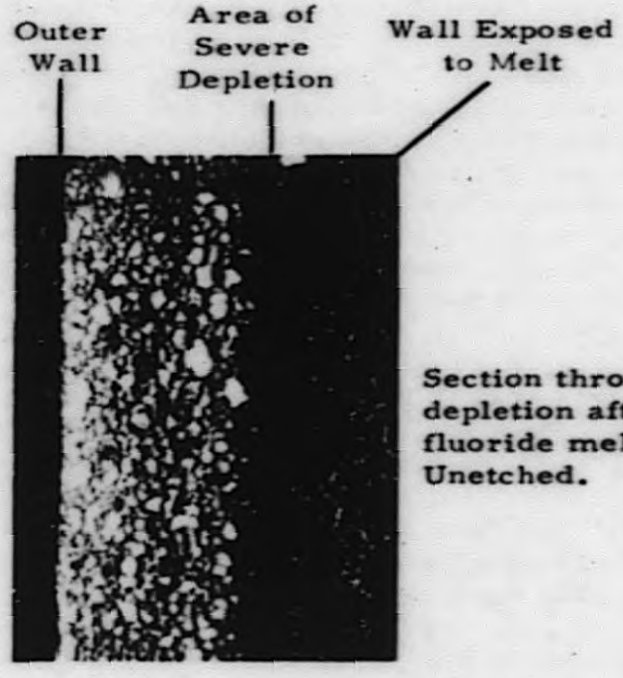

Figure 1

Section through wall of Monel liner showing copper depletion after exposure to hydrofluorinated fused fluoride melt (Run 73, 1188 hours at 600 C). 400X Unetched.

Copper depletion was also evident in the sectioned sparge tubes. (Data on the first sparger are reported in ANL-5633, page 21.) The second sparger appeared to have fractured due to severe attack of the metal on the internal surfaces above the impingement plate. An effect similar to this had been noted previously with nickel sparge tubes used for bromine pentafluoride corrosion tests at 600 C.

Run 91; "A" Nickel and Low-Carbon Nickel - A single liner was fabricated from vertical strips of "A" nickel and low-carbon nickel to determine differences in behavior, if any, toward a common environment. The tests were conducted for 327 hours at an average hydrogen fluoride sparge rate of 43 g/hr.

The liner was sectioned at two locations: one-quarter inch above the bottom, where little two-phase contacting was expected, and one inch above the bottom, where the two-phase contacting was expected to be at a maximum. Neither metal appeared to be embrittled. In the upper section the surfaces of both metals were roughened by selective attack at the grain boundaries. The depth of such attack was no greater than two grain diameters. Some deposits were evident, none of them being characteristically sulfurous. The surfaces of the lower section, where one-phase attack predominated, were considerably smoother. Intergranular effects were noted to a depth of two or three grain diameters, but these again were not sulfurous in nature. The grains in the "A" nickel were somewhat larger than those in the low-carbon nickel, but this was probably characteristic of the starting material. The dimensional changes did not exceed 1.5 mils in either material.

In summary, no gross differences existed between the two types of nickel, particularly with regard to intergranular effects.

3. Metals: One-Phase Exposure

The previous corrosion tests had been directed toward determining the behavior of nickel under extremely severe conditions where the metal was subjected to the gas and liquid alternately. A number of one-phase tests were begun to determine the characteristics of nickel exposed to more moderate conditions, i.e., to hydrogen fluoride-saturated melt only. Figure 2 shows the configuration used. In addition, data from earlier runs were re-examined to determine the dimensional changes in liner walls near the bottom, where the two-phase contacting was believed to have been low.

Run 92: "A" Nickel - The configuration shown in Figure 2 was used with a nickel liner and sparger and a Monel draft tube. The test period was 96 hours at a

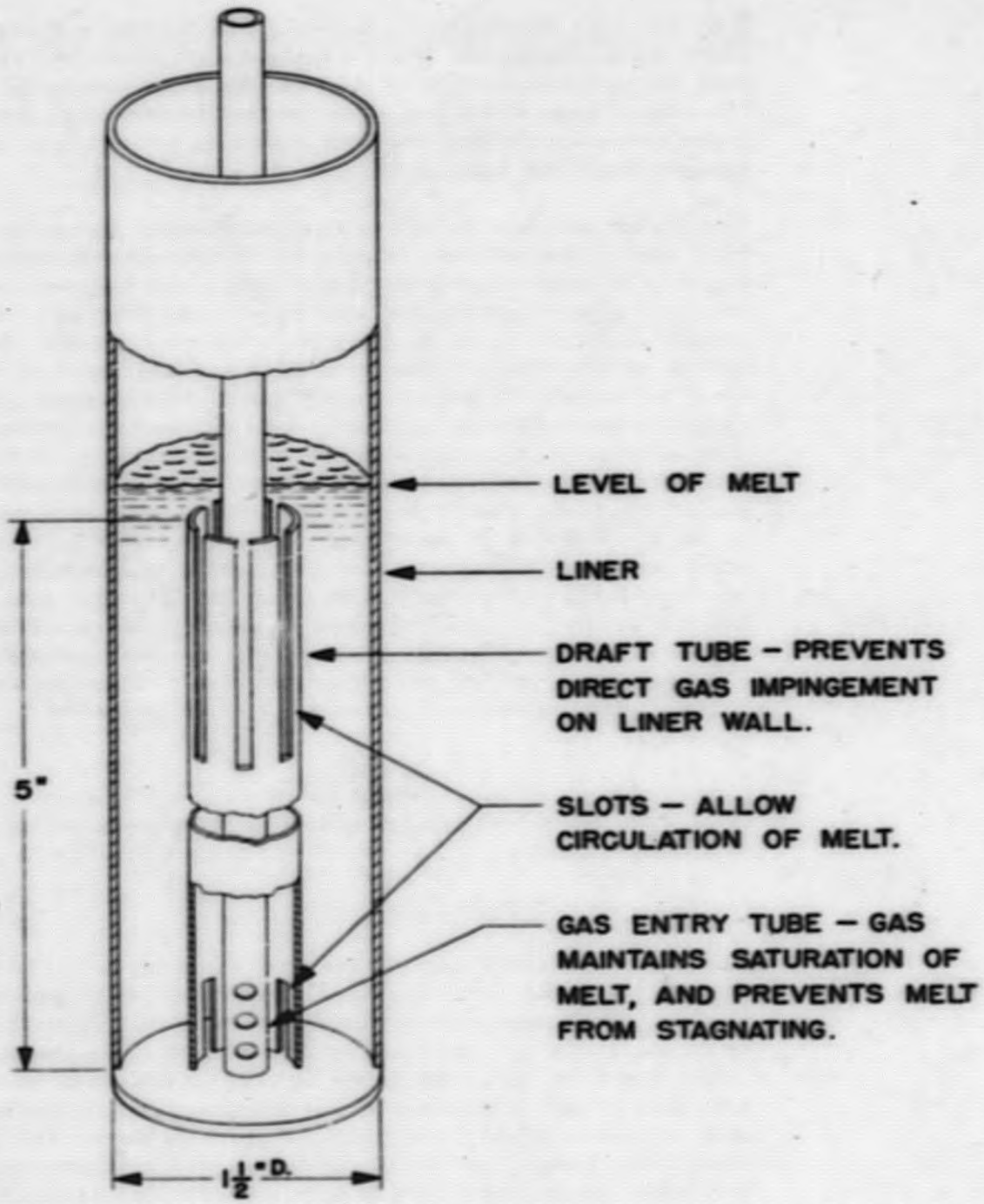

Figure 2

Configuration used for one-phase corrosion testing of metal liners (Provisions can be made for exposing coupons in annular space)

sparge rate of 38 g/hr. The maximum dimensional change occurring in the melt zone was 2.5 mils, while the interface penetration was 6 mils. The characteristically severe liner attack usually evident opposite the impingement plate was lacking. No intergranular effects were found.

Run 93: "A" Nickel - The draft tube in this run was also "A" nickel. The test was terminated after 996 hours without failure of the liner or draft tube. Evaluation has not yet been started.

Run 94: "A" Nickel - This test was identical to Run 93, except that 10 volume per cent hydrogen was added to the hydrogen fluoride sparge. Certain thermodynamic evidence suggests that the hydrogen addition should reduce the corrosive attack of nickel. The hydrogen fluoride used in the two runs was from different sources.

The test was terminated at 419 hours by a nearly complete embrittlement failure of all the components - the liner, sparger, thermocouple well and draft tube. A metallographic examination of the liner revealed sulfurous deposits in grain boundaries near the point of liner fracture, about 2¼ inches from the bottom. Contributing to the failure was excessive grain growth, which probably resulted from a temperature runaway due to a controller failure. Microscopic measurements of the wall showed uniformly small dimensional changes of 1 to 1.5 mils. Figure 3 shows a sulfurous inclusion in the metal wall near the point of fracture. Samples of the hydrogen fluoride are now being taken routinely for sulfur analyses.

Extrapolated One-Phase Corrosion Data from Earlier Tests - The data in Table 1 show the dimensional changes of liner walls near the bottom, where the two-phase attack should be very low. Data from the recent runs are also included. Dimensional changes of liner walls subjected to one-phase exposure appear to be less by factors of five to ten than walls subjected to two-phase exposure.

4. Carburization Tests

These tests are a continuation of those reported earlier (ANL-5633, page 21). A summary of the results to date is given in Table 2. Figure 4 shows the appearance of carburization in three of the metals tested.

Outer wall

Wall exposed to melt

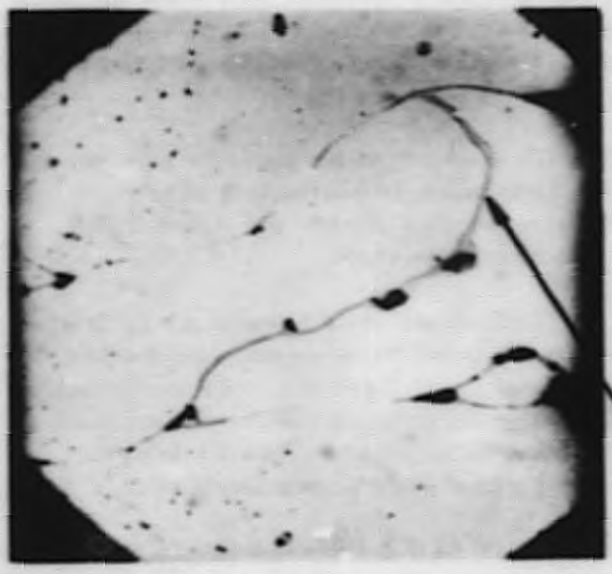

Continuous sulfurous deposit extending from wall to wall along grain boundary.

Figure 3

Embrittlement of Nickel Liner by Combined Grain Growth and Sulfidation

Single grains have grown to occupy entire wall thickness. (Run 94, 419 hours, 600C) 100X. Cyanide-persulfate etch.

Table 1

CORROSION OF "A" NICKEL LINERS IN HYDROGEN FLUORIDE-SATURATED MELT WITH AND WITHOUT IMPINGEMENT[a]

Most of the non-impingement data are extracted from earlier runs and are calculated from the dimensional change of liner walls near the bottom where gas impingement should be very low.

Melt: Equimolar $NaF-ZrF_4$

Run No.	Sparge Gas	Sparge Rate, g/hr	Temperature, C	Rate of Penetration, mils/day: Max Rate with Impingement	Rate of Penetration, mils/day: No Impingement
64[b]	HF	32	600	1.2	0.46
73[c]	HF	46	600	0.33	0.05
78[b]	HF	52	600	1.9	0.06
26	BrF_3	18.1	700	10.4	3.6
28-28A	BrF_3	6	700	3.6	0.6
35	BrF_3	15.4	600	1.4	0.5
92	HF	38	600	-	0.6
93	HF	20	600	0.48	0.02-0.14
94	10% H_2-HF	35	600	-	0.08

[a] Tests with impingement are two-phase exposures; without impingement one-phase exposures.

[b] "L" Nickel used in these runs.

[c] Monel used in this run.

Table 2

RESULTS OF CARBURIZATION TESTS

Samples packed in powdered graphite
under helium atmosphere at 600 C.

Total Exposure Time (weeks)	Total Depth of Attack (mils)[a]				
	3	4	7	8	11
Metal					
SS 347	0.4	-	0.9	-	1.7
Monel	1.1	-	0.8	-	1.1
Inconel	1.0	-	0.9	-	0.9
SS 330	1.5	-	3	-	3
Nickel	0.7	-	0.7	-	0.7
SS 304	0.5	-	0.3	-	0.3
Hastelloy B	0.05	-	0.2	-	0.3
SS 309	No Exposure	<0.05	-	<0.05	-
SS 310	No Exposure	0.2	-	0.2	-

[a]Slices were cut from exposed samples and evaluated; samples were then returned to test for additional exposure.

b. Behavior of Plutonium During the Volatilization of Uranium Hexafluoride
(S. Vogler)

In the fused fluoride process for the recovery of uranium from enriched reactor fuels, bromine pentafluoride can be used to volatilize the uranium from the melt at 600 C as the hexafluoride. As reported previously (ANL-5633, page 24), it was found that about 0.03 per cent of the plutonium present was collected in the cold traps under these conditions.

A further experiment has been performed to determine the effect of fluorine gas under conditions similar to those used with bromine pentafluoride vapor. An alloy of uranium containing 0.92 weight per cent plutonium was dissolved by fluorine sparged through an equimolar sodium fluoride-zirconium fluoride melt at 600 C at a fluorine flow rate of 45 cc/min. The off-gases were passed through cold traps, which consisted of 3/4-inch nickel tubes attached to the system by flare connectors. The traps contained copper mesh packing to aid in trapping the plutonium. These traps were maintained at -40 C and the lines from the furnace to the trap were held at 250 C in order to minimize the deposition of plutonium before it reached the traps. This equipment is shown in Figure 5. At the completion of the

Figure 4

Carburization Effects in Several Metals after Contact with Graphite for Eleven Weeks at 600C

All Photos Show Transverse Sections

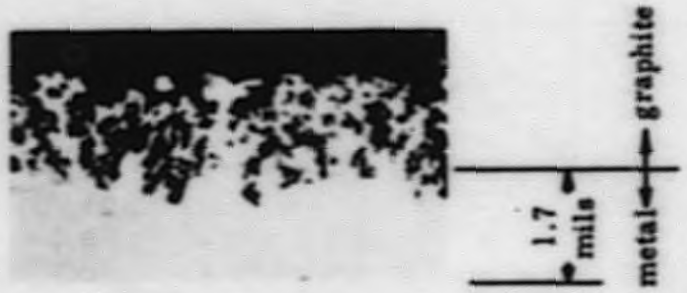

Type 347 Stainless Steel showing general carbide formation to depth of 1.7 mils. Attack appears to be progressive. 400X Unetched.

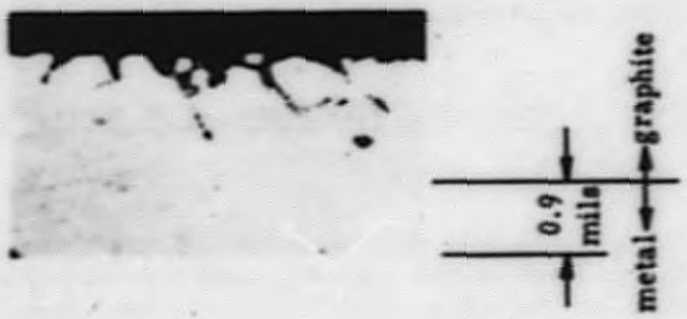

Carburization in Inconel along grain boundaries. Rate of attack is decreasing. 400X Unetched.

Detachment of grains from surface of Type 330 Stainless Steel following intergranular carburization. Rate of attack is decreasing. 400X Unetched.

FIGURE 5.

SCHEMATIC DIAGRAM OF LINE WASHES.

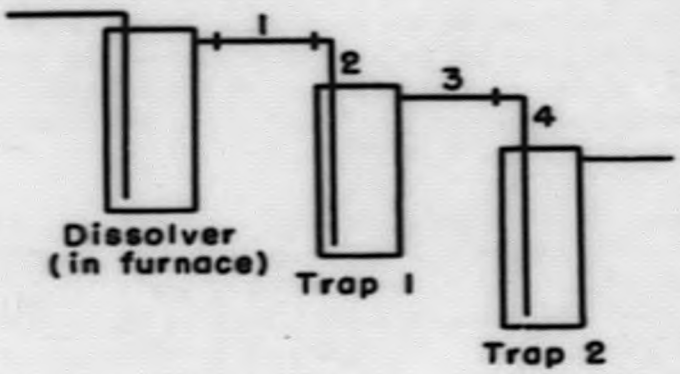

experiment, the traps and the melt were sampled and assayed for uranium and plutonium. The nickel traps were washed with hot 4 M nitric acid containing 0.05 M aluminum nitrate. The copper mesh was completely dissolved during the washing. The lines from the furnace to the traps were also washed with hot 6 M nitric acid.

The distribution of the plutonium and uranium in the traps, melt and lines is given in Table 3. As indicated in Figure 5 the line washes were collected in four fractions. The table also contains for comparison similar data obtained with bromine pentafluoride as the oxidizing gas.

Table 3

VOLATILIZATION OF PLUTONIUM AND URANIUM FROM EQUIMOLAR SODIUM FLUORIDE-ZIRCONIUM FLUORIDE MELTS WITH FLUORINE AND BROMINE PENTAFLUORIDE

Source of Plutonium: U-Pu alloy (0.92 w/o Pu) Melt: 40 g equimolar $NaF-ZrF_4$
Temperature: 600 C Gas Flow:[a] ~18 g/hr bromine pentafluoride
Time: 2 hours

Sparge Gas	Per Cent Found					
	F_2		BrF_5		BrF_5	
	Pu	U	Pu	U	Pu	U
Location						
Melt	110	0.02	167	0.7	168	0.3
Line Section 1	0.14	0.03	-	-	0.04	0.8
Line Section 2	6.5	12.5	-	-		
Trap 1	3.9	30.0	0.02	85.9	0.03	105
Line Section 3	0.14	8.0	-	-	-	-
Line Section 4	0.02	5.5	-	-	-	-
Trap 2	0.0004	0.9[b]	0.004	4.7	0.002	6.8

[a] These flow rates are approximately equal.

[b] Uranium material balance low due to poor trap design.

The data show that with fluorine sparging a small amount (~4%) of the plutonium was found in the first trap. The bulk of the plutonium found in the washings appeared in line section two, probably as a result of the lower portion of this section being cooled by the cold trap. Little plutonium was found in the washings from line section one which was kept hot throughout the experiment.

For comparison, after the experiments with bromine pentafluoride had been completed, washings of the lines corresponding to line sections one and two showed only 0.04 per cent of the plutonium and 0.8 per cent of the uranium (based on the material present in one experiment). In both cases the high plutonium material balances are believed to arise from poor melt sampling due to solidification of a portion of the melt on the cooler areas of the dissolver wall.

Qualitatively these data indicate that fluorine volatilizes several per cent of the plutonium from the melt, whereas bromine pentafluoride volatilizes negligible amounts, if any at all. In view of the differences in plutonium behavior in the presence of these two fluorinating agents, a second experiment appears to be warranted in the case of fluorine to confirm the results.

The uranium data indicate complete removal from the melt by either of the fluorinating agents.

2. Processing of Uranium-Plutonium Fuels - The Stability of Plutonium Hexafluoride
(M. D. Adams, D. V. Steidl)

Conditions affecting the handling of plutonium hexafluoride as a gas in nickel equipment are being studied. Plutonium hexafluoride has gained a reputation for instability. When handled as a gas it is difficult to prevent partial decomposition. A small amount of this decomposition is due to radiation damage, but the greater amount is due to the reactivity of the plutonium hexafluoride. It is apparently a better fluorinating agent for some metal surfaces than fluorine. For example, it will decompose on a surface at a lower temperature than that at which the surface was prefluorinated. As a result of the work presented it was found that under severe conditions of prefluorination much of the plutonium hexafluoride decomposition previously found could be prevented.

In previous experiments, such as Runs 89, 93, 95, and 97 in Table 4, the stability of plutonium hexafluoride in a current of helium was being studied as it was passed through a heated section of tubing packed with nickel wool (ANL-5602, page 32). Analyses of the contents of the various sections of the apparatus indicated a great deal of plutonium hexafluoride was

Table 4

EFFECT OF PREFLUORINATION ON COMPLETENESS OF VAPORIZATION OF PLUTONIUM HEXAFLUORIDE FROM A COLD TRAP

Plutonium hexafluoride prepared by passing fluorine over plutonium tetrafluoride at 500 C and condensed in a cold trap prefluorinated under conditions shown below.
Fluorine flushed out of apparatus with helium at 100 cc/min.
Cold trap warmed to temperatures indicated.
Diagram of equipment shown in ANL-5602, page 32.

Exp. No.	Pu Used (mg)	Prefluorination Time (min)	Prefluorination Temp. (C)	Trap Temperature (C)	Pu Remaining in Trap (mg)	Pu Remaining in Trap (per cent)
89	14.3	15	280	30	14.3	100
93	11.8	15	280	90	9.66	81.8
95	16.14	15	300	90	11.45	71.0
97	11.98	60	330	125	8.35	69.7
99	17.4	30	420	90	8.20	47.1
101	10.4	30	420	90	9.20	88.5
103	19.1	60	420	90	15.27	80.1
107	15.0	30	450	90	10.45	70.0
109	20.85	90	450	70	1.82	8.73
105	19.3	30	490	30	5.44	28.2
113	16.7	30	560	70	11.55	69.2
111	16.7	90	560	90	0.73	4.37

being lost because of decomposition in the condensing trap. Therefore, the effect on the decomposition of plutonium hexafluoride of various prefluorinations of nickel equipment in which condensation is to be effected was investigated.

A U-tube of 3/8-inch nickel tubing was constructed and placed in a system between a furnace for making plutonium hexafluoride and a cold trap. The U-tube was heated by a resistance wire winding. It was prefluorinated by heating it to a predetermined temperature in the range of 350 to 560 C and passing fluorine through the system at flow rates varying from 25 to 50 cc/min. After the required prefluorination time, the trap was cooled by immersion in liquid nitrogen.

Plutonium hexafluoride was then prepared by passing fluorine over plutonium tetrafluoride at about 500 C in the furnace tube. As it was produced it was carried by the fluorine stream into the nickel U-tube, where

it was condensed. Helium, which was purified by passing it through a charcoal trap at -196 C, was used to flush the fluorine from the system. The U-tube was warmed, usually to about 90 C, and the plutonium hexafluoride was carried into a cold trap by a helium stream which was regulated to 100 cc/min.

After about one hour the apparatus was disassembled and the contents of the trap were washed out with nitric acid. The solid matter was dissolved and the resulting solution was analyzed for plutonium.

The results of several experiments are listed in Table 4. Both the time and temperature of the prefluorination treatment appeared to have an effect upon the recovery of plutonium hexafluoride. For example, when the prefluorination was performed at 450 C for 30 minutes, 70 per cent of the plutonium remained in the U-tube. When the U-tube was pretreated with fluorine for 90 minutes at 450 C, however, less than 10 per cent of the plutonium remained behind.

It is planned to extend this investigation to include passing plutonium hexafluoride through various commonly used valves and other fittings in both fluorine and helium atmospheres.

3. Feed Materials Processing - The Conversion of Uranium Tetrafluoride to the Hexafluoride
(O. Sandus, W. A. Shinn)

Fluorination studies of uranium tetrafluoride in a fluidized bed reactor have been continued. The uranium tetrafluoride used in these experiments was produced by the semi-works fluidization group (page 37) by reduction and hydrofluorination of South African Rand ore concentrate in a fluidized bed reactor.

The experimental work reported previously (ANL-5633, page 31) has shown the possibility of using a solid inert diluent, calcium fluoride, during the fluorination of uranium tetrafluoride in a fluidized bed. As a result of difficulty in obtaining calcium fluoride of the desired purity and particle size (+100 mesh), an attempt was made to use magnesium fluoride as the solid diluent in the bed. Observations in a glass system showed that the magnesium fluoride and uranium tetrafluoride mixture tended to segregate with the uranium tetrafluoride at the bottom. This effect was caused by the low bulk density of the 100-mesh magnesium fluoride, which was about half that of the crude uranium tetrafluoride.

The second batch of crude uranium tetrafluoride was received by the laboratory group for further studies. The particle size was larger and the proportion of very fine particles was much smaller than the first batch (see Table 5). The better particle size distribution made unnecessary the

Table 5

PARTICLE SIZE DISTRIBUTIONS OF TWO BATCHES OF CRUDE URANIUM TETRAFLUORIDE

Source: South African Rand ore concentrate reduced and hydrofluorinated in a 3-inch fluidized bed at 450 C.
Method: Screen analysis.

	Per Cent	
Sieve No.	Batch 1	Batch 2
+20	2.1	0.1
-20, +40	29.5	46.1
-40, +60	11.5	29.0
-60, +100	12.2	14.0
-100, +200	13.8	8.0
-200, +325	9.3	1.3
-325	21.6	1.5

addition of an inert diluent (such as calcium fluoride) to improve fluidization characteristics. Although the present studies were made with the undiluted uranium tetrafluoride, it is possible that the solid diluent may be necessary in future work in order to handle the more finely divided gangue element fluorides. A partial analysis of the second batch of uranium tetrafluoride is shown in Table 6.

Two experiments have been completed in which the second batch of uranium tetrafluoride was fluorinated in the absence of a solid diluent. The results are shown in Table 7. These data indicate that under the conditions of the runs the concentration of fluorine in the gas stream does not affect the efficiency of the reaction. When the fluorine concentration was doubled, the rate of uranium hexafluoride production also increased twofold. The difference between the values for fluorine efficiency is within the experimental uncertainty. In both experiments some caking was noted in the material remaining in the reactor.

Since solid gangue element fluorides would be expected to accumulate in the fluidized bed as the uranium is removed, future work will be necessary to establish the nature of these residues.

4. Properties of Vanadium Fluorides
(L. E. Trevorrow, H. D. Tyler)

Experimental work on the properties of fluoride compounds of vanadium has been initiated to clarify the behavior of vanadium in the processing of uranium ores by fluoride volatilization methods. The first

Table 6

URANIUM COMPOUND CONTENT OF CRUDE URANIUM TETRAFLUORIDE PRODUCED FROM ORE CONCENTRATE

Source: South African Rand ore concentrate reduced and hydrofluorinated in a fluidized bed reactor at 450 C.

Analyses: Average values based on two samples from wet chemical methods.

Uranium Compound	Per Cent
UF_4	90.7
UO_2F_2	0.9
UO_3	1.7
UO_2	1.1
Impurities Containing No Uranium	5.6

Table 7

FLUORINATION OF CRUDE URANIUM TETRAFLUORIDE IN A FLUIDIZED BED REACTOR

Charge: 75 g crude UF_4 (71.8% U)
F_2 Added: One stoichiometric equivalent
Temperature: 450 C

Exp. No.	Flow Rate (cc/min)		Mole Ratio F_2/N_2	Time (min)	F_2 Efficiency[a] (per cent)
	Nitrogen	Fluorine			
20	2665	481	0.18	30.0	81
21	2310	836	0.36	17.3	79

[a] Fluorine Efficiency = $\frac{\text{amount of fluorine used to produce } UF_6}{\text{total amount of fluorine added}}$

compound of vanadium to be investigated is vanadium pentafluoride. Previous work at Argonne National Laboratory suggested that this compound is more volatile than indicated in chemical literature.

Vanadium pentafluoride was first prepared by the disproportionation of vanadium tetrafluoride by Ruff and Lickfett[1] who indicated that reaction of the elements was unsuitable for preparation of the pentafluoride. These workers described vanadium pentafluoride as a white solid with a sublimation point of 111.2 C and a melting point above 200 C. Emeleus and Gutmann[2] prepared vanadium pentafluoride by reaction of the elements at 300 C, and also by the reaction of vanadium metal with bromine trifluoride. However, they gave no description of the properties of the pentafluoride.

Experience in the present program has shown that the reaction of fluorine on vanadium metal in nickel apparatus at 300 C produced a volatile liquid which distilled out of the reaction site. A green solid also formed and remained in the hot reaction site. Emeleus also observed the production of this green solid, which he identified as vanadium trifluoride.

The properties of the volatile compound observed thus far in this work do not agree well with those described by Ruff for the vanadium pentafluoride. When the product issuing from the nickel apparatus was collected in a Fluorothene vessel, it was a dark reddish-brown liquid at room temperature. Simple distillation of this product gave a pale yellow, almost colorless, distillate. Preliminary vapor pressure measurements indicate that the normal boiling point of the liquid may be in the neighborhood of 50 C.

5. Kinetics of the Reaction of Fluorine with Iodine Pentafluoride to Form Iodine Heptafluoride
(J. Fischer, R. K. Steunenberg, W. Lechnick)

The rate at which iodine pentafluoride is oxidized to the heptafluoride by fluorine is important in fuel reprocessing by fluoride volatilization methods. Iodine, which is a major fission product activity in short-cooled fuel elements, is converted to iodine pentafluoride by strong fluorinating agents such as bromine trifluoride. For schemes in which uranium is dissolved in bromine trifluoride, fluorine is usually added after the dissolution to regenerate bromine trifluoride from bromine produced by the dissolution reaction. Therefore, the possible conversion of iodine pentafluoride to the heptafluoride during this fluorination step is of interest. Iodine heptafluoride is one of the most volatile fluorides produced (b.p. 4 C), while the pentafluoride (b.p. 100 C) is only slightly more volatile than bromine trifluoride.

---

[1] Ruff, O., and Lickfett, H., Ber., 44, 2539 (1911)

[2] Emeleus, H. J., and Gutmann, V., J. Chem. Soc., 2979 (1949)

The rate of the vapor-phase reaction of fluorine with iodine pentafluoride to form iodine heptafluoride was investigated from 55.6 C to 95 C. The rate was found to be second order with respect to the reactant pressures. The rate constants showed an Arrhenius temperature dependence, with an experimental activation energy of 14 kcal/mole. The reaction was homogeneous, suggesting that the rate-determining step is a bimolecular collision.

The preparation of iodine pentafluoride[3] and iodine heptafluoride[4] had been described by O. Ruff. The authors suggested that the reaction of iodine pentafluoride with fluorine, in the region of 100 to 270 C, resulted in an equilibrium mixture of the pentafluoride and the heptafluoride. Experimental limitations prevented them from observing whether complete conversion of the pentafluoride was possible.

This investigation was undertaken to establish the stoichiometry and kinetics of the reaction, and to obtain some insight of the mechanism involved. The materials, apparatus and procedure will be described in detail in an article recently accepted for publication by the Journal of the American Chemical Society. The iodine pentafluoride was prepared by the direct combination of fluorine and reagent grade resublimed iodine in a reaction vessel at 0 C. Very little iodine heptafluoride was formed at this temperature. The apparatus and experimental technique were similar to those described in connection with the rate study of bromine trifluoride and fluorine in the previous quarterly report (ANL-5633, page 38).

The rate of the reaction was obtained from the change in total pressure, with time, after known partial pressures of the reactants were mixed in the reaction vessel. Iodine pentafluoride vapor was added to the vessel first, and its pressure was measured. Fluorine was then added from a metering vessel and its partial pressure in the reaction vessel was calculated from the pressure decrease in the metering vessel. The volume factors between the two vessels were measured, using both fluorine and helium individually.

Since the measurements were all based on pressure data, it was necessary to show that the concentrations were related to the pressures by the ideal gas law. Vapor densities of iodine pentafluoride and iodine heptafluoride were determined by measuring the pressures of weighed amounts of the materials added to a vessel of known volume at a fixed temperature. Iodine pentafluoride at temperatures around 80 C and pressures of 200 to 250 mm gave an average value of 224.3 ± 1.5 g/G.M.V. (Formula weight: 221.9 g/mole.) The heptafluoride at 28 C and over a pressure range of 129

---

[3] Ruff, O., and Braida, A., Z. anorg. u. allgem. Chem., 220, 43 (1934)

[4] Ruff, O., and Keim, R., ibid, 193, 176 (1930)

to 258 mm gave a value of 260.9 ± 2.0 g/G.M.V. (Formula weight: 259.9 g/mole.) The same cylinder of fluorine had been shown previously[5] to exhibit ideal behavior. (Gas density: 38.00 ± 0.15 g/G.M.V.; Formula weight: 38.00 g/mole.) Thus, all three gases were considered ideal within the over-all accuracy of the measurements.

Before meaningful rate determinations could be made, the stoichiometry of the reaction had to be demonstrated. The data in Table 8 indicate that the formation of the heptafluoride occurs quantitatively within the temperature range of these measurements. Physical separations or chemical analyses of the reactants and products in this system are difficult. In order to confirm the quantitative nature of the reaction, an additional experiment was performed. At the conclusion of the second experiment in Table 8, the mixture in the reaction vessel was cooled with liquid nitrogen, and the system was evacuated to remove the residual fluorine. When the system was warmed to 75.3 C, an observed total pressure of 103.6 mm was in good agreement with the theoretical yield of 101.2 mm of iodine heptafluoride.

Table 8

STOICHIOMETRIC BEHAVIOR OF THE REACTION $IF_5 + F_2 \longrightarrow IF_7$

Temp. (C)	Initial Pressures (mm) F_2	Initial Pressures (mm) IF_5	Final Pressure (mm)	Elapsed Time (min)
55.7	562.1	99.4	563.6	1402
75.0	575.2	101.2	574.2	197
85.7	560.2	102.4	561.5	1098

Therefore it was possible to calculate the partial pressures of the reactants at any time during the reaction from the difference between the total initial pressure and the total pressure at that time.

The reaction under study may be expressed as

$$IF_5 + F_2 \longrightarrow IF_7 \quad . \qquad (1)$$

If the product results from the homogeneous bimolecular interaction of iodine pentafluoride and fluorine molecules, the rate of reaction will be second order with respect to the partial pressures of the reactants. Graphical methods were employed to obtain the rate constants.

---

[5]Steunenberg, R. K., and Vogel, R. C., J. Am. Chem. Soc., 78, 90 (1956)

The rate data obtained from the experiments are given in Table 9. The initial partial pressures of the reactants are given to show the variations in the initial pressures used. The pressures were assumed to be reliable to ± 0.2 mm and the temperatures to ±0.05 C. The rate constants, in dimensions of $(mm^{-1})(hr^{-1})$, were computed from the slopes of lines drawn through the plotted data.

Table 9

SECOND-ORDER RATE CONSTANTS FOR THE REACTION $IF_5 + F_2 \rightarrow IF_7$

Expt. No.	Temp. (C)	Initial Pressures (mm) F_2	Initial Pressures (mm) IF_5	Rate Constant, k $(mm^{-1}\ hr^{-1})$
1	55.6	99.5	98.8	2.02×10^{-3}
2	55.6	106.0	99.4	2.02
3	55.6	99.8	99.6	2.01
4	55.7	562.1	99.4	2.01
5	55.7	560.8	99.5	2.07
6	65.0	100.8	100.1	3.86
7	65.0	99.7	100.0	3.97
8	65.0	299.0	99.6	3.75
9	65.0	299.5	99.5	3.77
10	65.0	569.0	100.0	3.63
11	65.0	568.7	99.6	3.65
12	69.8	100.2	100.0	5.03
13	75.3	99.6	99.8	6.94
14	75.3	100.8	100.2	6.79
15	75.3	298.3	99.5	6.93
16	75.3	575.0	101.0	7.09
17	80.3	99.8	99.8	8.57
18	85.1	100.5	100.4	10.5
19	85.1	99.7	99.8	11.9
20	85.1	100.1	99.7	12.1
21	85.1	299.8	99.4	10.6
22	95.0	100.6	101.1	18.9

In Experiment 7, the surface area of the reaction vessel was increased by a factor of about five by placing nickel wire mesh in it. The volume change was negligible. In Experiments 3, 5 and 9, another reaction vessel of approximately twice the original volume was used. The fact that variations in the surface and volume had no effect on the rate indicates homogeneous behavior of the reaction.

The activation energy for the reaction was determined by plotting the logarithm of the rate constant against the reciprocal absolute temperature as shown in Figure 6. The activation energy calculated from the slope of the line was 14 kcal/mole. This activation energy is a reasonable value for a homogeneous bimolecular reaction. The linear nature of this plot is also in accord with a reaction of this type.

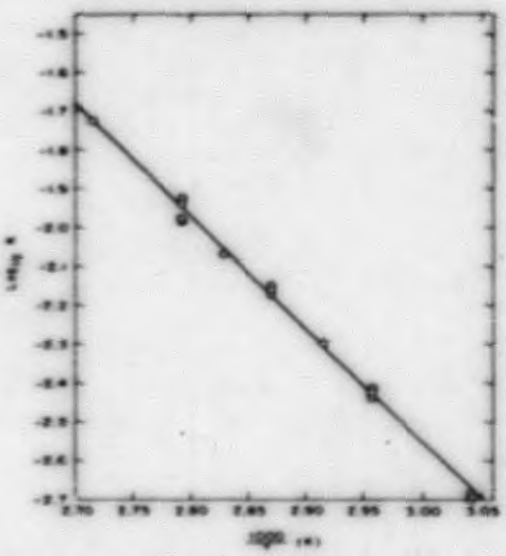

6. The Reactions of the Iodine Fluorides with Iodine, Bromine and the Bromine Fluorides
(J. Fischer, R. K. Steunenberg, W. Lechnick)

The importance of the reaction of iodine pentafluoride with fluorine was discussed in the previous section. For similar reasons, the reactions of iodine pentafluoride and iodine heptafluoride with iodine, bromine, bromine trifluoride and bromine pentafluoride may also be pertinent to fluoride volatilization processes. Several experiments were performed to outline in a general way the chemical reactions which may be expected in these systems.

A study of the visible and ultraviolet absorption spectra of bromine trifluoride, bromine pentafluoride, bromine, iodine pentafluoride and iodine heptafluoride indicated that spectral absorption in the gas phase would be useful in a study of their interactions. Serious interferences in the absorption curves prevented their exclusive use, however. Iodine has an absorption peak in the region 5010 to 5020 Å, but the molar absorbency index has not been determined satisfactorily. Iodine tended to condense

on the cell windows in these experiments, but trace amounts (less than 1 mm pressure) were easily detected in the 10-cm cell. The apparatus and procedures for the spectrophotometric determinations have been described previously.[5]

The iodine pentafluoride was prepared by the direct combination of fluorine gas and reagent grade, resublimed iodine at 0 C. The residual fluorine was removed by evacuation of the system at -196 C.

Iodine heptafluoride was prepared by the reaction of iodine pentafluoride with excess fluorine at 100 C. The excess fluorine which remained after the reaction was distilled from the reaction mixture at liquid nitrogen temperature. The iodine heptafluoride was separated from the unreacted pentafluoride by distillation at -25 C.

FIGURE 7.
BEER'S LAW BEHAVIOR OF IODINE HEPTAFLUORIDE.
Optical Path of Cell: 10 cm
Temperature: 25 C.

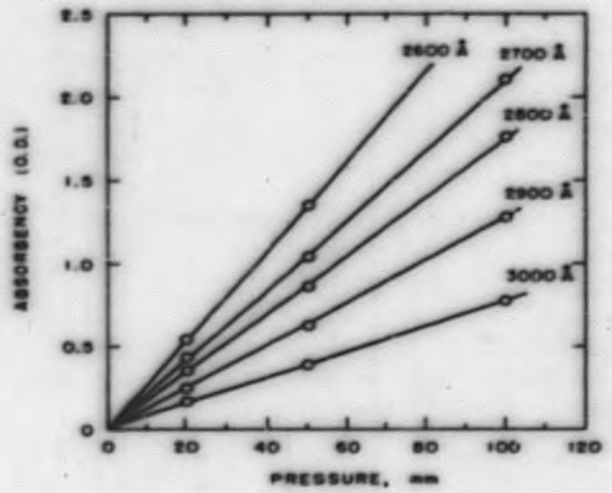

The absorption spectra of the iodine fluorides were investigated in the visible and ultraviolet regions. Positive absorption regions were found for both compounds in the ultraviolet. The absorption at various wavelengths of iodine heptafluoride as a function of pressure at 25 C is shown in Figure 7. The Beer's Law behavior* permits the calculation of molar absorptivities of iodine heptafluoride from the slopes of the lines in Figure 7.

The values of molar absorptivity for iodine pentafluoride at 2300, 2400 and 2500 Å were calculated in a similar manner from absorption measurements at 78 C using pressures of 100 and 200 mm.

The effect of temperature on the absorptivity of iodine heptafluoride is indicated in Figure 8, where the molar absorptivity is plotted as a function of wavelength for temperatures from 25 C to 87 C.

---

*$a_M = A/dc$

where a_M = molar absorptivity (extinction coefficient), $(\text{moles/liter})^{-1}\text{cm}^{-1}$
A = absorbency (optical density)
d = cell path, cm
c = concentration, moles/liter

FIGURE 8.

ABSORPTION SPECTRUM OF IODINE HEPTAFLUORIDE.

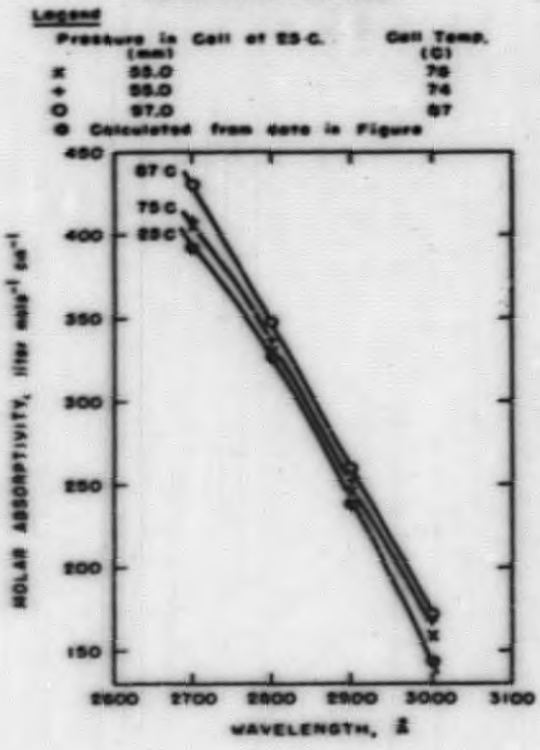

The curves of molar absorptivity for iodine pentafluoride and iodine heptafluoride are shown in Figure 9, along with the curves determined previously for bromine, bromine trifluoride and bromine pentafluoride. It is evident that iodine heptafluoride can be determined quantitatively in the presence of the other substances.

The reactions listed in Table 10 were studied at 77 C by mixing the components, in the vapor phase, in a nickel vessel at known partial pressures and observing any change in the pressure with time. The mixed vapors were expanded into a 10-cm absorption cell which was heated to 77 ± 2 C. The absorption was determined from 2400 to 6000 Å, using the Cary recording spectrophotometer. The absorptions in the visible and ultraviolet regions were then used for qualitative and quantitative detection of the gaseous components present.

The experimental observations are summarized in Table 10. No reactions were observed between iodine pentafluoride and bromine pentafluoride or between iodine pentafluoride and bromine trifluoride, as indicated under reactions 1 and 2.

In reaction 3, iodine pentafluoride and iodine vapors were mixed to determine whether any intermediate compound would be formed. No change was noted in the pressure or the spectra, indicating that no reaction takes place.

A mixture of iodine heptafluoride and bromine trifluoride showed no change in pressure in a 24-hour period. The partial pressure of the iodine heptafluoride, calculated from the optical absorption, did not

FIGURE 9.

ABSORPTION SPECTRA OF Br_2, BrF_3, BrF_5, IF_5, AND IF_7.

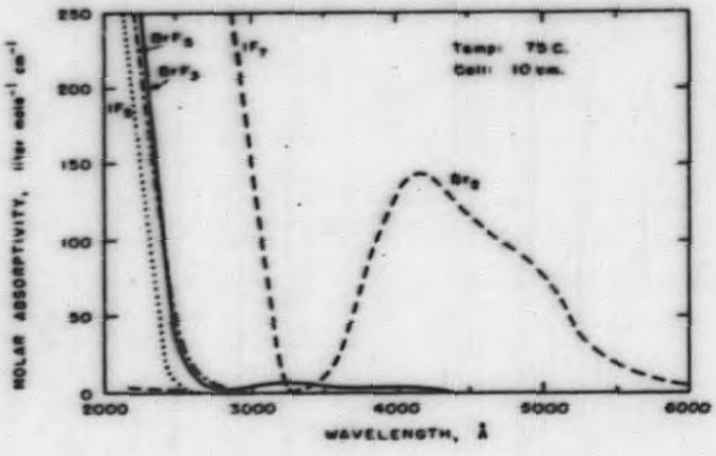

Table 10

VAPOR-PHASE REACTIONS OF IODINE PENTAFLUORIDE AND IODINE HEPTAFLUORIDE

Reaction	Reactants A	Reactants B	Initial Partial Pressure (mm) A	Initial Partial Pressure (mm) B	Temp. (C)	Change in Total Pressure (mm)	Observations of Absorption Spectra: Ultraviolet (2400-4000 Å)	Observations of Absorption Spectra: Visible (4000-6000 Å)
1	IF_5	BrF_5	69.8	70.0	77	None	No IF_7 formed	-
2	IF_5	BrF_3	54.9	55.5	77	None	No IF_7 formed	-
3	IF_5	I_2	40.3	13.5	77	None	-	Iodine present
4	IF_7	BrF_3	101.3	50.1	77	None	Very slow decrease in IF_7 concentration in absorption cell.	-
5	IF_7	I_2	101.6	12.0	77	113.1 to 126.5 (Very rapid - less than 1 min.)	Decrease in IF_7 concentration.	Iodine absent
6	IF_7	Br_2	124	21	77	145.0 to 167 (slow reduction)	Decrease in IF_7 concentration.	Bromine concentration decreased with time, disappeared in 5 hrs.
7	IF_7	Br_2	119	20.8	77	-	Decrease in IF_7 concentration.	Bromine concentration decreased with time, disappeared in 5 hrs.
8	IF_7	BrF_3	102.6	51.0	100	None	Slow decrease in IF_7 concentration.	Slow decrease in BrF_3 concentration.

change after 24 hours. When the mixture had been in the spectrophotometer cell for 90 minutes, however, the absorption curve indicated a decrease in the partial pressure of iodine heptafluoride, corresponding to 9 mm in the reaction vessel. This is listed under reaction 4.

Reaction 5, between iodine heptafluoride and iodine, was observed to occur rapidly. A spectrophotometric observation, made 20 minutes after mixing the reactants, indicated no iodine. The decrease in iodine heptafluoride, as shown by the spectra and the total pressure change, indicated that the reaction proceeds stoichiometrically according to the equation

$$5\ IF_7 + I_2 \longrightarrow 7\ IF_5 \quad . \qquad (1)$$

Iodine heptafluoride and bromine reacted at a slow rate (reaction 6). The increase in total pressure with time is given below as an indication of the rate of the reaction at 77 C.

Time After Mixing (minutes)	Total Pressure (mm)
0	145
2	150
23	161
60	165
126	167

The final total pressure for the complete conversion of bromine to bromine trifluoride is 166 mm, according to the reaction

$$3\ IF_7 + Br_2 \longrightarrow 3\ IF_5 + 2\ BrF_3 \quad . \qquad (2)$$

The optical absorption due to bromine decreased slowly until it was below the limit of detection at 5.5 hours after mixing.

In a similar experiment, 7, the iodine heptafluoride and bromine were admitted to the cell soon after mixing. If the reaction had proceeded according to equation (2), the final partial pressure of iodine heptafluoride in the reaction vessel would have been 56.6 mm. The final iodine heptafluoride suggests that some of the iodine heptafluoride may have been converted to iodine pentafluoride by oxidizing some of the bromine trifluoride to bromine pentafluoride. This is in agreement with the results of reaction 4, indicating that, at 77 C, iodine heptafluoride is capable of oxidizing bromine trifluoride to the pentafluoride at a slow rate.

Reaction 8 was performed at 100 C in order to reach a more easily measured rate. At this temperature the bromine trifluoride was slowly oxidized to the pentafluoride by iodine heptafluoride:

$$BrF_3 + IF_7 \longrightarrow BrF_5 + IF_5 \quad .$$

In a 24-hour period, approximately one-half of the original bromine trifluoride was converted to bromine pentafluoride.

B. Pilot Plant Operations

(W. J. Mecham, R. C. Liimatainen, R. W. Kessie, G. J. Vogel, G. E. Goring*)

1. Fused Salt Process for Dissolution of Fuel Alloys

a. Equipment Development

Work is continuing on the installation and testing of equipment for fused salt dissolution of zirconium-uranium fuel alloys. Initial melting and transfer of salt in the fused salt system has been made with helium as a sparge gas. The fused salt sampler was installed.

An examination of the fused salt make-up tank which failed was made by the metallography section of the Metallurgy Division. Extensive cracks apparently were produced in the forming of the dished heads. Sulfide deposits were identified in the cracks and on the inner surface of the nickel wall which was in contact with the molten fluoride.

b. Tests on the Ignition of 1020 Steel in Fluorinating Atmospheres

Since 1020 steel has been under consideration as a cheap material of construction for a disposable fluorinator in the fused salt process, it seemed desirable to determine whether or not there was a possibility of ignition at temperatures in the range of 500 to 700 C.

One-half-inch long samples of 1/4-inch OD x 0.030-inch wall 1020 steel tubing were cleaned and dried. In each run two samples were placed in a horizontal 3/4-inch OD nickel or copper tube which was heated by a resistance furnace. In all but one of the runs the unit was brought up to temperature in a helium atmosphere. The fluorinating agent was then introduced continuously at a slow rate (~100 cc/min) without the helium.

In all runs ignition was evident from the rapid rise in temperature. Also, the steel was completely fluorinated into a powder. In Run 4 (Table 11) a nickel sample of the same size as the steel was placed between the two steel samples. The nickel sample remained intact although it was covered with a heavy fluoride film.

---

*Special Scientific Employee on loan from Union Carbide Nuclear Company.

Table 11

IGNITION DATA ON 1020 STEEL

(Steel completely fluorinated to a powder in all runs.)

Test Number	Fluorinating Agent	Temp. at which Fluorinating Agent was Introduced (C)	Max. Temp. Reached During Reaction (C)	Furnace Tube	Condition of Furnace Tube after Reaction
1	F_2	650	1100	Copper	Melted and Fluorinated
2	F_2	650	960	Nickel	Intact
3	BrF_3	670	775	Nickel	Intact
4	BrF_5	655	760	Nickel	Intact
5	F_2	22	1400	Nickel	Melted

In Run 5 fluorine was introduced continuously, starting from room temperature; the temperature rose approximately 10 C/min until the steel ignited at 570 C; the temperature then increased at approximately 100 C/min. This temperature was measured by a thermocouple wired to the furnace tube near the sample position. A summary of the ignition data is given in Table 11. These data indicate that 1020 steel is not a suitable material of construction for a disposable fluorinator.

2. Fractionation of Uranium Hexafluoride-Bromine Pentafluoride Mixtures

In previous fractional distillations involving uranium hexafluoride, bromine pentafluoride and bromine trifluoride, the purity of uranium hexafluoride appears to have been limited by side reactions rather than by the relative volatilities of the above components. With bromine trifluoride present there is always the possibility of it reacting to form bromine. Since bromine trifluoride can be fluorinated with fluorine to bromine pentafluoride, it was decided to investigate the fractionation of the uranium hexafluoride-bromine pentafluoride binary system.

The still pot of a 16-foot column was charged with 48.2 lb uranium hexafluoride and 336 g bromine pentafluoride. Three runs were carried out on this charge. Initially fluorine was introduced to a total pressure of approximately 40 psia with the still pot temperature maintained slightly above the melting point of uranium hexafluoride and was left in contact for over 50 hours. The column was then operated for 54 hours on total reflux (Run C-3); in all runs the boilup rate was 46 lb uranium hexafluoride/hr

and the pressure 3 atm. The column was isolated from the still pot and the column hold-up was removed from the system as product. A similar second run (C-4) was made for 56 hr on total reflux using the remaining still pot material. Again the column hold-up was removed and, after a fluorination similar to that following the initial charge, a third run (C-5) was made at total reflux. The data obtained are shown in Figures 10, 11 and 12.

During the first two runs a light yellow or pink color could be seen in some of the overhead samples (particularly toward the end of the run). Thus it appears that corrosion of nickel is producing some elemental bromine. Also, the data in the second run suggest that some bromine trifluoride was also formed. A fourth run (C-6) was made (see Figure 13) with continuous, slow fluorine sparge in an effort to eliminate the bromine problem. No bromine color was observed in the samples from this run. The final still pot liquid from Run C-6 showed <1 ppm bromine pentafluoride: thus, the specifications on the bromine impurity were met.

FIGURE 10.
URANIUM HEXAFLUORIDE - BROMINE PENTAFLUORIDE DISTILLATION. Run C-3

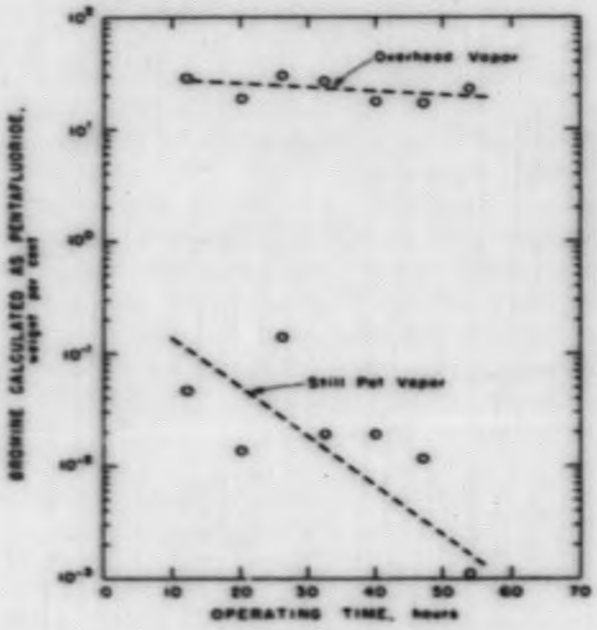

FIGURE 11.
URANIUM HEXAFLUORIDE - BROMINE PENTAFLUORIDE DISTILLATION. Run C-4

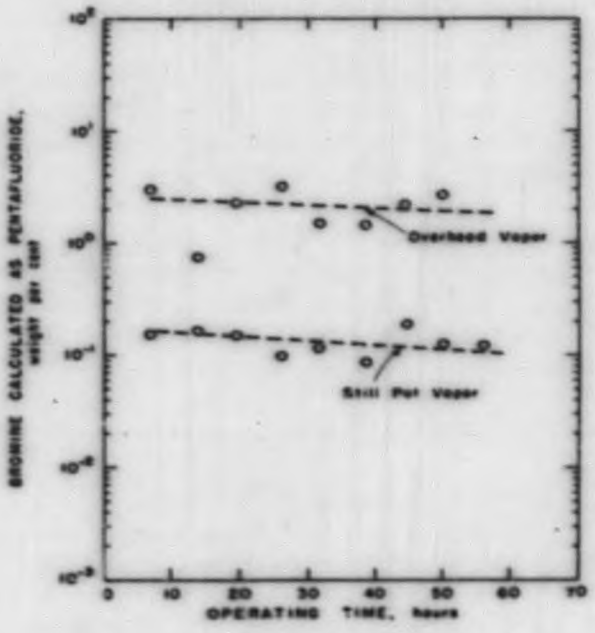

FIGURE 12.
URANIUM HEXAFLUORIDE - BROMINE PENTAFLUORIDE DISTILLATION. Run C-5

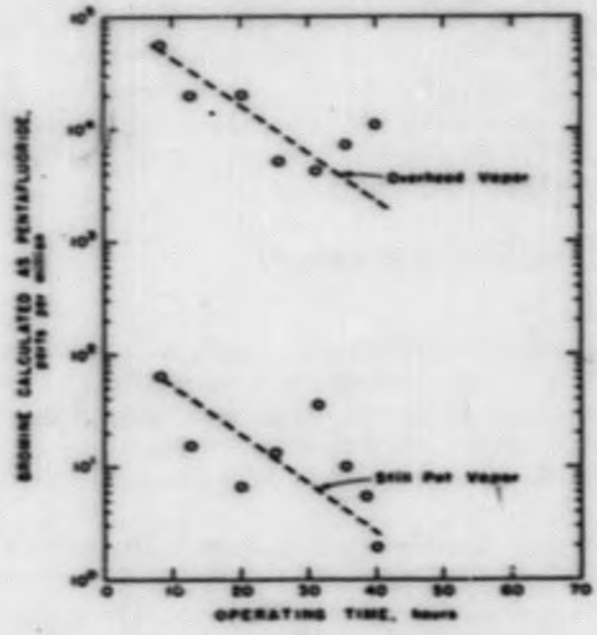

FIGURE 13.
URANIUM HEXAFLUORIDE - BROMINE PENTAFLUORIDE DISTILLATION. Run C-6
(Continuous Fluorine Bleed)

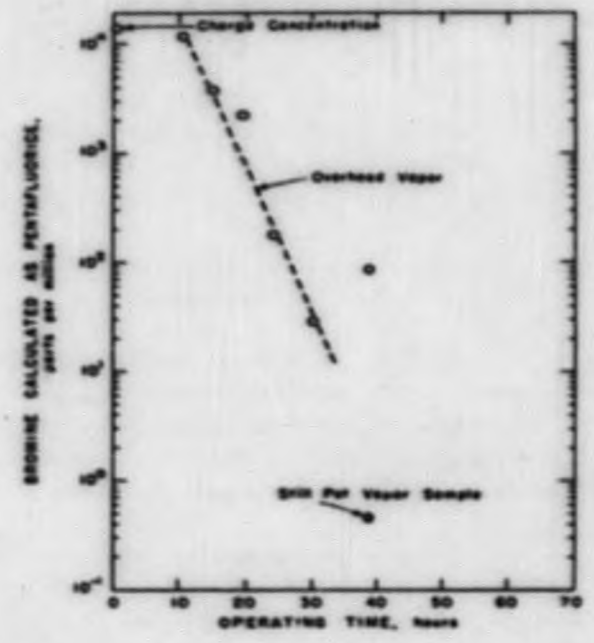

III. FLUIDIZATION

(A. A. Jonke)

Work during this quarter was directed primarily toward the installation and shakedown of new fluidized-bed equipment. More complete analytical data were obtained on the crude green salt produced from ore concentrates in runs made in the previous quarter.

The green salt pilot plant, consisting of two multistage fluidized-bed reactors with associated equipment, was completed, and several shakedown runs were made with refined uranium oxide feed. Operability was generally satisfactory, although some minor modifications are necessary. No caking was observed and green salt of good appearance was produced. Some difficulty was encountered in maintaining downcomer seals in the hydrofluorination reactor, but this condition is believed to be capable of correction.

Installation of the shielded calciner for converting radioactive waste solutions to solid oxides was about 90 per cent completed, and initial runs are planned for the next quarter.

The fundamental study of particle size distribution in fluidized beds was concluded.

Mr. H. Neumark of Allied Chemical and Dye visited Argonne October 30 to discuss fluidized-bed processing of uranium ore concentrates. On November 30 W. Burkhardt, H. Muhlhauser and C. Fetner of National Lead discussed fluidization. A conference was held with R. Walton, Jr. of AEC office, Idaho and D. Paige, Idaho Chemical Processing Plant, on December 13 to discuss waste calcination. Mr. R. Stahl of Allied Chemical and Dye visited Argonne from December 10 to 19 for an exchange of information on fluidized bed processing of uranium ore concentrates.

A. Crude Green Salt From Uranium Ore Concentrates

(N. Levitz, T. Cannon)

In the process under development for the purification of uranium ore concentrates by fractional distillation of crude uranium hexafluoride, the initial process steps involve the production of crude uranium tetrafluoride by reduction and hydrofluorination of the ore concentrates. The use of the fluidized-bed technique for crude green salt production is being investigated.

Previous studies with six different ore concentrates, one South African and five domestic, yielded encouraging results. A feed preparation step consisting of crushing and screening was necessary to convert the concentrates to a fluidizable powder. In some cases an initial agglomeration

step, which could be accomplished by continuous briquetting, was also necessary. Satisfactory conversion to crude green salt was obtained in batch, fluidized-bed experiments, and in several continuous runs.

The results of the series of batch experiments on five domestic ore concentrates were partially reported in the previous report (ANL-5633, page 63). Additional analytical data have since been obtained on the crude green salt product and are reported in Table 12, together with the analyses of the starting concentrates for comparison.

The analytical procedures for tetravalent uranium and unhydrofluorinated uranium in the crude green salt are incompletely developed at present, and the accuracy of the reported values is somewhat uncertain. The procedures developed for refined uranium compounds are not directly applicable because of the presence of impurities and the uncertain nature of the uranium compounds present. Development of improved analytical methods is being carried out.

The data in Table 12 substantiate the previously reported conclusions. The reactivity of the concentrates, as denoted by the percentage of unhydrofluorinated uranium in the crude green salt, appears to be a function of the method by which the concentrates were produced. The two Bluewater concentrates, made by diuranate precipitation and drum drying at moderate temperatures, were the most reactive, the crude green salt containing about 2 per cent of unhydrofluorinated uranium. The Uravan and Rifle concentrates, produced by diuranate precipitation and roasting at 600 C, were slightly less reactive, the crude green salt having about 8 per cent of unhydrofluorinated uranium. The Durango material, which undergoes a high temperature fusion in the final step, was least reactive, the product having 27 per cent of unhydrofluorinated uranium.

The sulfur impurity was substantially reduced by the reduction and hydrofluorination treatment, but the residual sulfur was sufficiently high to constitute a possible corrosion problem in nickel alloy equipment. The phosphorus content was substantially unchanged by the treatment. Silicon and boron were reduced to very low values, and vanadium and molybdenum were partially removed.

No additional runs were made during the past quarter because efforts were concentrated on completing the green salt pilot plant. It is planned to continue process development on crude green salt production on a pilot scale during the next quarter.

B. Green Salt Pilot Plant
(N. Levitz, E. Petkus, M. Jones, T. Cannon)

Installation of the green salt pilot plant was completed during the quarter and several shakedown runs were made.

Table 12

ANALYSES OF CRUDE GREEN SALT PRODUCED FROM ORE CONCENTRATES

(Batch Fluidized-Bed Runs. See ANL-5633, page 61 for details.)

Analyses (W/O)	Bluewater Acid Leach		Bluewater Carb Leach		Durango		Uravan		Rifle	
	Ore Conc[a]	Crude UF_4[b]	Ore Conc[a]	Crude UF_4[b]	Ore Conc[a]	Crude UF_4[b]	Ore Conc[a]	Crude UF_4[b]	Ore Conc[a]	Crude UF_4[b]
Total Uranium	72.6	68.0	63.2	59.6	71.0	64.6	64.8	60.1	66.0	62.2
U (IV)[c]	-	65.2	-	45.6	-	63.2	-	52.6	-	60.4
Unhydrofluorinated Uranium[d]	-	2.3	-	1.8	-	27	-	8.1	-	7.0
Total Fluoride	-	20.6	-	24.5	-	24.2	-	-	-	-
Sulfur	0.63	0.21	0.06	0.0035	0.75	0.06	0.64	0.06	2.41	0.20
Phosphorus	0.09	0.1	0.06	0.02	0.013	0.015	1.22	0.80	0.20	0.15
Silicon	-	0.02	-	0.02	-	0.05	-	0.01	-	0.02
Vanadium	0.03	-	0.53	0.12	0.067	-	1.99	1.07	1.62	1.2
Molybdenum	0.01	-	0.01	0.0012	0.01	-	0.07	-	0.03	0.0052
Boron	0.0005	<0.0001	0.0002	<0.0001	<0.0001	<0.0001	0.014	<0.0001	0.012	0.001

[a] Analyses by Grand Junction Operations Office.

[b] Analyses by ANL Chemical Engineering Division.

[c] Determined by reducing power analyses.

[d] Determined by analysis for uranium content of ammonium oxalate insoluble.

1. Description of the Pilot Plant

A photograph of the equipment prior to installation of the thermal insulation is shown in Figure 14, and a schematic drawing of the facility is shown in Figure 15.

The pilot plant consists of two multistage reactors, together with feeders, filters, and associated equipment. The two reactors are similar except for size and material of construction, the stainless steel reduction reactor being five inches in diameter with four stages, and the Monel hydrofluorination reactor being six inches in diameter with five stages. Each stage consists of a fluidized bed 10 inches deep supported by a perforated plate. The latter was drilled with 60° conical holes spaced on 1-inch centers and tapering to a 5/64-inch diameter opening at the bottom. The conical holes prevent stagnant solids (which might cake during reaction) from collecting on the surface of the distributor plate. To prevent downflow of solids through the perforations during shutdown a thin, perforated baffle plate is fixed one-fourth inch below the gas distributor plate. A photograph of a bed support and downcomer is shown in Figure 16.

The reactors are constructed of 2 foot long, flanged, pipe sections, bolted together, with the bed support and downcomer unit clamped between the flanges. Any number of stages can thus be connected together.

Each stage of the reactors is heated by three 1000-watt tubular heaters bonded to the reactor wall by sprayed copper metal. In addition the top stage of the hydrofluorination reactor is provided with a cooling coil, also bonded to the wall, to remove some of the heat generated in the reaction. Both reactors are insulated with three inches of preformed, asbestos insulation. Thermocouples are installed in each fluidized bed and at other appropriate points to measure heater and wall temperatures. Pressure taps and manometers indicate the amount of material on each stage.

In starting the empty reactors, it is necessary to charge enough material into each stage to seal the bottom of the downcomers, since the fluidizing gas would flow up the downcomers rather than through the beds if no seal were provided. For this initial charging operation a 1/2-inch pipe nipple is welded into the wall of each stage into which solids are charged from a small container. Once filled, the reactors can be shut down and restarted at will.

In operating the pilot plant, uranium trioxide is fed from a hopper to a screw feeder, then to a gas-lift conveyor where nitrogen gas carries the solids through a 3/8-inch OD tube to the top stage of the reduction reactor. The oxide passes downward by overflow through the downcomers, leaving at the bottom. A preheated hydrogen-nitrogen mixture,

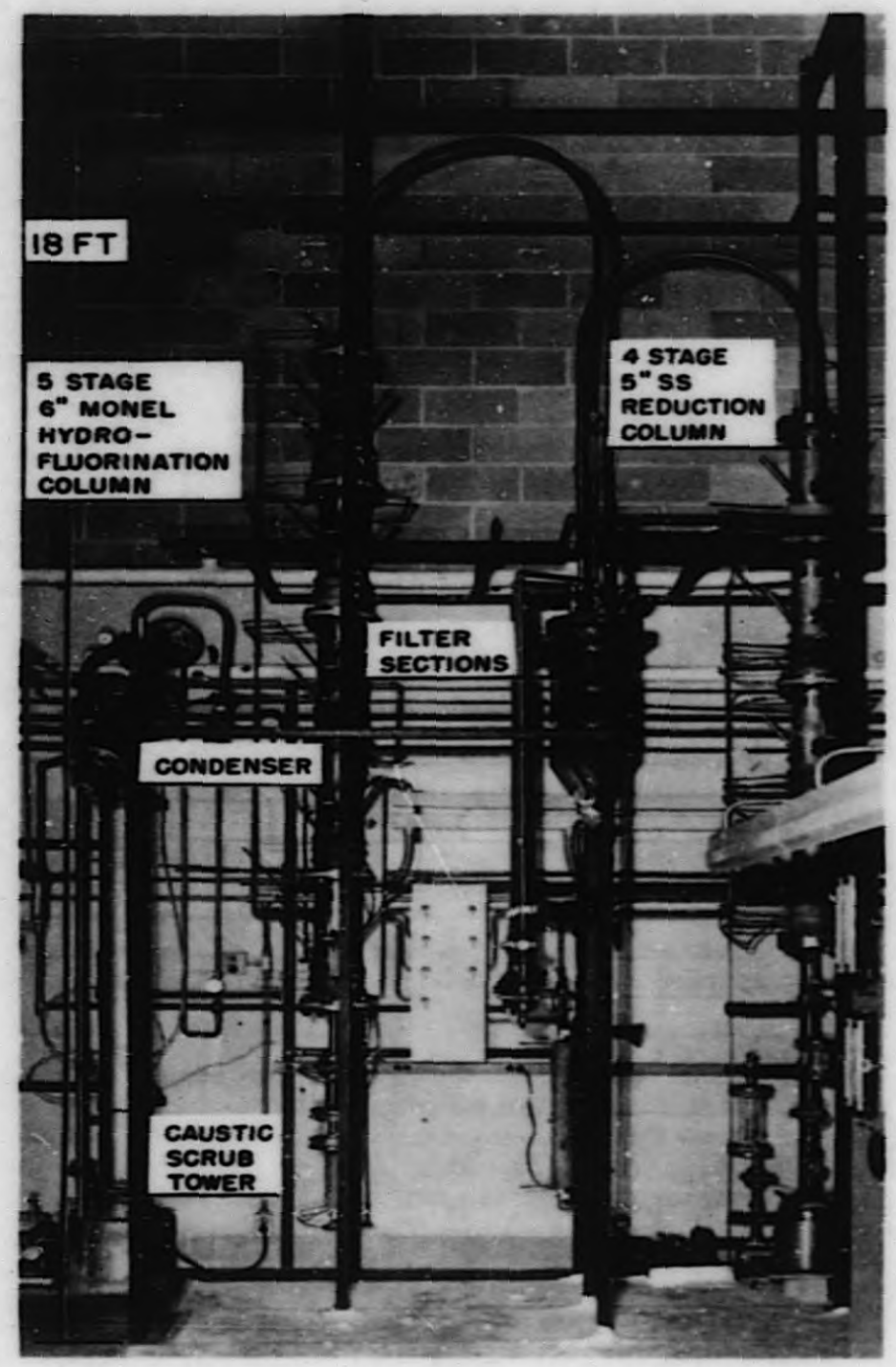

FIGURE 14

FIGURE 15

SCHEMATIC DIAGRAM OF FLUIDIZED-BED GREEN SALT PILOT PLANT

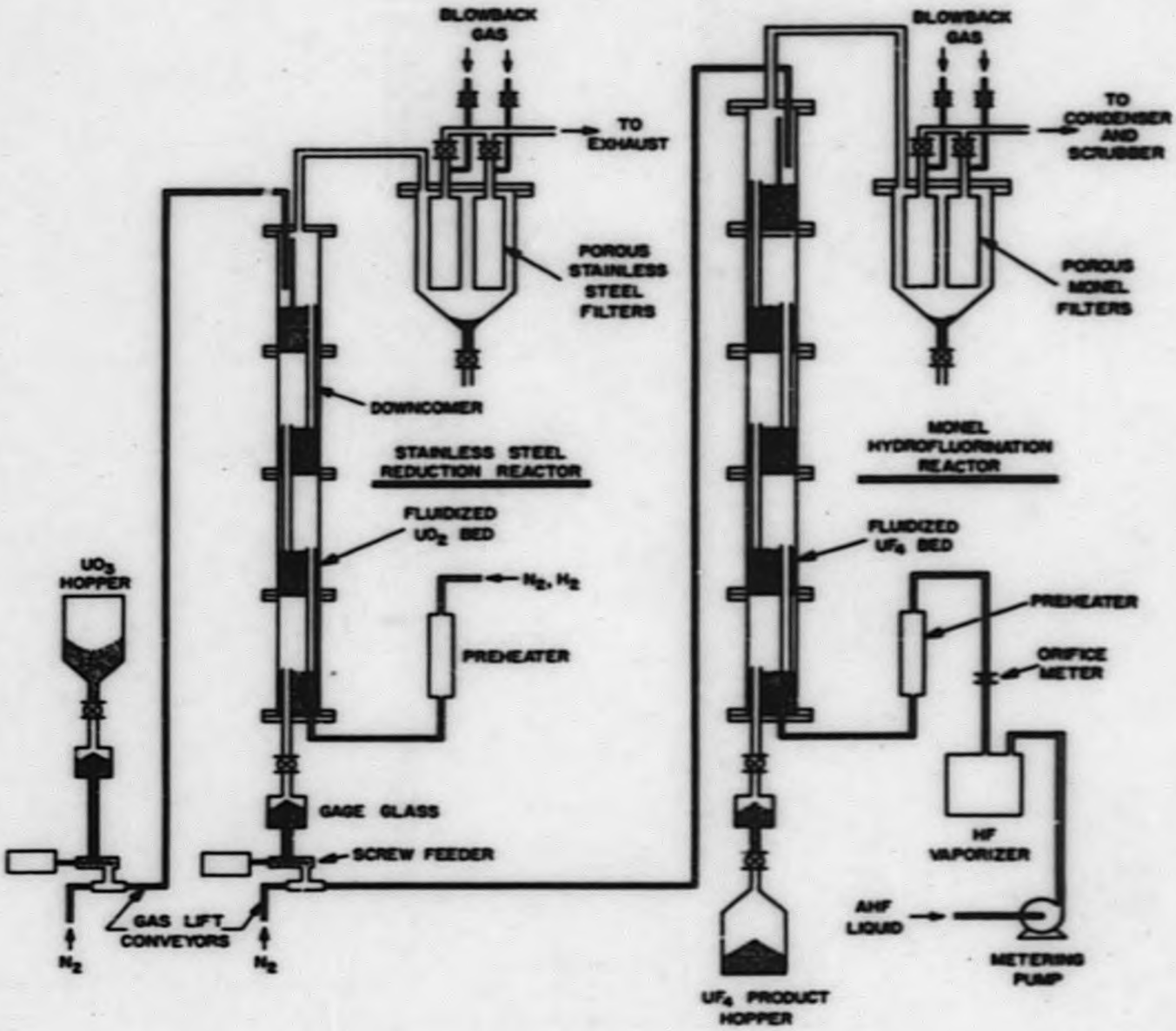

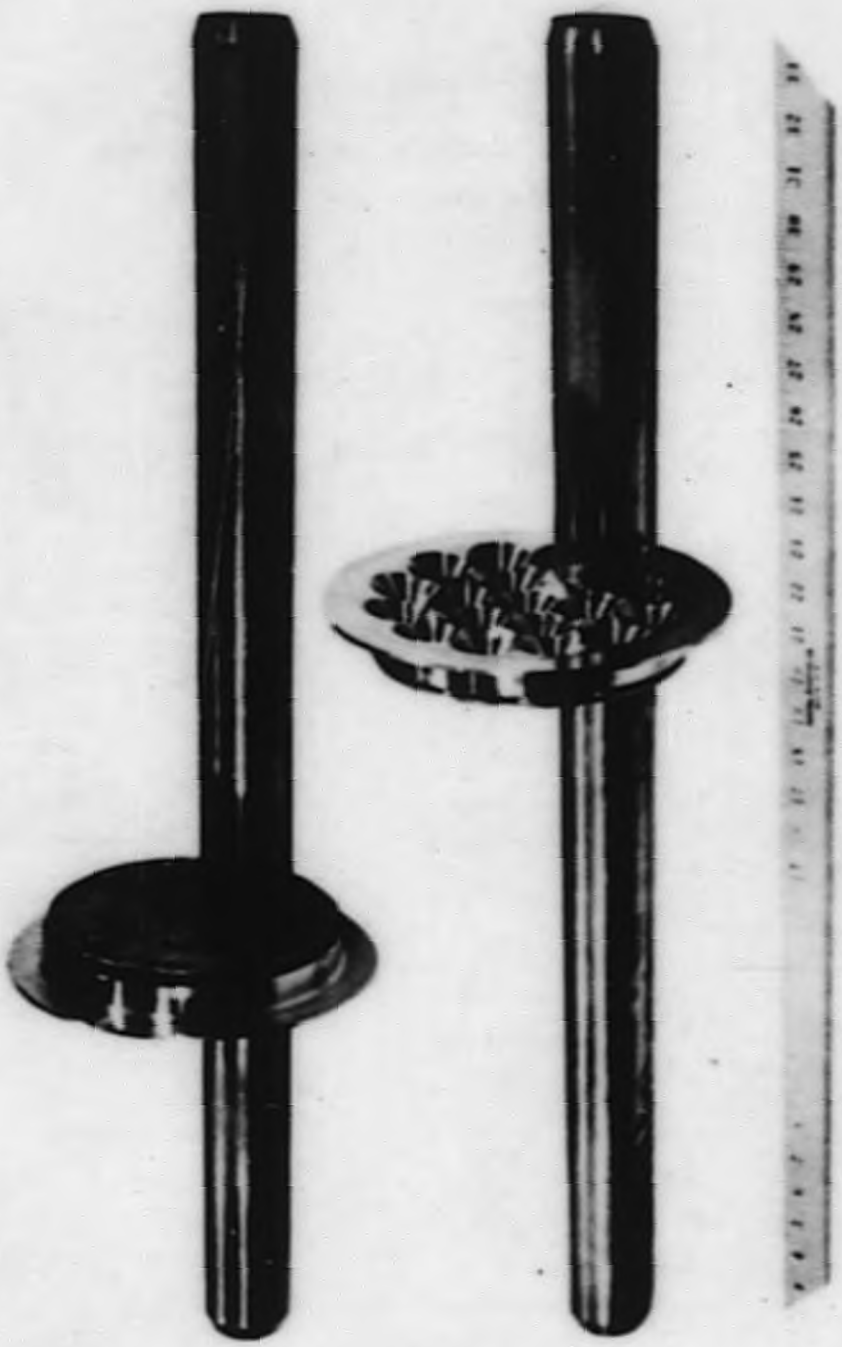

Figure 16

Bed support and downcomer of reactor in the fluidized-bed green salt pilot plant

simulating dissociated ammonia, flows upwards countercurrent to the solids flow, and, after leaving the reactor, passes to a filter chamber containing four porous, stainless steel filters, then to an air jet which dilutes the hydrogen before exhausting it to the ventilation system. The product uranium dioxide is collected in a standpipe from which it is fed by screw feeder to a second gas-lift conveyor and carried to the top stage of the hydrofluorination reactor. Liquid anhydrous hydrogen fluoride, cooled to about 5 C in a refrigerated box, is metered by a diaphragm pump to a vaporizer, then to a preheater before entering the bottom of the reactor. The off-gas is filtered through porous Monel filters, then condensed, and the uncondensed gas is finally scrubbed with caustic in a packed tower. The green salt product overflows from the bottom stage of the reactor and is collected in a hopper.

The preheaters for the reactant gas are constructed of 2-inch standard pipe, packed with Raschig rings and heated by tubular heaters bonded with sprayed copper. The hydrogen fluoride vaporizer is a small nickel tank heated by an electric mantle. The rates of flow of hydrogen fluoride are determined by weight measurements of the storage cylinders, and by orifice meter. The rates of flow of solids are determined by the measurements of the time required to feed a measured amount from a sight glass, and by weight measurements on the green salt product.

2. Design Considerations

Before the reactors were completely assembled, tests were made to determine the pressure drop across the gas distributor plates at various gas velocities. When the plates were drilled with seventeen 1/16-inch diameter openings at the bottom of the cones, the pressure drop was found to be about 39 inches of water for an air flow of 0.6-ft/sec superficial velocity in the 5-inch diameter reactor. This value was higher than desired, since it would cause the level of solids in the downcomers to be very high and might prevent downflow of solids. The holes were therefore enlarged to 5/64 inch in diameter, after which the pressure drop at 0.6-ft/sec velocity was determined to be about 16 inches of water.

Since the pressure drop across a 10-inch deep bed of fluidized, high-density uranium oxide is about 24 inches of water, the distributor pressure drop was about two-thirds of that of the fluidized bed itself. Under these conditions it is believed that good gas distribution should be obtained, and it is likely that adequate gas distribution would be obtained with even less pressure drop across the plate.

With a total pressure drop across the plate and the bed of 40 inches of water, the nominal level of solids in the downcomer for a solid whose fluidized density is 3 g/cc would be about 13 inches above the upper surface of the bed into which the downcomer feeds. However, momentary increases in gas velocity in the downcomer, such as might occur if a large pocket of gas entered the downcomer, could cause the solids to spurt considerably

above the nominal level. Moreover, the natural tendency for slugging or surging to occur in fluidized beds of large height-to-diameter ratio, such as exists in the downcomers, would also cause the level of solids to rise substantially at times. These considerations emphasize the need for adequate spacing between stages in order to maintain downcomer seals at all times.

It is worth pointing out that for solids of lower density (such as uranium ore concentrates), it may not be possible to maintain downcomer seals with the present design unless the pressure drop across the plates is reduced to maintain about the same plate-to-bed pressure drop ratio as with the high-density oxide, or unless the depth of bed on each stage is reduced. Moreover, if the operating gas velocity is greatly increased above the design velocity of approximately 0.5 ft/sec, the pressure drop across the plate will increase, causing the level of solids in the downcomers to rise. Thus any mal-operation which causes the gas flow to surge momentarily to two or three times the normal flow rate may cause a loss of downcomer seals. These considerations point to the need for additional research to determine the minimum plate pressure drop suitable for adequate gas distribution. If it is possible to use a low plate pressure drop, then a considerably greater flexibility in operating conditions could be tolerated.

By direct geometric scale-up of the design of the prototype, 3-inch diameter, multistage reactor, a bed depth of 10 inches was obtained for the pilot-scale reactors. It was decided, however, to test the reactors with a 12-inch bed depth first, and then to reduce the depth if necessary.

3. Shakedown Runs

The columns were first loaded with refined uranium trioxide having an untapped bulk density of approximately 4.0 g/cc and were operated with continuous solids feed to study the "hydraulic" behavior and solids flow characteristics. It was found in several test runs that, after a short period of satisfactory operation, the solids would cease to flow through one or more of the downcomers and the levels of solids on these stages would continually increase as long as solids were fed into the unit. Lack of solids flow could be caused either by bridging in the downcomers or by the loss of downcomer seals. The operating behavior indicated the latter condition to be the more likely.

Since the levels of solids in the downcomers could be reduced by decreasing the bed depth, it was decided to shorten the downcomers to give a 10-inch deep bed. At the same time the downcomers were shortened by one inch on the discharge end, so that the distance from the bottom of the tube to the next lower distributor plate was increased from 2 inches to 3 inches.

With these changes the reactors were satisfactorily operated for periods of 4 to 6 hours with uranium trioxide as the solid and air as the fluidizing gas. Tests were made at both room temperature and at operating temperatures.

Following these tests the uranium trioxide was removed from both reactors; uranium dioxide was charged into the reduction reactor and uranium tetrafluoride into the hydrofluorination unit. Two shakedown runs were then made under representative operating conditions; the first run was for a period of about 3 hours and the second for a period of 12 hours. The uranium trioxide used as feed was produced by fluidized-bed denitration, and represented an accumulation of oxide produced under a variety of conditions. Therefore no attempt was made in the shakedown runs to obtain data representative of the conversion to green salt which could be expected in the pilot plant. Some samples were taken, but these have not yet been analyzed. Visually, the product had the appearance of good green salt.

The following observations on mechanical operability of the equipment were made.

(1) Downflow of solids was not entirely satisfactory in the hydrofluorination reactor, since the levels of solids occasionally rose above the downcomers on one or another of the stages, and the solids ceased to flow to the next stage. This could be corrected by vibrating the column briefly with several mallet blows, but it indicated that the problem of maintaining downcomer seals was not completely solved. This condition was not observed in the reduction reactor, however, probably because of the higher density of uranium dioxide as compared to uranium tetrafluoride and because the pressure drop across the plates of this unit was lower than for the hydrofluorination reactor. The lower pressure drop was due to the lower volume flow of gas in the reduction reactor, which has the same number of holes per plate as the hydrofluorination reactor. It appears, therefore, that a slight additional enlargement of the holes in the plates of the latter reactor may be desirable.

(2) A large amount of heat was generated by chemical reaction in the second reduction stage and very little in the first stage. This indicates either that an induction period was required before the reaction occurred or that the solids feed was largely bypassing the first stage. The latter could occur if the solids flowed over the top of the inlet baffle in stage one rather than under the baffle.

It should be noted that the heat generated in the hydrofluorination reaction was almost entirely in stage one.

(3) The temperatures in the bottom stages of the reactors were not quite as easily controlled as in the other stages. In addition, the solids occasionally did not flow freely from the bottom stage discharge pipe. It is possible that these effects were due to a low gas velocity in this stage - insufficient for complete fluidization - because the inlet gases were only partially preheated (400 C) and therefore not completely expanded before entering the fluidized bed. This condition should be readily corrected by preheating to a higher temperature or by using a slightly higher gas velocity.

(4) The uranium trioxide feed rate varied from 15 to 30 lb/hr due to variations in rpm of the feed screw. This will be corrected by replacing the variable speed drive with a more reliable unit.

(5) The heat input to the hydrogen fluoride vaporizer was insufficient to evaporate the liquid at the desired rate of 9 lb/hr. An additional heater will be installed on the bottom of this vessel.

The results of the shakedown runs indicate that satisfactory operability of the pilot plant should be obtained after slight modifications are completed. It is planned next to test the equipment with uranium ore concentrates which have bulk densities about one-half that of the refined uranium oxide used in the previous tests. After satisfactory mechanical operation is achieved, several runs will be made to study crude green salt production on a pilot scale.

C. Calcination of Reactor Fuel Processing Wastes
(J. Loeding, W. Pehl, K. Pelletier)

Work during this quarter has been spent in the construction of a shielded fluidized-bed calciner for experimental studies on diluted reactor fuel processing wastes. Installation of this unit is about 90 per cent completed, and shakedown operations are scheduled to begin early in the next quarter.

Initial studies will be directed toward wastes of the type being produced at the Idaho Chemical Processing Plant. It is planned to obtain data and operational experience with radioactive wastes to aid in the design of a production-scale calciner for the ICPP. The first "hot" runs will be made with tracer-level solutions; these will be followed by work with increasingly higher activity levels, up to the maximum permitted by the 18-inch thick concrete shielding of the cell.

D. Fundamental Studies
(H. Katz)

The study of particle size distribution in fluidized beds was concluded, and a final report on this work is in preparation. No additional fundamental studies are planned for the immediate future because of a shortage of personnel.

IV. REACTOR CHEMISTRY

A. Metal Oxidation and Ignitions

(H. A. Porte, J. G. Schnizlein, R. C. Vogel, J. Bingle, D. Fischer, A. Porter)

The frequency and severity of ignitions and explosions[6] involving uranium, zirconium, thorium and plutonium are great enough to constitute a serious hazard. Increased efforts to understand the factors governing their pyrophoric nature are demanded by the increased use of these metals. It is likely that conditions which accelerate their oxidation will lower the ignition temperature and increase the possibility of spontaneous ignition. Thus, an understanding of the kinetics of oxidation and the mechanism of the reaction should help to predict when these metals will be unusually sensitive to spontaneous ignition. The great variation of reported rates of oxidation of pure uranium was previously pointed out. The reasoning behind the experimental approach for this program is outlined in ANL-5494, pages 104 to 109.

Although the data available on zirconium oxidation do not show as great a variation as those for uranium, there are still several unresolved disagreements. A summary of the literature data for zirconium has been presented in ANL-5602, pages 77 through 86. Experimental work on zirconium has just started.

A literature search on the oxidation kinetics of thorium and plutonium is now underway.

1. Uranium

The major effort this past quarter has been devoted to the establishment of the base line data in order to appraise critically the influence of specific variables on the oxidation and pyrophoric properties of uranium metal.

a. Apparatus Modification and Standard Run

After comparison of data of the first stage of uranium oxidation given in ANL-5633, page 81, with more recent data, the presence of a factor due to the apparatus was suspected. Blank runs without a metal sample present were made early in the investigation. These showed that the apparatus was giving dependable data. However, more recent blank runs showed that the apparatus (described in ANL-5602) behaved incorrectly and indicated that a small amount of oxygen was consumed during the first few

[6] Smith, R. B., "Pyrophoricity, A Technical Mystery Under Vigorous Attack," Nucleonics 14, No. 12, 28-33 (December 1956).

minutes of a run. Various experiments demonstrated the cause to be centered in the slant-tube mercury manometer used as a pressure regulator. The difficulty was probably caused by mercury erratically "sticking" to the glass wall in the slant tube.

Because no metal oxidation rate is sufficiently well defined to be used as a standard, a standard type of run was achieved by the use of a leak. This leak was constructed by sealing a 19-gauge copper wire, about five cm long, inside a Pyrex tube. On cooling, the difference in coefficients of expansion of copper and Pyrex caused the appearance of a very small annular-shaped space which allowed gas to escape at a slow rate. The leak was attached to the apparatus in place of the sample chamber and the other side of the leak was connected to a vacuum pump. Such a home-made leak gave variable rates, but the leak would be linear with time. When the leak was used with the vertical tube mercury pressure regulator it was demonstrated that the apparatus was behaving properly. The same kind of leak has been used on three different sets of apparatus and has given identical leak rates within the errors of measurement.

b. Base Line Oxidation Data

As reported in ANL-5602, pages 71 to 77, and ANL-5633, page 81, the oxidation of uranium has been found to take place in two stages. At temperatures below 200 C and at all pressures the second stage is linear. Above 200 C it appears that the rate of the second stage reaches a maximum and then falls off. This is shown in Figure 23, page 77, ANL-5602. During the early phases of the investigation the rate law of the first stage was in doubt. However, when runs were made with a vertical tube pressure regulator it became apparent that the first stage was also linear. These runs were carried out over the ranges of pressures from 20 to 800 mm and of temperatures from 125 to 250 C - a total of fourteen additional runs under eleven sets of conditions. This further study showed that the erroneous data collected during the first few minutes of the early base line runs made with the slant tube pressure regulator could be corrected. This has been done and an essentially complete set of the data for uranium oxidation is presented in Tables 13, 14, 15, and 16. Figure 17 shows a graphical presentation of a typical run with an illustration of the manner of calculating the data.

The oxidation behavior of uranium at various temperatures and pressures can be further defined by indicating the time and amount of oxygen consumed by the sample when the transition occurs from the first stage to the second stage. The method of selection of these data is somewhat arbitrary. The method which seems most reasonable at the present time is demonstrated in Figure 17. The data for the break weights and break time are also presented in Tables 13, 14, 15, and 16. It is also thought likely that the break weight, which is related to film thickness is the more fundamental quantity.

Table 13

OXIDATION OF URANIUM IN 20 mm OXYGEN PRESSURE

Analytical, metallurgical, and surface preparation data given in ANL-5602, pages 67 to 71.

	First Stage Rate			Second Stage Rate			Break Weight[a]			Break Time[a]		
Temp (C)	μg/sq cm	Avg Dev Mean (%)	No. of Runs	μg/sq cm	Avg Dev Mean (%)	No. of Runs	μg/sq cm	Avg Dev Mean (%)	No. of Runs	min	Avg Dev Mean (%)	No. of Runs
125	0.026	38	2	0.11	12	3	30	40	2	1180	4.6	2
150	0.073	34	3	0.47	8.3	3	27	37	3	384	7.8	3
200	0.31	23	5	3.5	18	4	42	7.1	4	148	30	4
250	1.1	9.3	3	10[b]	17	3	82	6.1	3	77	13	3

[a]Intersection of extrapolated first and second stage rate (see text).

[b]Rate decreases near the end of the run.

Table 14

OXIDATION OF URANIUM IN 50 mm OXYGEN PRESSURE

Analytical, metallurgical, and surface preparation data given in ANL-5602, pages 67 to 71.

	First Stage Rate			Second Stage Rate			Break Weight[a]			Break Time[a]		
Temp (C)	μg/sq cm	Avg Dev Mean (%)	No. of Runs	μg/sq cm	Avg Dev Mean (%)	No. of Runs	μg/sq cm	Avg Dev Mean (%)	No. of Runs	min	Avg Dev Mean (%)	No. of Runs
125	0.029	6.9	2	0.13	4.8	3	18	17	2	630	13	2
150	0.086	28	5	0.59	4.6	5	29	24	5	320	16	5
200	0.39	25	5	5.1	3.5	6	35	17	5	90	7.8	5
250	1.4	4.4	4	18[b]	11	4	69	23	4	52	21	4

[a]Intersection of extrapolated first and second stage rates.

[b]Rate decreases near the end of the run.

Table 15

OXIDATION OF URANIUM IN 200 mm OXYGEN PRESSURE

Analytical, metallurgical and surface preparation data given in ANL-5602, pages 67 to 71.

	First Stage Rate			Second Stage Rate			Break Weight[a]			Break Time[a]		
Temp (C)	μg/sq cm	Avg Dev Mean (%)	No. of Runs	μg/sq cm	Avg Dev Mean (%)	No. of Runs	μg/sq cm	Avg Dev Mean (%)	No. of Runs	min	Avg Dev Mean (%)	No. of Runs
125	0.032	31	3	0.11	15	3	19	21	3	570	25	3
150	0.11	18	5	0.60	8.5	6	38	21	5	360	23	5
175	0.25	26	3	1.8	19	3	28	14	3	120	14	3
200	0.49	6.9	8	6.6	9.7	9	57	28	8	120	25	8
225	1.1	12	2	14[b]	9.9	2	58	10	2	46	22	2
250	3.2	47	7	32[b]	13	8	62	31	7	25	32	7
275	7.0	11	3	55[b]	23	3	145	20	3	21	10	3
295	10	32	3	71[b]	3.4	3	170	22	3	19	16	3

[a]Intersection of extrapolated first and second stage rates.

[b]Rate decreases near the end of the run.

Table 16

OXIDATION OF URANIUM IN 800 mm OXYGEN PRESSURE

Analytical, metallurgical and surface preparation data given in ANL-5602, pages 67 to 71.

	First Stage Rate			Second Stage Rate			Break Weight[a]			Break Time[a]		
Temp (C)	μg/sq cm	Avg Dev Mean (%)	No. of Runs	μg/sq cm	Avg Dev Mean (%)	No. of Runs	μg/sq cm	Avg Dev Mean (%)	No. of Runs	min	Avg Dev Mean (%)	No. of Runs
150	b			0.54	4.4	2	b			b		
200	0.81	36	3	8.2	3.4	4	62	8.1	3	89	26	3
250	5.8	25	2	40[c]	1.8	2	80	48	2	15	33	2
295	b			225[c]		1	b			b		

[a]Intersection of extrapolated first and second stage rates.

[b]Unable to distinguish satisfactorily to date.

[c]Rate decreases.

Temperature Dependence of the Linear First Stage Rate: Arrhenius plots of first stage rate are shown in Figures 18, 19, and 20. The data points denoted by circles indicate the mean value of the first stage rate and the bar represents the average deviation from the mean. It is not appropriate to present an Arrhenius plot for the experiments at 800 mm since data are available for only two temperatures. The data for the first stage rates at the various pressures were fitted to an Arrhenius equation of the type $\log k = \log A - (\Delta E/2.303\ RT)$ by the method of least squares. The measured values of the rate and temperature for each run were used in the least square calculations, whereas averages of rates and rounded-off temperatures are presented in Tables 13, 14, 15, and 16. The resulting equations, in which k is the linear rate constant for the first stage are as follows:

$\log k = 5.2260 - 2.719 \times 10^3\ (1/T)$ for 20 mm

$\log k = 5.3825 - 2.747 \times 10^3\ (1/T)$ for 50 mm

$\log k = 6.7234 - 3.288 \times 10^3\ (1/T)$ for 200 mm .

From these data the activation energies ΔE with their standard deviations and the constants, A, are the following:

$\Delta E = 12.4 \pm 0.9$ kcal ; $A = 1.7 \times 10^5$ μg/sq cm-min for 20 mm

$\Delta E = 12.6 \pm 0.7$ kcal ; $A = 2.4 \times 10^5$ μg/sq cm-min for 50 mm

$\Delta E = 15.0 \pm 0.6$ kcal ; $A = 5.3 \times 10^6$ μg/sq cm-min for 200 mm .

It is clear that the activation energy has a pressure dependence. The theoretical significance of this is not clear at this time.

Pressure Dependence of Linear First Stage Rate: The influence of pressure on the rate during the first stage is shown in Figure 21. If one assumes a dependence of the data on pressure according to the equation

$$\text{First Stage Rate} = kP^{\alpha} \quad ,$$

the values of α are:

0.09 at 125 C
0.18 at 150 C
0.21 at 200 C
0.5 at 250 C .

It is apparent that the effect of pressure is greater at higher temperatures.

FIGURE 17.

RATE DETERMINING DATA FOR A TYPICAL URANIUM OXIDATION RUN. (150 C and 50 mm oxygen pressure)

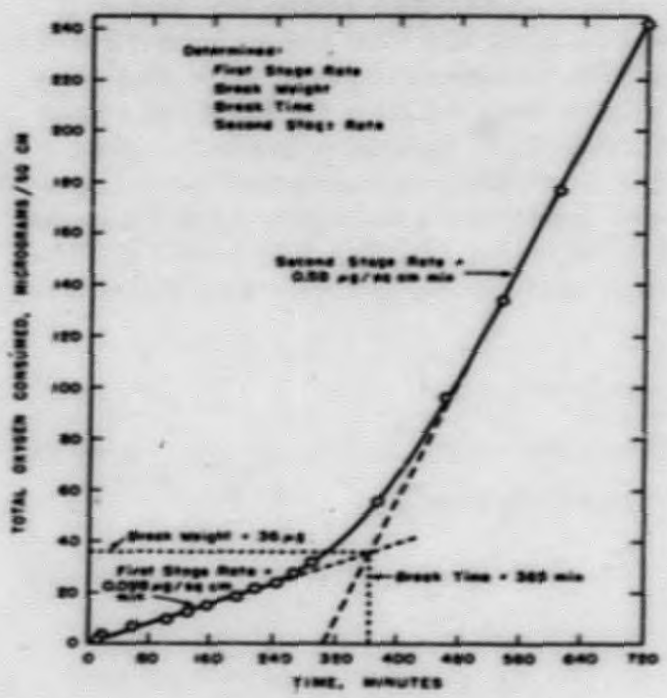

FIGURE 18.

ARRHENIUS PLOT OF FIRST STAGE RATE vs. INVERSE TEMPERATURE 20 mm OXYGEN PRESSURE

(Average deviation from the mean are indicated by the bar above and below the average point)

$\Delta E_{(act)}$ = 12.4 ± 0.9 kcal

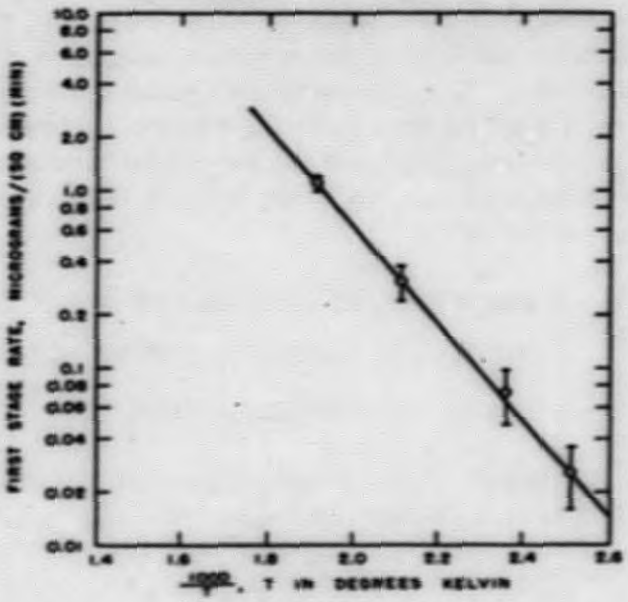

FIGURE 19.

ARRHENIUS PLOT OF FIRST STAGE RATE vs. INVERSE TEMPERATURE 50 mm OXYGEN PRESSURE

(Average deviation from the mean are indicated by the bar above and below the average point)

$\Delta E_{(act)}$ = 12.6 ± 0.7 kcal

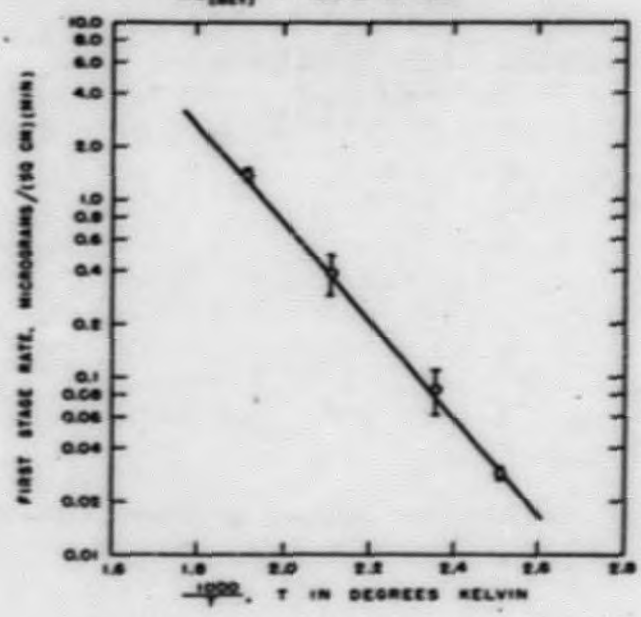

FIGURE 20.

ARRHENIUS PLOT OF FIRST STAGE RATE vs. INVERSE TEMPERATURE 200 mm OXYGEN PRESSURE

(Average deviation from the mean are indicated by the bar above and below the average point)

$\Delta E_{(act)}$ = 15.0 ± 0.6 kcal

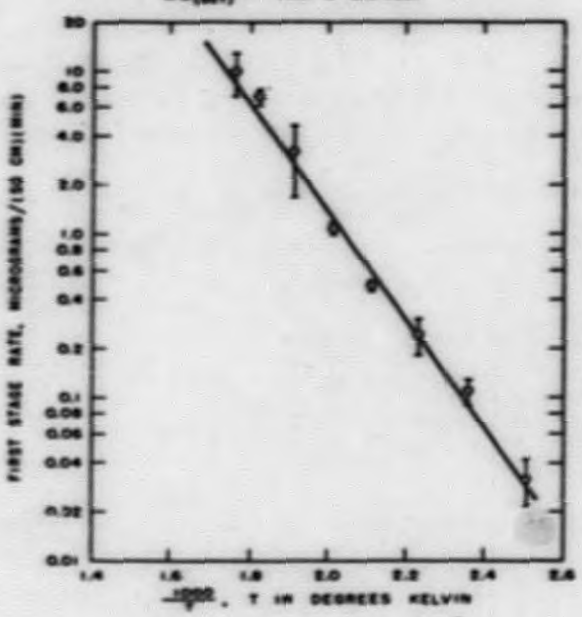

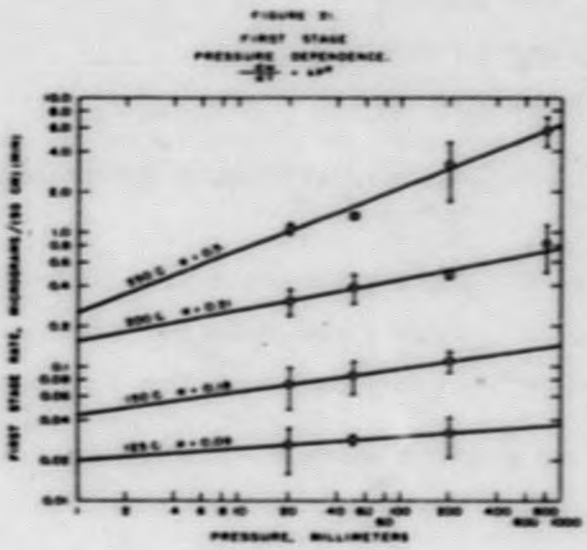

Temperature Dependence of the Break Weight: In earlier reports it was indicated that the break weight was independent of the run temperature. Carrying out more runs and obtaining the rate law for the first stage has permitted a more exact evaluation of the data. It is now clear that the break weight is not constant, but increases from about 25 μg/sq cm to 70 μg/sq cm as the temperature increases from 125 to 250 C. Perhaps the break from the first to the second stage is due to a cracking or blistering of an oxide film. If this is eventually proven to be true, the temperature dependence of the break weight may be related to the variation of the strength of the oxide with temperature and rate of formation. The break weight does not appear to be a function of pressure.

Temperature Dependence of Second Stage Rate: At temperatures of 200 C and less the rate of the second stage is linear for a considerable period of time. At temperatures over 200 C the rate goes through a maximum after approximately 1000 μg/sq cm oxygen are consumed and then decreases. At 295 C in 200 mm oxygen a second maximum is observed. The trend of these data is shown in ANL-5602, page 77, Figure 23. Experiments conducted at 200 C or less, for unusually long periods of time showed a slight decrease in rate after approximately 1500 μg/sq cm oxygen was consumed.

Arrhenius plots of the rates for the linear portion of the second stage are shown in Figures 22, 23, and 24. The data points denoted by circles indicate the mean value of the first stage rate and the bar represents the average deviation from the mean. The maximum rate is also shown in these figures at the higher temperatures, but these data were not used in the determination of the activation energy. The data for the second stage rates at the various pressures were fitted to an Arrhenius equation of the type $\log k = \log A - (\Delta E/2.303\ RT)$ by the method of least squares. The measured values of the rate and temperature for each run were used in the least squares calculations, whereas averages of rates and rounded-off temperatures are presented in Tables 13, 14, 15, and 16. The resulting equations in which k is the linear rate constant for the second stage are as follows:

$\log k = 8.3184 - 3.678 \times 10^3 (1/T)$ for 20 mm

$\log k = 9.1290 - 3.979 \times 10^3 (1/T)$ for 50 mm

$\log k = 10.0126 - 4.353 \times 10^3 (1/T)$ for 200 mm .

From these data the activation energies ΔE with their standard deviations and the constants, A, are as follows:

$\Delta E = 16.8 \pm 0.7$ kcal ; $A = 2.1 \times 10^8$ μg/sq cm-min for 20 mm

$\Delta E = 18.2 \pm 0.3$ kcal ; $A = 1.4 \times 10^9$ μg/sq cm-min for 50 mm

$\Delta E = 19.9 \pm 0.5$ kcal ; $A = 1.0 \times 10^{10}$ μg/sq cm-min for 200 mm .

It is clear that there is a variation of the activation energy with pressure similar to that for the first stage.

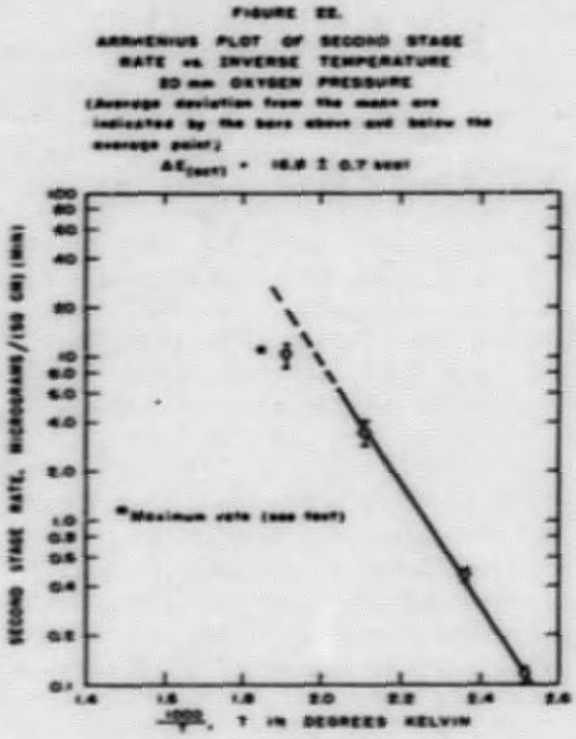

FIGURE 22.

ARRHENIUS PLOT OF SECOND STAGE RATE vs. INVERSE TEMPERATURE 20 mm OXYGEN PRESSURE

(Average deviation from the mean are indicated by the bars above and below the average point)

$\Delta E_{(av)}$ = 16.8 ± 0.7 kcal

SECOND STAGE RATE, MICROGRAMS/(100 CM²) (MIN)

*Maximum rate (see text)

$\frac{1000}{T}$, T IN DEGREES KELVIN

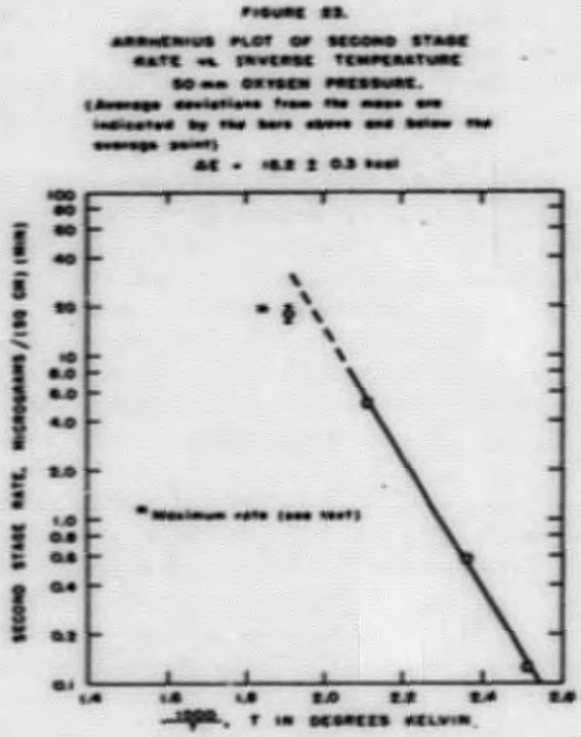

FIGURE 23.

ARRHENIUS PLOT OF SECOND STAGE RATE vs. INVERSE TEMPERATURE 50 mm OXYGEN PRESSURE.

(Average deviations from the mean are indicated by the bars above and below the average point)

ΔE = 18.2 ± 0.3 kcal

SECOND STAGE RATE, MICROGRAMS/(100 CM²) (MIN)

*Maximum rate (see text)

$\frac{1000}{T}$, T IN DEGREES KELVIN

Pressure Dependence of Second Stage Rate: The influence of pressure on the second stage rate is shown in Figure 25. If one assumes a dependence of the data on pressure according to the equation

Second Stage Rate = kP^{α} ,

it can be seen that α has the following approximate values:

Temp (C)	α
125	0
150	0.04
200	0.19
250	0.4 (Maximum rates)

It can be seen that at 125 and 150 C the pressure dependence is small, while at 200 C it is considerably greater. For linear rates at 200 C and the maximum rates at 250 C the pressure dependence is very nearly the same for both first and second stage rates.

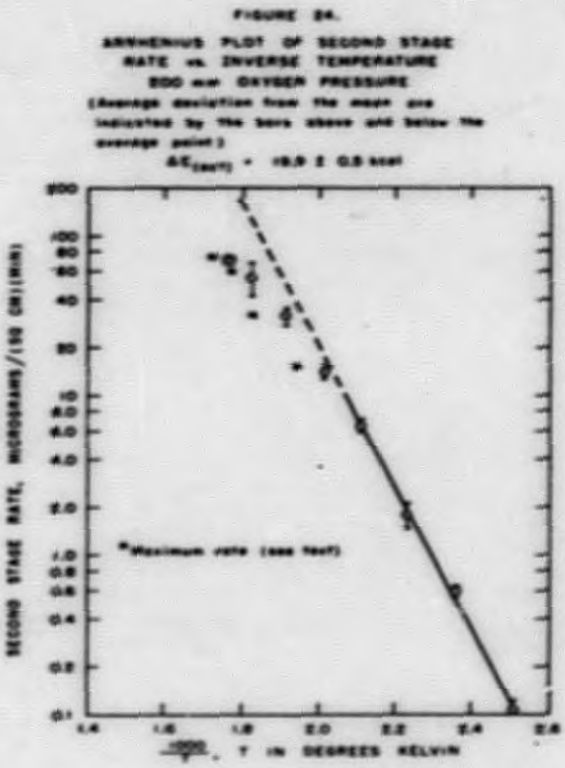

FIGURE 24.
ARRHENIUS PLOT OF SECOND STAGE RATE vs. INVERSE TEMPERATURE
200 mm OXYGEN PRESSURE
(Average deviation from the mean are indicated by the bars above and below the average point.)
$\Delta E_{(act)}$ = 19.9 ± 0.5 kcal
SECOND STAGE RATE, MICROGRAMS/(150 CM)(MIN)
*Maximum rate (see text)
$\frac{1000}{T}$, T IN DEGREES KELVIN

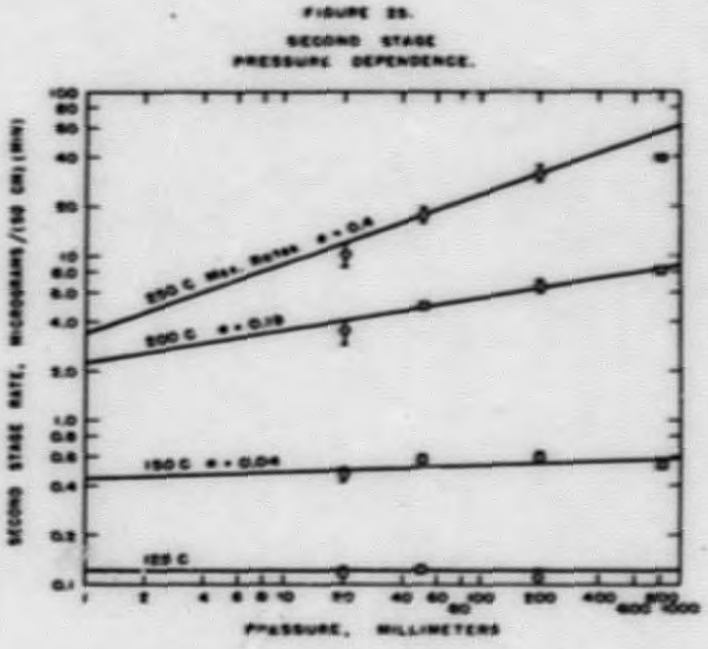

FIGURE 25.
SECOND STAGE PRESSURE DEPENDENCE.
SECOND STAGE RATE, MICROGRAMS/(150 CM)(MIN)
250 C MAX. RATES α = 0.4
200 C α = 0.19
150 C α = 0.04
125 C
PRESSURE, MILLIMETERS

c. Metallurgical Variables

Samples of the same base metal with different metallurgical histories were available. These were: (1) cast, (2) rolled (less than 50% reduction of cross-sectional area), (3) high-alpha quenched and (4) beta quenched. All the base-line data have been collected using the beta-quenched metal. The data from experiments performed on these samples at a few temperatures and pressures are presented in Tables 17, 18, and 19; they

Table 17

OXIDATION RATE DATA OF URANIUM WITH VARIED METALLURGICAL HISTORY IN 200 mm OXYGEN PRESSURE AT 150 C

Analytical and surface preparation data the same as for base line beta-quenched metal which are given in ANL-5602, pages 67 to 71.

Metallurgical History	First Stage Rate			Second Stage Rate			Break Weight[a]			Break Time[a]		
	μg eq cm	Avg Dev Mean (%)	No. of Runs	μg eq cm	Avg Dev Mean (%)	No. of Runs	μg eq cm	Avg Dev Mean (%)	No. of Runs	min	Avg Dev Mean (%)	No. of Runs
Cast	0.074	9.5	2	0.32	20	2	35	2.9	2	481	12	2
Rolled	0.087	4.0	2	0.43	2.1	2	36	0.0	2	413	4.6	2
α Quenched	0.081	5.6	2	0.37	22	2	39	9.1	2	485	11	2
β Quenched[b]	0.11	18	5	0.60	8.5	6	38	21	5	360	23	5

[a]Intersection of extrapolated first and second stage rates.

[b]See base line data.

Table 18

OXIDATION RATE DATA OF URANIUM WITH VARIED METALLURGICAL HISTORY IN 200 mm OXYGEN PRESSURE AT 200 C

Analytical and surface preparation data the same as for base line beta-quenched metal which are given in ANL-5602, pages 67 to 71.

Metallurgical History	First Stage Rate			Second Stage Rate			Break Weight[a]			Break Time[a]		
	μg eq cm	Avg Dev Mean (%)	No. of Runs	μg eq cm	Avg Dev Mean (%)	No. of Runs	μg eq cm	Avg Dev Mean (%)	No. of Runs	min	Avg Dev Mean (%)	No. of Runs
Cast	1.01	0.5	2	5.0	1.8	2	70	0.7	2	69	1.4	2
Rolled	0.50	32	2	6.2	0.3	2	49	20	2	102	14	2
α Quenched	0.57	25	3	5.9	9.5	3	50	14	3	92	16	3
β Quenched[b]	0.49	6.9	8	6.6	9.7	9	57	28	8	120	25	8

[a]Intersection of extrapolated first and second stage rates.

[b]See base line data.

Table 19

OXIDATION RATE DATA FOR URANIUM WITH VARIED METALLURGICAL HISTORY IN 200 mm OXYGEN PRESSURE AT 250 C

Analytical and surface preparation data the same as for base line beta-quenched metal which are given in ANL-5602, pages 67 to 71.

Metallurgical History	First Stage Rate			Second Stage Rate			Break Weight[a]			Break Time[a]		
	μg eq cm	Avg Dev Mean (%)	No. of Runs	μg eq cm	Avg Dev Mean (%)	No. of Runs	μg eq cm	Avg Dev Mean (%)	No. of Runs	min	Avg Dev Mean (%)	No. of Runs
Cast	2.5	-	1	23[c]	-	1	86	-	1	36	-	1
Rolled	4.4	0	2	26[c]	6.4	2	135	14	2	30	15	2
α Quenched	3.7	43	2	38[c]	27	2	112	8	2	37	32	2
β Quenched[b]	3.2	47	7	32[c]	13	8	62	31	7	25	32	7

[a]Intersection of extrapolated first and second stage rates.

[b]See base line data.

[c]Rate decreases.

show very little or no systematic difference. Because the "as rolled" sample had not been subjected to a large enough reduction of area to achieve maximum orientation, a new sample will be prepared with a very high degree of rolling orientation.

d. Proposed Studies

Plans are underway to study (1) the influence of hydrogen in the metal, (2) the influence of certain alloying agents in small concentrations, and (3) the ignition temperature directly.

Equipment which will make it possible to observe the sample directly with a microscope while measuring the oxidation rates has been ordered. It is hoped that these and other types of observations will lead to an understanding of the change in oxidation rate from the first stage to the second stage.

2. Zirconium

The apparatus which will be used in the study of the rate of oxidation of zirconium has been completed. It is essentially the same type of apparatus which has been used in the uranium oxidation studies (ANL-5602, pages 65 to 77).

One of the important phases of the zirconium program will be the determination of the effect of impurities on the rate of oxidation. In this regard, an order has been placed for a series of binary zirconium alloys.

At present, a series of runs has been initiated on pure zirconium (arc melted, grade I crystal bar) to establish base line data at various temperatures and pressures with which the alloys may be compared. Since the literature data are in reasonable agreement, it is hoped that a less extensive series of experiments than for uranium will suffice.

3. Thorium

On September 22, 1956, a spontaneous fire occurred in a shipment of 1-inch diameter, half-inch thick, thorium pellets. The pellets were contained in a plastic bag which was sealed at the top and then had been placed in a rather heavy gauge metal drum.

A chemical and spectrochemical analysis has been made on undamaged thorium similar to that which burned. These data are given in Table 20.

A literature search on the kinetics of thorium oxidation is being made to aid program planning.

Table 20

ANALYSIS OF THORIUM PELLETS

Element[b]	ppm	Element	ppm
Ag	2	Mn	20
Al	2000	N[a]	247
B	100	Na	50
C[a]	2100	Ni	5
Ca	400	O[a]	4900
Cu	5	Pd	200
Fe	500	Si	800
H[a]	396		
Mg	30		

[a]Chemical analysis for C, O, N, H; all other elements analyzed by spectrochemical analysis.

[b]The following elements were less than their listed limit of detection:
As 10, Ba 5, Be 1, Bi 1, Ce 1000, Co 5, Dy 200, Er 200, Eu 100, Gd 500, Ho 1000, K 20, Li 1, Lu 100, Mo 20, Nd 500, P 50, Pr 1000, Sb 1, Sc 50, Sm 1000, Sn 5, Sr 100, Tb 1000, Ti 100, Tm 500, V 20, W 200, Y 50, Yb 50, Zn 50.

B. The Yield of Cesium-137 in Fast Neutron Fission of Uranium-235 and Plutonium-239
(C. Crouthamel, P. Kafalas, D. Stupegia, R. R. Heinrich, B. Tani)

The yield of cesium-137 for fast fission of uranium-235 and plutonium-239 has been determined and the results have been written in final manuscript form which is being reviewed in our Division prior to being submitted for publication in the Journal of Inorganic and Nuclear Chemistry.

C. Determination of Alpha, the Ratio of Capture to Fission Cross Sections, in EBR I
(P. Kafalas, M. Levenson, C. M. Stevens,* D. C. Stupegia, M. Homa, G. McCloud, F. Ferry)

The determination of alpha for uranium-235 and plutonium-239 in EBR-I has also been completed. A manuscript will be submitted to Nuclear

*Special Materials Division, responsible for mass spectrometric analysis.

Science and Engineering for publication. The determination of alpha for uranium-238 in EBR-I is in progress. The burn-up determinations are completed and the only remaining work is the determination of the capture events (plutonium-239). It was necessary to prepare plutonium-236 for use as a tracer in the alpha pulse analysis of plutonium-239. This has been accomplished by a deuteron bombardment of a target of enriched uranium-235. Sufficient plutonium-236 has now been isolated to complete this work.

Samples of uranium-233 which were also exposed throughout the EBR-I are now being analyzed to obtain the burn-up patterns in the reactor for this isotope. No capture data will be obtained on these samples because of the original high uranium-234 content. This will then complete the analysis of samples irradiated in the last EBR-I run.

V. CHEMICAL-METALLURGICAL SEPARATION PROCESSES

A study of the kinetics of uranium-ceramic oxide reactions is being carried out with high purity uranium and uranium alloys. Studies have been made of beryllia-uranium and zirconia-uranium systems. The reaction of beryllia with uranium shows that the rate of beryllium pickup increases with exposure time. Zirconium pickup in uranium is too small to permit kinetic studies. Additional tests of the effect of adding alloying agents on the corrosion of alumina, beryllia and thoria by uranium have been made.

Experiments to determine the removal of cerium from "fissium" alloys by melt refining have been made in ceramic oxide crucibles. The "fissium" alloys contained cerium, ruthenium, molybdenum, palladium and zirconium in various combinations. Various degrees of cerium removal were accomplished in the ceramic oxide crucibles tested. Magnesia removes cerium effectively and shows the best resistance to cracking by thermal shock or chemical reaction.

A sessile drop method is being used to measure the physical properties of liquid uranium, including its density and surface tension. The surface tension of uranium at about 1250 C is 825 ± 83 dynes/cm and its work of adhesion to five stable ceramic materials having close packed oxygen anion surfaces is 240 ± 50 ergs/sq cm.

The preparation of the compound $2CaO \cdot 3BeO$ in the lime-beryllia system was studied.

The variables affecting extraction of plutonium from uranium powder produced by hydriding were further studied.

Data on the partition of various fission product elements between liquid magnesium and uranium-chromium eutectic alloy (5 per cent chromium) have been obtained. Zirconium, molybdenum and ruthenium strongly favor the uranium phase, while rhodium, palladium, silver and cadmium favor the magnesium phase.

A full-scale uranium melting furnace, a prototype of the one to be used in the EBR-II pyrometallurgical pilot plant for fuel purification, was received and installed in the last quarter. Shakedown testing was begun.

Uranium ingots, purified by melt refining, will have equilibrium temperatures of the order of 600 C as a result of fission product heating. It was shown that at this temperature essentially no attack of the uranium by the nitrogen in the argon cell gas (5 vol per cent nitrogen) will occur.

A large number of materials have been screened with regard to their efficacy in trapping metals volatilized at high temperatures during the melt refining process. Surface-active materials have been found to be effective. Three materials: activated alumina, an activated charcoal, and "Molecular Sieves," have been selected for further study.

Work on purification of uranium by fractional crystallization from zinc was continued. The individual solubilities of uranium and a number of fission product elements in zinc have been determined as a function of temperature.

The five-kilogram-scale batch extraction unit of the magnesium extraction process for plutonium has operated satisfactorily in inactive runs using magnesium and a 5-w/o chromium-uranium alloy. A magnesium distillation unit has operated very well with a sodium-cooled condenser. A magnesium "freeze" valve has been developed.

A. Laboratory Studies
(H. M. Feder)

1. Control of Dross in Melt Refining
(N. Chellew, C. Cushing, J. Schilb, D. Finucane)

a. Kinetics of Uranium-Ceramic Oxide Reactions

(1) High Purity Uranium

Data from two additional experiments have been added to the study of the kinetics of the beryllia-uranium reaction. These experiments were performed under the conditions of 1330 C and 5 and 6-hour melt periods. The data from these experiments and those previously reported (ANL-5633, page 95) are shown in Figure 26. The observation that the corrosion rate increases with time is in agreement with the two-step mechanism postulated previously.

The kinetic study of the zirconia-uranium reaction has been terminated. Analyses of zirconium concentration in the ingots produced from nine melts at temperatures as high as 1325 C and for melt times as long as 4 hours indicated an upper limit of 5 ppm for the zirconium concentration. The inaccuracy of currently available methods for the analysis of zirconium in uranium at these low concentrations limits the value of the results obtained in these experiments.

(2) Uranium Alloys

The effects of alloying elements in uranium on the corrosion behavior of alumina, beryllia and thoria have been summarized in Figures 27 and 28 in which contamination of alloyed uranium by aluminum,

beryllium or thorium is compared with the contamination of unalloyed uranium under similar melt conditions. (The weight per cent of the alloying constituents are indicated in the figures.) These charts summarize the data from 16 melts, four of which were made this quarter. Data for essentially duplicate runs have been averaged in this presentation. The base corrosion rates for uranium were taken from plots of the relevant kinetic studies. The variations in corrosion rates due to alloying have been discussed in previous quarterly reports (ANL-5633, page 96 and ANL-5602, pages 95 and 96).

The accumulated data on the corrosion of ceramic oxides by uranium and its alloys will be presented in a topical report to be issued shortly.

FIGURE 26.

CONTAMINATION OF URANIUM BY BERYLLIUM
BERYLLIA CRUCIBLE MELTS AT 1330 C

Charge: Maximum impurities – 39 ppm carbon, <10 ppm nitrogen, 8 ppm oxygen and <1 ppm beryllium.

Conditions: Helium atmosphere. Uranium charges liquated in crucible.

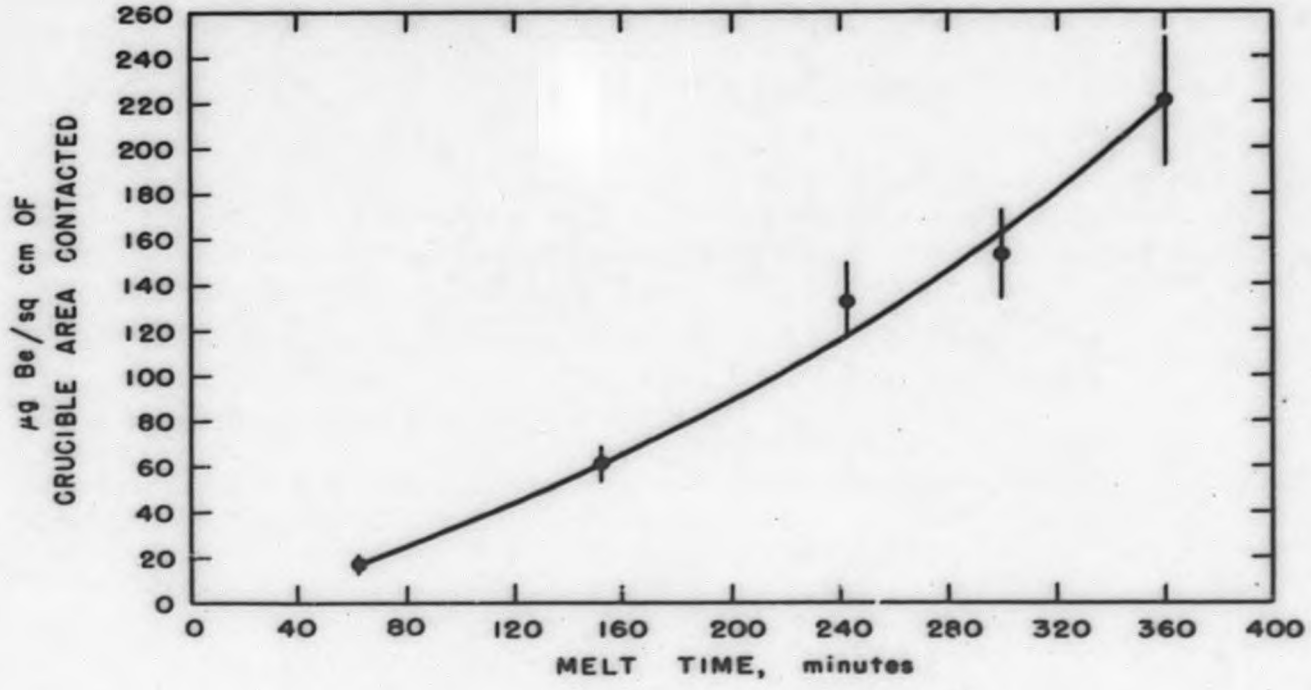

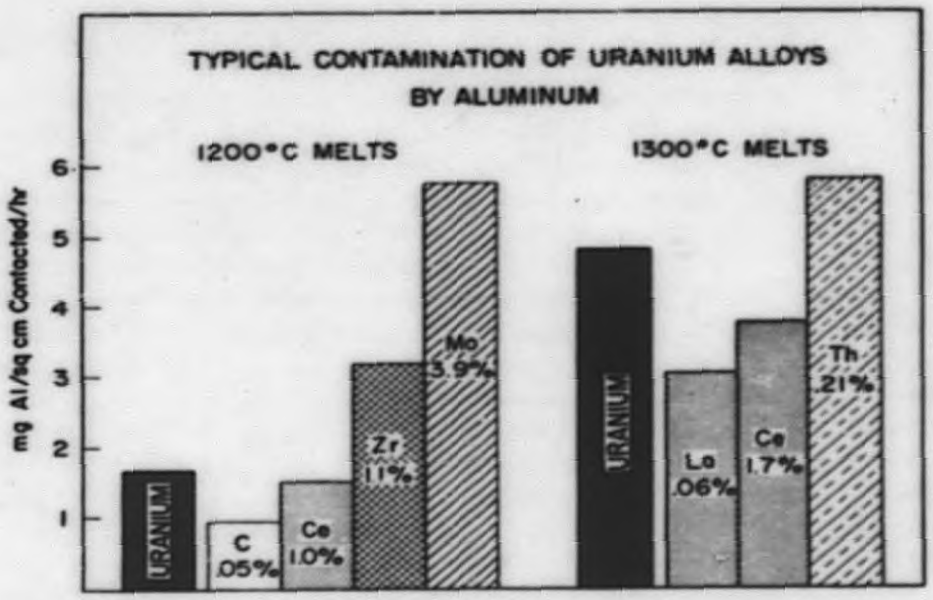

Figure 27

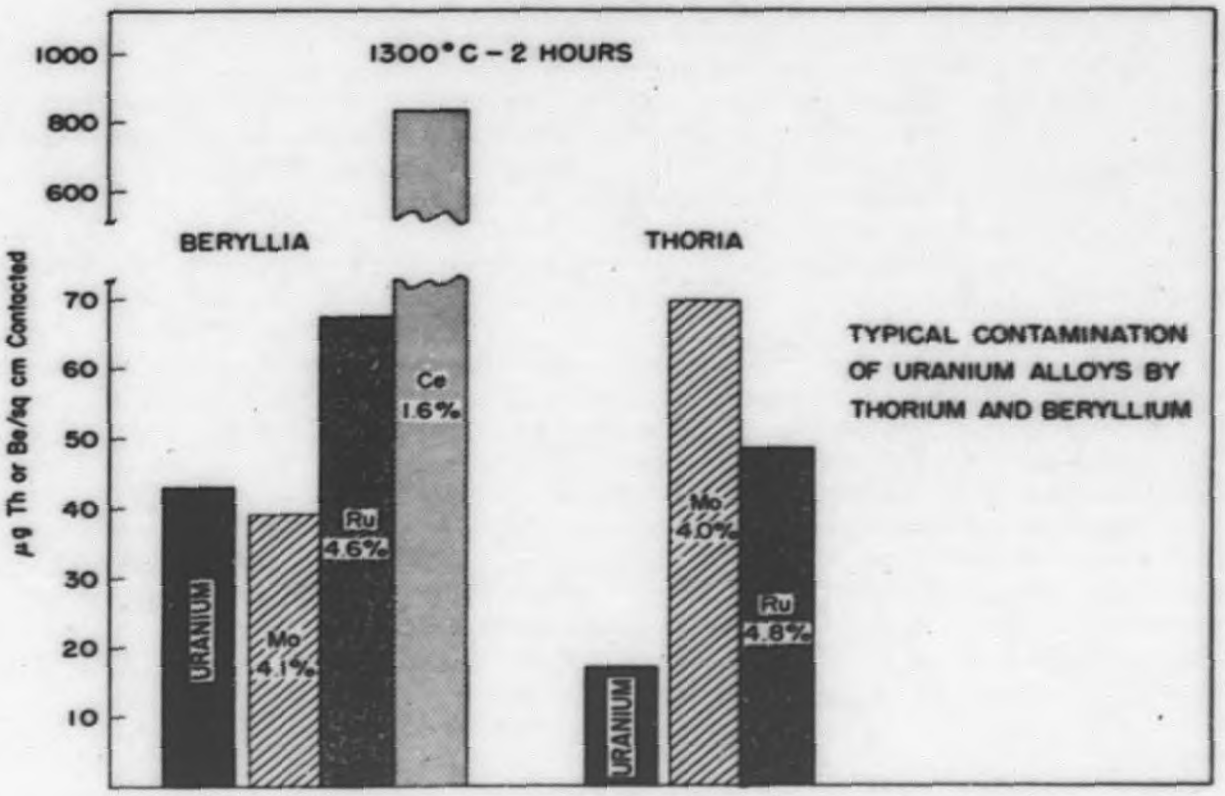

Figure 28

b. Removal of Cerium from Uranium and Uranium Alloys

A program of experimentation on the removal of alloying elements from uranium by melt refining (ANL-5633, page 96) has been continued with emphasis on the behavior of cerium because of its importance in the processing of nuclear fuels. The purpose of the present study was to determine appropriate melt conditions for removal of cerium at about the one per cent level by reaction with a ceramic crucible. Crucible materials investigated were alumina, magnesia, thoria, beryllia and zirconia. The initial work was done with uranium-cerium alloys and results from these experiments are reported in Table 21. From these preliminary results and from earlier work on crucible corrosion the following conclusions were drawn. The removal of cerium by reaction with thoria is too slow for practical use. Removal of cerium by reaction with alumina appears to be possible, but the high corrosion rate of alumina rules against its use in practice because of contamination of the uranium by aluminum. Liquation of cerium-uranium alloys in magnesia was accompanied by considerable agitation of the melt due to volatilization of magnesium from the molten metal-ceramic interface. Although bubbling gradually subsided, the melt surface never appeared free from disturbance. Metallographic examination of specimens of material retained in the crucible after Runs 128 and 126 indicated the reaction layer to be fragmented. Based on the hypothesis that bubbling causes dislodgement of the cerium oxide from the crucible surface, it was concluded that in future experiments with magnesia a downspout should be used to retain floating dross during the top-pour. Accordingly, in subsequent experiments with magnesia an alumina cylinder of small diameter was cut longitudinally and a half-section was tied with molybdenum wire to the crucible to form an inside skimmer tube extending from the pouring edge to approximately one-quarter inch above the bottom.

A second series of experiments to survey the removal of cerium from "fissium" alloys was then conducted using magnesia, beryllia and zirconia crucibles. The synthetic "fissiums" contained cerium, ruthenium, molybdenum, palladium and zirconium in various combinations in the concentrations shown in the footnotes to Table 22. The results of these experiments are given in Table 22. Although the large number of variables prevents the drawing of sound conclusions about the effect of each variable, it is apparent that with optimum selection of time and temperature adequate removal of cerium can probably be attained with any of these crucible materials. However, in a large number of the runs listed in Table 22 it was found that the crucible was cracked at the end of the run. By duplicate experiments with and without fissium charges it was shown that the cracking was due to chemical reaction rather than to thermal shock. Of the crucible types investigated magnesia showed the best resistance to cracking from either cause, so that further experimentation on the kinetics of cerium removal will concentrate on this crucible material.

Table 21

REMOVAL OF CERIUM FROM CERIUM-URANIUM ALLOYS BY MELTING IN OXIDE CRUCIBLES

Alloy: Maximum impurities in preparation-carbon 39 ppm, oxygen 10 ppm and nitrogen 10 ppm.

Conditions: Helium atmosphere. Ingot separated from dross by top-pour technique unless otherwise indicated. 500-gram charges.

Crucible	Run	w/o Ce in Alloy	Melt Conditions: Nominal Temp, C	Melt Conditions: Total Time, min	Ce Remaining in Ingot, Per Cent[c]
Alumina (recrystallized)	138[a]	1.02[b]	1170	6	85
	137[a]	1.08[b]	1170	19	78
	130	1.04[b]	1200	180	6
	125	1.06	1300	180	29
Magnesia (slip cast)	128	0.75	1200	60	68
	126	0.75	1300	60	96
	136	0.98[b]	1330	60	81
Thoria (slip cast)	99	0.98	1200	120	100
	132	0.97[b]	1200	180	100
	123	0.60	1300	180	100
Beryllia (slip cast)	131	0.96[b]	1200	180	81
	111	1.49	1300	120	71
	14E, 15E[a]	1.70	1300	122	72 (avg)
	127	0.79	1300	180	68
Zirconia (slip cast)	129	0.78	1200	180	2
	124	0.76	1300	180	5

[a] Melt liquated in crucible. Dross separated from ingot with cutting wheel.

[b] Cerium added to molten uranium at 1170 C. All other experiments employed pre-formed cerium-uranium alloys.

[c] Estimated accuracy ± 10%.

Table 22

REMOVAL OF CERIUM FROM FISSIUM ALLOYS BY MELTING IN OXIDE CRUCIBLES

Conditions: Helium atmosphere. Ingot separated from dross by top-pour technique except for Run 146. Metal poured at 1300 to 1330 C unless otherwise indicated.

		Alloy Charge		Conditions		
Crucible	Run	Alloy Composition[a]	Initial w/o Ce	Nominal Temp, C	Total Time, min	Ce Remaining in Ingot, Per Cent[e]
Magnesia	149	Ru, Mo, Zr, Pd, Ce	0.91	1200	180	36
(slip cast)	153	Ru, Mo, Zr, Pd, Ce	0.58	1200	180	30
(slip cast)	155	Ru, Mo, Zr, Pd, Ce	0.76	1250[d]	180	37
(slip cast)	157	Ru, Mo, Zr, Pd, Ce	1.06	1300[d]	180	22
(dry pressed)	159	Ru, Mo, Zr, Pd, Ce	0.43	1250[d]	180	9
	161	Ru, Mo, Zr, Pd, Ce	0.88	1250[d]	330	3
Beryllia	151	Ru, Mo, Zr, Pd, Ce	0.61	1200	180	41
(slip cast)	144	Ru, Mo, Zr[b], Pd[b], Ce[b]	0.88	1330	244	18
	146[c]	Ru, Mo, Zr[b], Pd[b], Ce[b]	0.95	1330	244	9
	145	Ru, Mo, Zr[b], Pd[b], Ce[b]	0.98	1330	264	7
	142	Ru, Mo, Pd, Ce[b]	0.99	1330	337	6
	140	Ru, Mo, Pd, Ce[b]	1.04	1330	362	9
Zirconia	143	Ru, Mo, Ce[b]	1.13	1200	126	54
(slip cast)	150	Ru, Mo, Zr, Pb, Ce	0.61	1200	180	36
	139	Ru, Mo, Pd, Ce[b]	1.08	1330	184	34

[a] When present the concentrations of alloying elements in weight per cent were: Ru, 2.5-3.5; Mo, 3.0-4.1; Zr, 1.3-2.1; Pd, 0.2-0.3.

[b] Added, with shaking, to molten alloy at 1170 C.

[c] Melt liquated without pouring. Dross separated from ingot by cutting.

[d] Poured at nominal temperature shown.

[e] Estimated analytical precision ± 10%.

2. Physical Properties of Molten Uranium
(C. L. Rosen, R. U. Sweezer)

a. Density of Liquid Uranium

The volume expansion of uranium on melting is being determined by measuring, on photographic negatives, the heights and diameters of the profiles of sessile drops of uranium on thoria plaques.

The ratio of the dimensions of the liquified and solidified drops are approximately

$$\frac{r_\ell}{r_s} = 1.024; \quad \frac{z_\ell}{z_s} = 1.048; \quad \frac{x_\ell}{x_s} = 1.0 \quad ,$$

where r (one-half the maximum diameter), z, and x are defined in the following sketch (the subscripts ℓ and s refer to the liquid and solid states respectively):

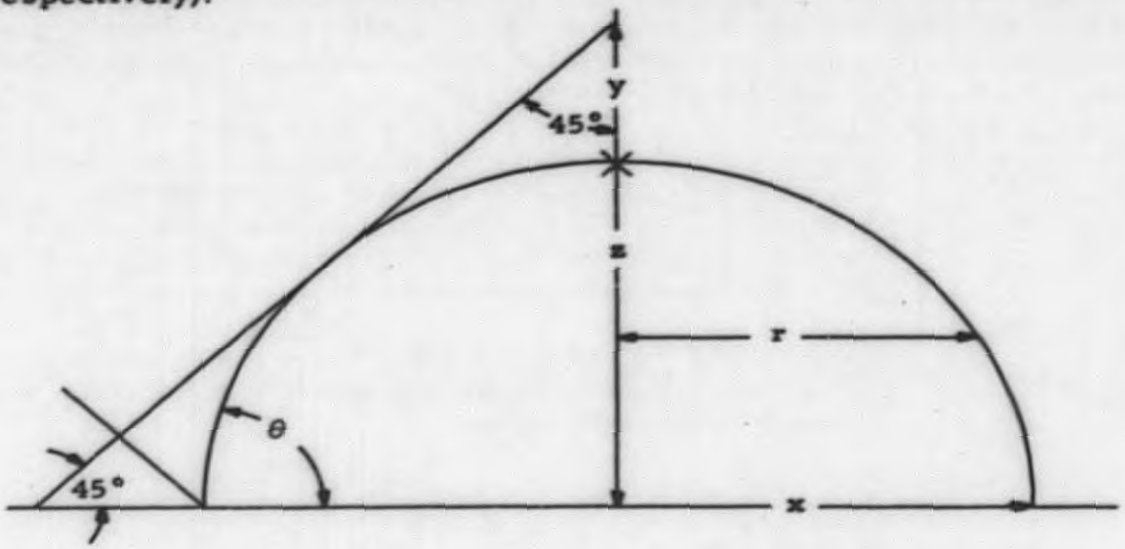

One of the difficulties in determining the volume expansion on melting from these data is the fact that the drops do not expand and contract isotropically and the base area of a drop does not change. As a rough approximation one may consider the drop to be a cylinder with radius r and height z. In this case the volume expansion would be $(r^2_\ell \, z_\ell / r^2_s z_s)^{1/3}$ or 3 per cent from the above data. Since the assumption of cylindrical geometry is probably not very satisfactory, a better value of the volume expansion will be obtained from new measurements of the negatives using a calibrated eyepiece marked with both radial and coordinate units so that one can obtain values of "y," as well as of "r" and "z." The tables and equations of Bashforth and Adams[7] will also be used to obtain the volumes as functions of the measured coordinates.

---

[7] Bashforth, F. and Adams, S. C., "An Attempt to Test the Theories of Capillary Action," University Press, Cambridge (1883).

b. Surface Tension of Liquid Uranium

Using the relation developed by Dorsey[8] a surface tension of 825 ± 83 dynes/cm has been obtained for liquid uranium drops on thoria and stabilized zirconia at temperatures in the neighborhood of 1250 C.

While it has been assumed that the liquid uranium drops used in these calculations take the form of unrestrained sessile drops (data in ANL-5602, page 100 showed that the geometry of the original ingot had no large effect on the shape of the final drop), certain experiments have indicated that large hysteresis effects may occur after the liquid drop is formed. These experiments were as follows:

(1) Uranium was melted in the right angle of an "L"-shaped cut in stabilized zirconia. Some of the uranium dripped over this groove and it was found that the uranium adhering to the bottom of the plaque wet it while the uranium remaining in the angle did not.

(2) It was found that above 1600 C the contact angle on thoria recedes from 135° to below 90° but it does not increase again on cooling.

(3) It was found that if molten uranium is dropped from a height onto a zirconia plaque the contact angle is much closer to 90°.

(4) If part of the uranium from a frozen sessile drop is removed, the remaining uranium, on melting, wets the same base area as did the larger quantity of uranium.

Two alternative explanations fit these observations. In the first it is assumed that the smaller contact angle is the equilibrium value, but that some activation energy must be supplied to overcome a large initial value of the interfacial tension so that the drop may spread. In the second it is assumed that the larger contact angle is the equilibrium value, but that activation energy must be supplied to permit the molten uranium to retract from a once-wetted area. Since the latter phenomenon has been classically observed in many cases, it is the more likely explanation.

From simple considerations of the equilibrium forces at the interface one can determine the relation

$$\gamma_s = \gamma_{su} + \gamma_u \cos \theta \qquad (1)$$

---

[8] Dorsey, N. E., J. Wash. Acad. Sci., 18, 505 (1928).

where

γ_s = solid surface energy

γ_{su} = interfacial tension

γ_u = liquid uranium surface tension

and θ = the contact angle.

The work of adhesion, or the increase in free energy, needed to separate the uranium-ceramic interface into clean surfaces is given by the Dupre equation:

$$W_{Ad} = \gamma_u + \gamma_s - \gamma_{su} \quad . \tag{2}$$

Combining (1) and (2) we get

$$W_{Ad} = \gamma_u (1 + \cos\theta) \quad . \tag{3}$$

Therefore, the work of adhesion is dependent only on the uranium surface tension and the contact angle. Using the measured value of 825 dynes/cm for the surface tension and the observed initial contact angles one finds that the work of adhesion is approximately 240 ± 50 ergs/sq cm for thoria, alumina, beryllia, lime-stabilized zirconia and magnesia. The approximate agreement for all five substrates indicates that this work of adhesion is characteristic of the interface between liquid uranium and a surface of closely packed oxygen ions.

3. Reactions of Uranium with Container Materials
(C. L. Rosen, R. U. Sweezer)

An effusion apparatus for measuring the vapor pressures of tantalum borides, or of other materials which may possibly be used to construct containers, has been built and is now being tested.

4. Phase Diagram Studies of Oxide Systems
(M. Ader, D. Fredrickson)

Lime-Beryllia System: During the past quarter effort was concentrated on the study of the preparation of the compound 2 CaO·3 BeO (ANL-5602, page 107) in high purity in order that some minor discrepancies in its formulation might be cleared up and to obtain single crystals sufficiently large for X-ray study.

A recent patent statement[9] that "calcium beryllate" may be precipitated from an alkaline solution of beryllium hydroxide by the addition of calcium chloride was investigated. The outlined procedure was

[9]Derge, G. and Monet, G. P., U.S.A. Patent 2,743,173, April 24, 1956.

followed, mixing the reactants in the mole ratio of calcium to beryllium of 2:3. The solid obtained has not been identified as yet. On drying by heating to 500 to 900 C the material gave X-ray patterns of lime and beryllia only. On heating to 1450 C the compound 2 CaO·3 BeO with a small amount of excess calcium oxide was formed. It is apparent that the intimacy of mixing of calcium and beryllium compounds that can be obtained by simultaneous precipitation is conducive to ready reaction on heating.

Numerous experiments now completed show that the formation of the compound depends critically on the reactivity of its constituents. Thus, when the grade of calcium carbonate (Baker and Adamson, 1540, Reagent Special) used in the earlier, successful experiments was replaced by a slightly purer and lower density grade (Mallinckrodt, 4071, Primary Standard), no compound was formed in repeated experiments. The same batch of beryllia was used throughout. The variables that were tested were as follows:

(1) Magnesia was added to simulate the major impurity in the Baker and Adamson calcium carbonate;

(2) Platinum, graphite and tantalum were used as crucibles;

(3) The mixtures were thermally cycled above and below the eutectic temperature;

(4) The melts were cooled slowly and rapidly;

(5) The atmosphere of untreated air was replaced by dry air or helium.

The compound was finally produced from this batch of calcium carbonate by seeding the melt at about 1400 C with a few small crystals of previously prepared compound. It was observed that the extensive supercooling of the melt usually 30 to 40 degrees below the eutectic temperature of 1385 C was markedly decreased. This information will be of value when the earlier thermal analysis experiments are repeated. The exact nature of the difference in reactivity is still unknown, but it is likely that the failure of earlier investigators to notice the formation of a compound in the lime-beryllia system is connected with their use of unreactive starting materials.

The preparation from the above-mentioned seeding experiment contained 58 mole per cent beryllia. In order to obtain the compound free of excess lime this material was powdered and washed with cold, dilute hydrochloric acid. The washed preparation failed to show any X-ray powder diagram lines of calcium oxide; thereby an upper limit of 2 to 3 mole per cent is set for its calcium oxide content. The density (by pycnometer) of this sample was 2.66 g/ml.

The analytical techniques required to establish the ratio of beryllia to lime in the compound are being re-examined because it is suspected that a small systematic error due to the presence of alumina as an impurity may have occurred. At present it can only be stated that the lower limit of this ratio is 1.442.

5. Magnesium Extraction Studies
(E. Greenberg, M. W. Nathans, K. E. Anderson)

a. Extraction of Plutonium from Liquid Uranium or its Alloys

In the previous quarterly report (ANL-5633, page 107) data were reported on a number of runs with uranium-chromium-plutonium alloy as the heavy metal phase. It was shown that 10 to 30 per cent of the plutonium had concentrated in a finely divided residue which remained after dissolving the magnesium phase away from the heavy metal phase. In order to determine whether this effect was caused by either an increased rate of reaction between the charge and the alumina crucible, or by inadequate cleaning of the surface charged metal, two additional runs were made at about 1000 C with a tantalum crucible in one and an alumina crucible in the other. The cleaning of the surface of the heavy-metal charge was carried out to a much higher degree than in the earlier runs. The results are shown in Table 23. Run 39, which has been reported previously, has been included for comparison. It is clear from these data that neither the crucible nor the condition of the metal charge surface was primarily responsible for the concentration of plutonium in the residue.

Table 23

DISTRIBUTION OF PLUTONIUM BETWEEN MAGNESIUM AND URANIUM-CHROMIUM EUTECTIC ALLOY

			Plutonium Found							
Run No.	Temp[a] (C)	Time at Temp (hr)	in Mg (mg)	in U (mg)	in Residue (mg)	Total (mg)	Alloy Charge[d] (g)	Pu Charged (mg)	Pu Recovered (%)	Pu in Residue (%)
39[b]	1055	3	90.1	24.4	35.3	150	19.3	160	94	22
44	1070	3	54.3	31.9	30.8	117	13.5	112	104	27
45[c]	1070	3	58.7	38.7	19.9	117	14.9	123	95	16

[a] Temperatures are reported to the nearest 5 C.

[b] Previously reported (ANL-5633, page 107).

[c] A tantalum crucible was used in this run. Morganite alumina crucibles were used in the other runs.

[d] Magnesium charge was ~18 g in each run; alloy was a nominal 1% plutonium - 5% chromium - uranium alloy.

It is likely that the original ingot contained occlusions and impurities which formed stable plutonium compounds. These would subsequently concentrate in the metal-metal and metal-crucible interfaces and be dislodged when the magnesium phase was dissolved. Because of this possibility a new batch of uranium-chromium-plutonium alloy has been prepared with special attention devoted to keeping contamination to a minimum. In addition, equilibration experiments are currently in progress in which the plutonium is initially in the magnesium phase.

b. Extraction of Plutonium from Powdered Uranium
(R. Nuttall, J. Settle)

Several additional experiments have been made in which plutonium was extracted from powdered uranium - one weight per cent plutonium alloy with liquid magnesium. Analytical results from five runs are given in Table 24. The extraction obtained in these runs can be compared with runs using tracer amounts of plutonium (ANL-5602, page 110).

Table 24

EXTRACTION OF PLUTONIUM FROM POWDERED URANIUM

Run No.	Crucible Material	Charge (g)		Temp (C)	Contact Time (hr)	Per Cent in Mg		Material Balance (%)	
		Mg	1% Pu in U			Pu	U	Pu	U
24	Al_2O_3	10.47	51.10	800	1	48.0	0.001	94.0	98.2
25	Al_2O_3	11.44	29.25	800	3	60.3	0.05	99.0	97.0
26	Graphite	14.26	3.02	900	1	14.6	0.03	91.3	97.1
27	Graphite	15.6	34.7	900	1	24.9	0.03	98.6	98.8
28	Graphite	19.2	49.2	800	1/4	4.6	0.05	96.7	92.6

There are as yet insufficient analytical data from which to draw conclusions concerning the effect of contact time, temperature, crucible material, and relative amounts of uranium and magnesium.

c. Extraction of Fission Products from Uranium Alloys
(G. R. B. Elliott, R. U. Sweezer)

Work has continued on the distribution of fission product elements between molten magnesium and low melting uranium alloys. The equilibrations have tested the individual partition coefficients of zirconium, niobium, molybdenum, ruthenium, rhodium, palladium, silver and cadmium

between uranium - 5 w/o chromium and magnesium. This report presents preliminary results on all the elements mentioned above with the exception of niobium. In addition further results from last quarter's equilibrations of ruthenium and palladium between magnesium and uranium-iron eutectic are listed.

(1) Experimental

The equipment and procedure have been described in detail in the previous quarterly report (ANL-5633, page 111). Briefly, a weighed charge in an inert container is encapsulated in an inert atmosphere and shaken in a controlled-temperature furnace. After three hours equilibration with agitation and five minutes settling to allow phase separation, the capsule is removed from the furnace and allowed to quench in air. The ingot is cut and polished to provide samples for analysis.

Analyses for zirconium, molybdenum, ruthenium, palladium, chromium, uranium, and magnesium were performed by the analytical group using standard techniques. If the analyses showed complete dissolution of the tested element into the metallic equilibrium mixture, and if the distribution strongly favored one phase, then only the phase containing the minor amount of fission product was analyzed in succeeding runs. Only the magnesium phases were analyzed when the solute metal was rhodium, cadmium or silver. The rhodium analysis consisted of a dissolution of the cleaned magnesium sample in acetic acid and weighing of the dried residue. The residue, which in each case weighed only a few milligrams more than would be expected from complete extraction of the charged rhodium into the magnesium phase, was then submitted for X-ray analysis and magnesium analysis.

Cadmium in magnesium was analyzed by weighing as cadmium sulfide.

Silver in magnesium was analyzed by separation of the bulk of the magnesium by acetic acid dissolution, dissolution of the silver residue in nitric acid, and precipitation and weighing as silver chloride.

Eighteen experimental equilibrations were carried out with uranium-chromium-magnesium-fission product element systems to test distribution behavior. The results are shown in Table 25.

Table 26 gives information on the ruthenium-iron-uranium-magnesium system which was not available for the last quarterly report (ANL-5633). It belongs in Table 42, page 113, of that report. Table 26 also indicates the distribution of palladium in the system palladium-uranium-iron-magnesium.

Table 25

THE DISTRIBUTION OF FISSION PRODUCT ELEMENTS BETWEEN MAGNESIUM AND URANIUM - 5 w/o CHROMIUM

Run No.	Element Tested	Concentration,[a] (Atom Fraction)	Crucible	Temp (C)	Time Heated (hr)	Partition Ratio[b] of Element
22-2-E	Zr	0.027	ZrO_2	936	3	3.2×10^{-3}
23-1-E	Zr	0.030[d]	Thoria Coated Graphite	926	4	1.8×10^{-3}[c]
27-2-E	Zr	-d	ZrO_2	936	3	-d
28-2-E	Nb	-d	MgO	942	3	-d
21-2-E	Mo	0.028	MgO	937	3	$\leq 3.6 \times 10^{-5}$
24-2-E	Mo	0.034	MgO	948	3	-d
26-2-E	Mo	0.035	ZrO_2	930	3	-d
22-1-E	Ru	0.042	MgO	936	3	1.7×10^{-4}
25-2-E	Ru	0.052	MgO	944	3	-d
27-1-E	Ru	0.114	Al_2O_3	936	3	-d
25-1-E	Rh	0.0046	MgO	944	3	Extracts strongly into Mg[e]
28-1-E	Rh	0.0080	MgO	942	3	Extracts strongly into Mg[e]
21-1-E	Pd	0.0064	MgO	937	3	≥ 1000
24-1-E	Pd	0.0071	MgO	948	3	-d
26-1-E	Pd	0.0030	ZrO_2	930	3	-d
29-1-E	Ag	0.0023	Al_2O_3	930	3	Extracts strongly into Mg[e]
29-2-E	Cd	0.0034	Al_2O_3	930	3	Extracts strongly into Mg[e]

[a] Concentration in the preferred phase; each phase weighed ~25 g.

[b] Ratio of atom fraction in magnesium to atom fraction in uranium-chromium.

[c] Approximate value only.

[d] Incomplete analysis.

[e] Only Mg phase analyzed. Essentially total extraction into this phase with 10 moles of Mg per mole of U-Cr.

Table 26

THE DISTRIBUTION OF RUTHENIUM AND PALLADIUM BETWEEN MAGNESIUM AND URANIUM-IRON EUTECTIC

Run No.	Partition Ratio[a]
Series A: Ruthenium	
11-1-E	<0.04
12-1-E	<0.004
16-2-E	1.3×10^{-3}
18-1-E	5.7×10^{-4}
Series B: Palladium	
20-2-E	≥ 75

[a]Ratio of atom fraction in magnesium to atom fraction in uranium-iron; each phase weighed ~25 g.

(2) Discussion of Results

The data of Table 25 show that, in the equilibration of magnesium with uranium-chromium eutectic alloy, zirconium, molybdenum, and ruthenium strongly favor the uranium phase while rhodium, palladium, silver, and cadmium favor the magnesium phase. A similar distinction between ruthenium and palladium is also exhibited when uranium-iron eutectic alloy is used. It will be of some interest to determine whether the qualitative change in behavior which takes place as atomic number of the solute element increases from ruthenium to rhodium can be understood in terms of parameters such as atomic radius, electronegativity, etc.

With respect to quantitative determinations of the partition ratios for rhodium, silver and cadmium it should be pointed out that the determination of the concentration only in the strongly favored phase makes the value depend on a small difference between large numbers and hence is subject to very large errors.

Determinations of the solubility of uranium and chromium in magnesium and of magnesium in the uranium-chromium phase were carried out during the course of the equilibrations. Difficulties were encountered which arose from possibilities of physical occlusion of heavy-metal phase in the magnesium and from interference of a manganese

impurity in the magnesium with the analysis for chromium. For this reason the discussion of these results will be deferred until they are all collated. They will be published in the terminal report which will be written on this project.

B. Semi-Works Studies of High Temperature Processes
(L. Burris, Jr.)

Evaluation and testing of various equipment and process steps considered for use in the EBR-II pyrometallurgical pilot plant was continued.

1. Design and Testing of Components for Pilot Plant
(G. J. Bernstein, V. N. Thelen)

The principal effort during this period was directed toward the installation and testing of a melting furnace, a prototype of one to be used in the EBR-II pyrometallurgical pilot plant. The furnace was designed, using information of previous semi-works and laboratory studies, in the Design Group of J. H. Schraidt by D. C. Hampson and associates.

The furnace is inductively heated by an uncooled copper coil using a tantalum susceptor and will handle charges up to 10 kg of uranium. It will be operated under an atmosphere of purified argon but will be capable of being evacuated for degassing of the interior. The equipment is designed to permit remote operation and servicing. Materials of construction were selected to withstand the high radiation field anticipated in actual plant use.

Figure 29 shows the equipment with the bell-jar cover suspended over the furnace platform. The crucible frame and coil assembly can be seen with the cast-iron mold in position. Surrounding the base is the electrically heated, fusible metal seal. To the left can be seen, in order, the two connectors for the induction coil, the connectors for the metal seal heater, the thermocouple conduit, three argon supply lines (which were put in solid but would actually have disconnects), an argon supply line with fusible couplings and a similar vacuum line. The connections on the left simulate the connectors to be permanently mounted in the operating cell. All these contacts can be made or broken with a manipulator, thus permitting remote removal of the entire furnace assembly.

Figure 30 shows the bell jar sealed to the base and the protective cover over the electrical leads. Figure 31 shows the furnace interior with the flexible coil connectors and the fume trap mounted above the crucible.

Figure 29

Uranium Melting Furnace - Bell Jar Partially Removed.

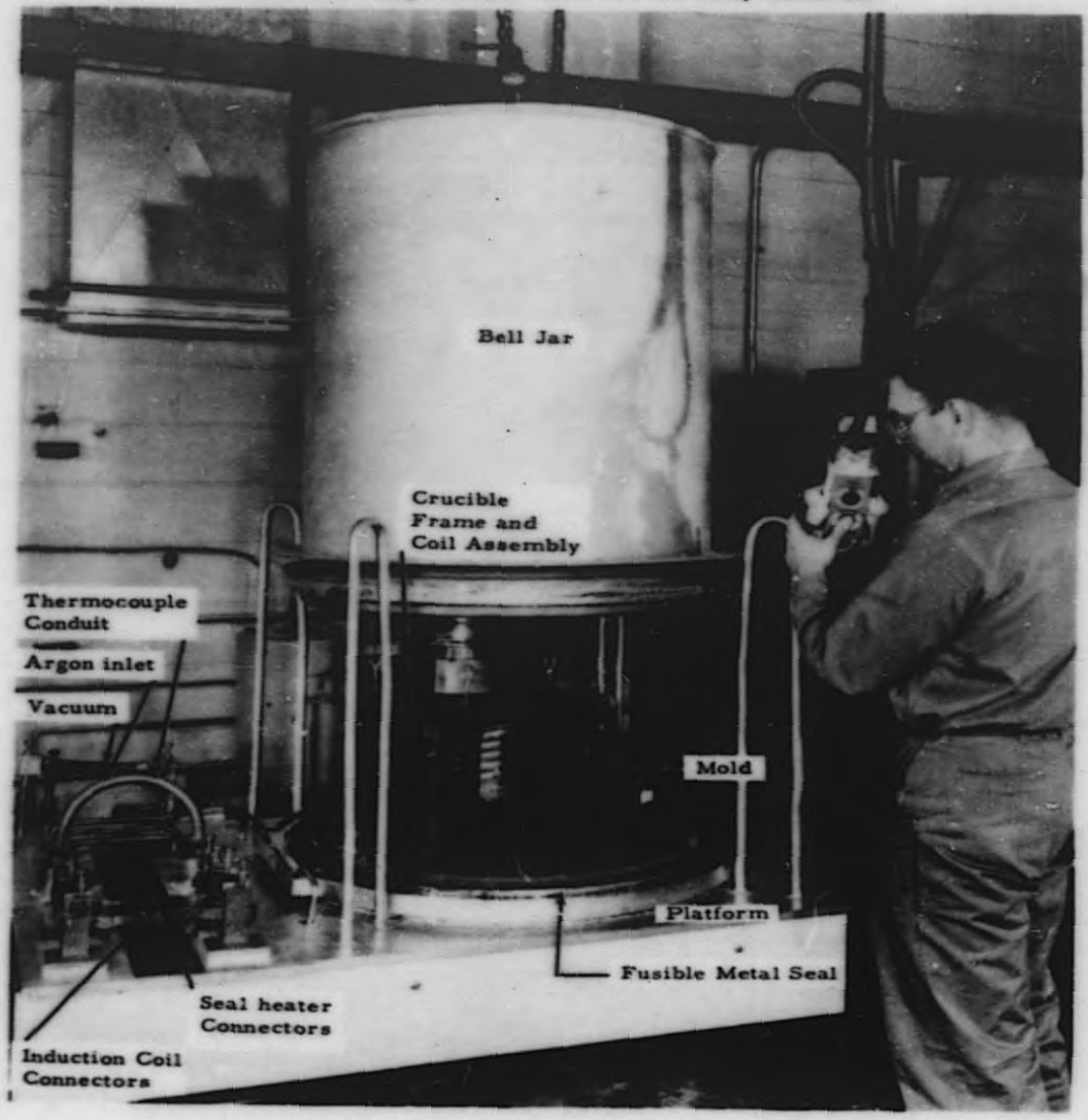

Figure 30

Bell Jar Cover in Position

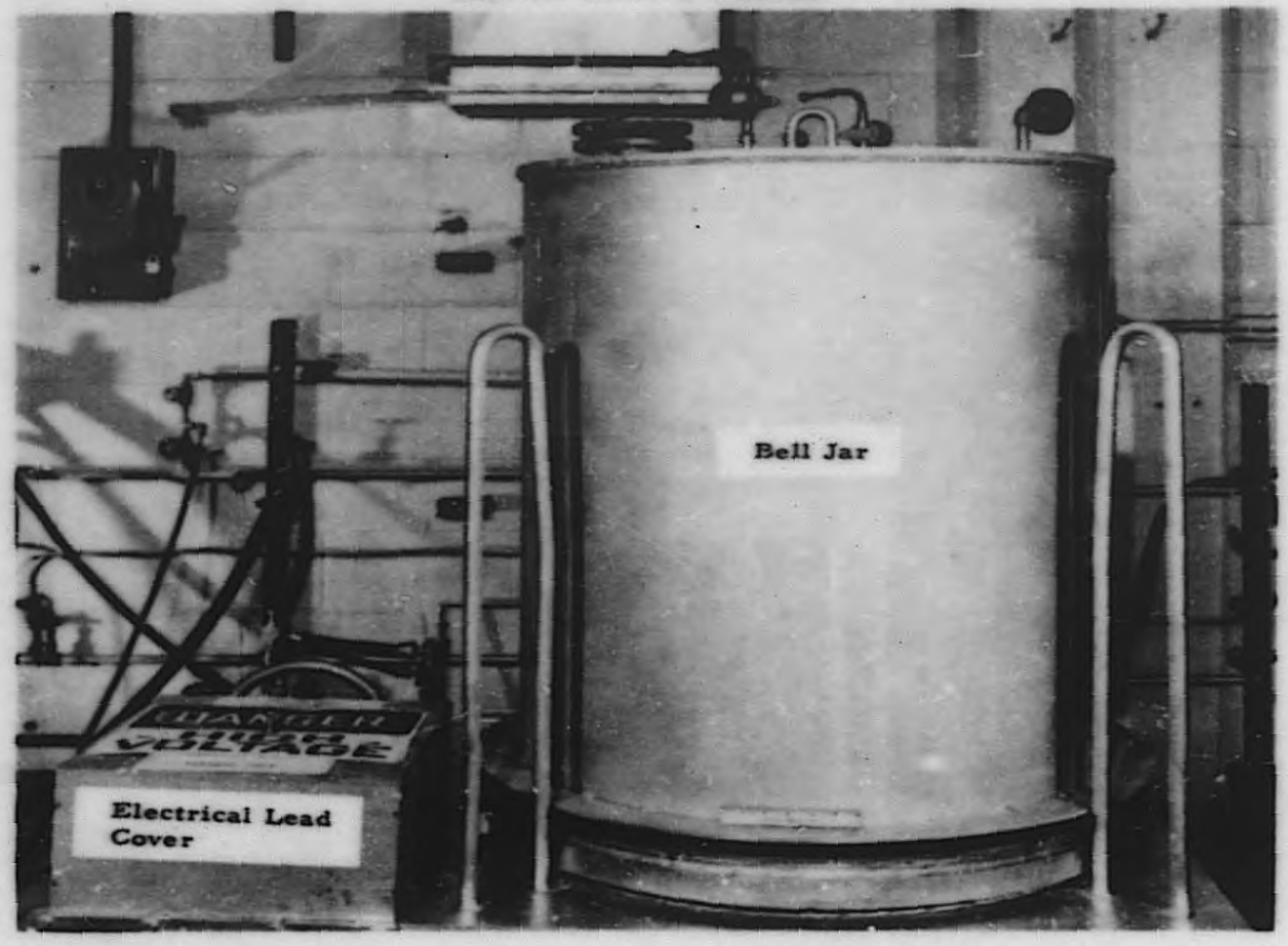

Figure 31

Furnace Interior

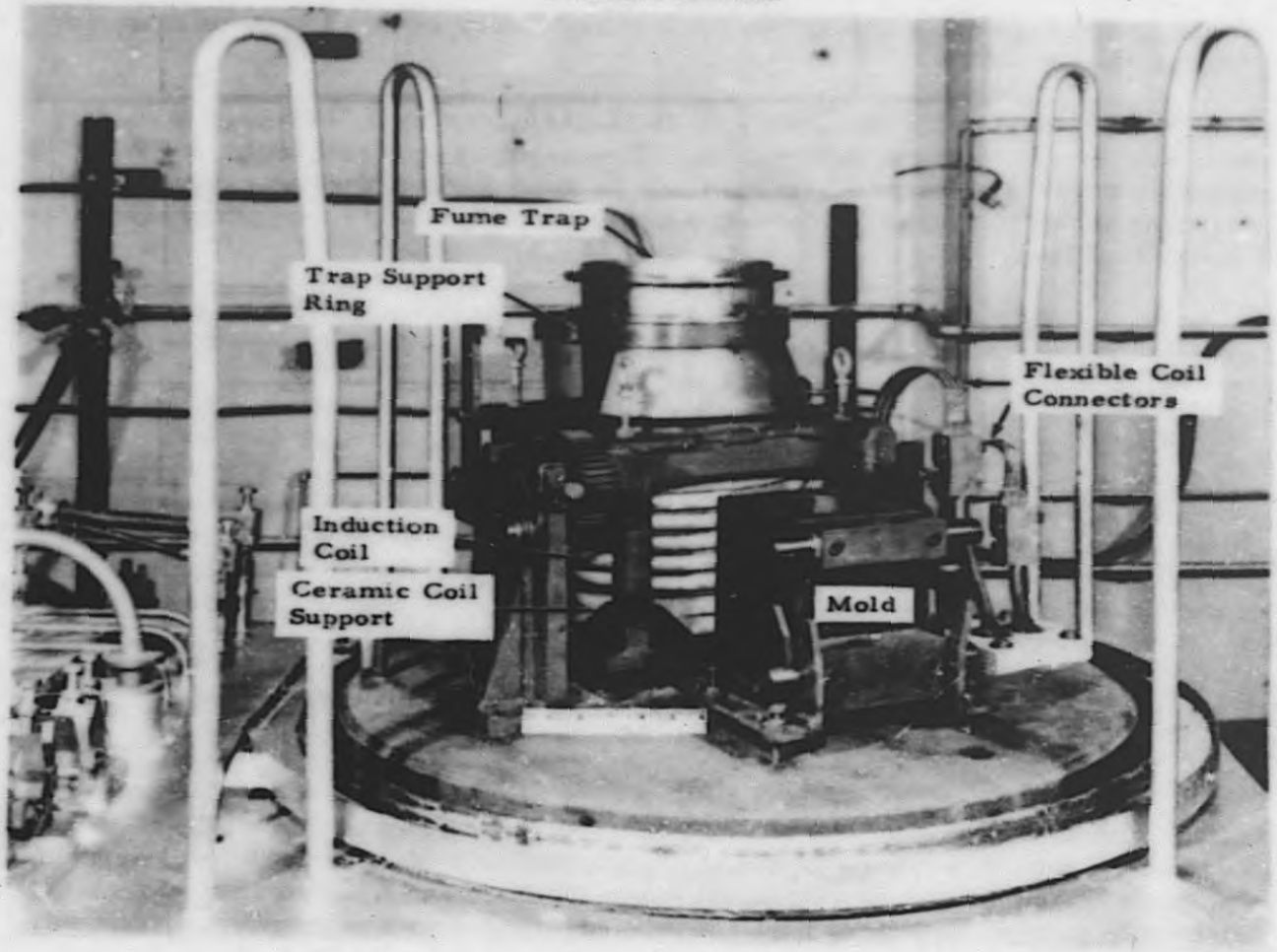

Figure 32 shows the crucible in a partially tilted position. The fume trap is raised by its support ring to allow the molten metal to pour. The rack which drives the tilting gear is actuated by a shaft which passes through a sleeve in the base. Beneath the frame can be seen the reference thermocouple lead connector which makes contact with a chromel-alumel thermocouple mounted beneath the tantalum susceptor.

Figure 33 is a close-up of the furnace interior. The flexible leads are connected to the bus bars with sliding clips which can be disconnected with the manipulator. Removal of the pin shown just in front of the gear permits raising the entire assembly by the use of a crane to engage the eyebolts.

The mold has two 1/8-inch diameter by 1/4-inch deep holes in the base to provide ingot samples. The ingot is dumped from the mold in the apparatus shown in Figure 34. It is then moved with the manipulator into the sampling position where a cutter bar removes the protrusions as shown in Figure 35.

Tests are in progress to establish the operability of the various components. A 10-kg charge of uranium has been melted and poured, the ingot yield being 96.4 per cent.

2. Removal of Cerium by Oxide Slagging

A series of experiments is in progress to determine the effectiveness of cerium removal from equilibrium fission alloys* by oxide slagging in magnesia crucibles. In the first run, cerium, initially at a concentration of 0.59 w/o, was reduced to 0.19 w/o by liquation at 1300 C for three hours.

3. Reactions of Fissium in the EBR-II Cell Atmosphere
(A. Chilenskas, P. Kelsheimer)

It is expected that fuel pins and ingots of fissium, which may attain temperatures of 600 C, will have to be stored in the cell atmosphere for considerable periods of time. It is, therefore, important to know how much reaction might be expected when fissium is exposed to an inert cell atmosphere containing various levels of oxygen and nitrogen impurities. The previous quarterly (ANL-5633, page 120) showed that the fissium ingot in an argon atmosphere containing nitrogen and oxygen and at 600 C was attacked primarily by the oxygen and did not appear to be attacked significantly by the nitrogen. It was also found that the corrosion rate was sensitive to the oxygen concentration.

---

*See definition of equilibrium fissium on page 64.

Figure 32

Crucible assembly in Partially Tilted Position

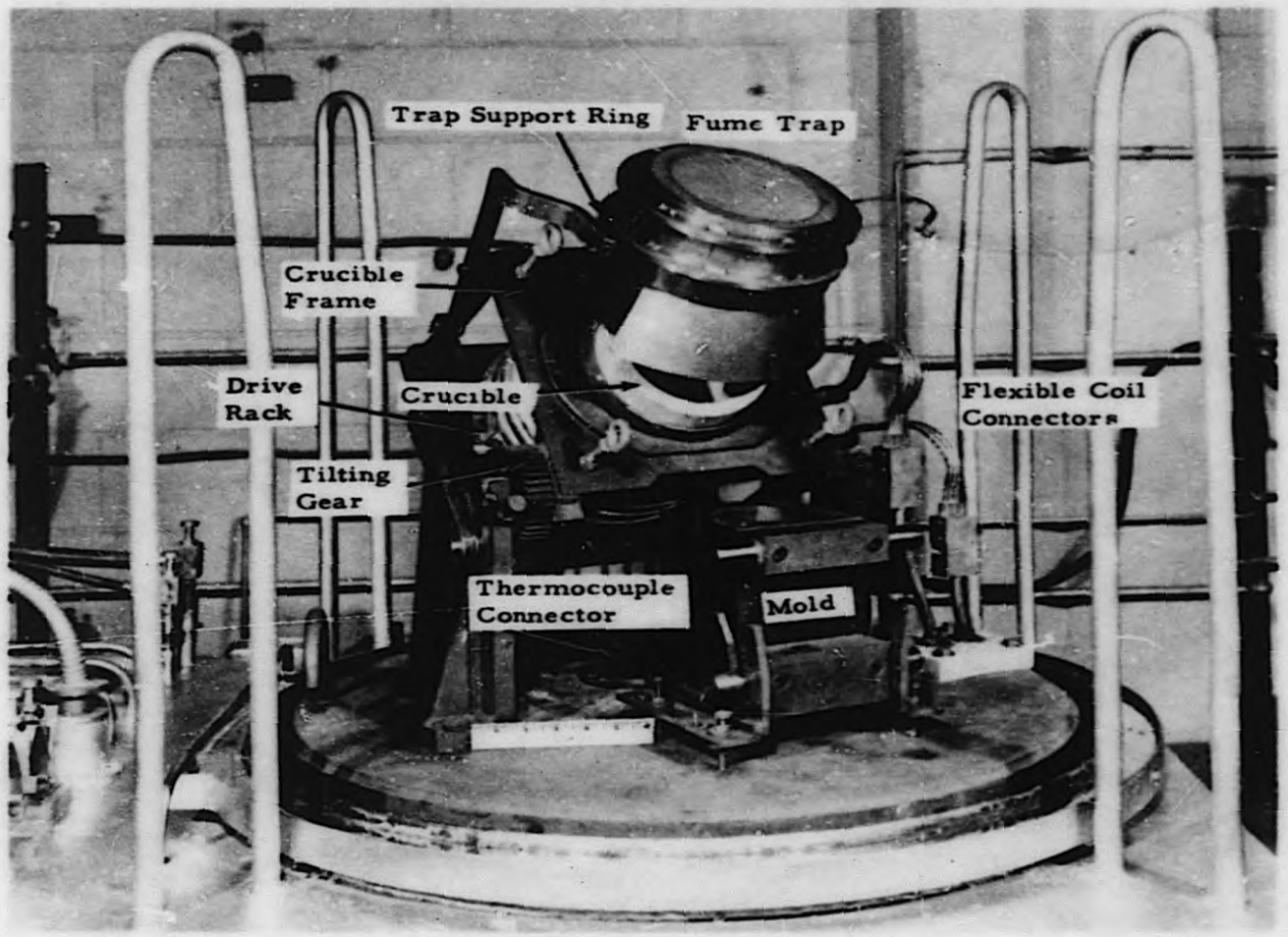

Figure 33

Close - Up of Furnace Interior

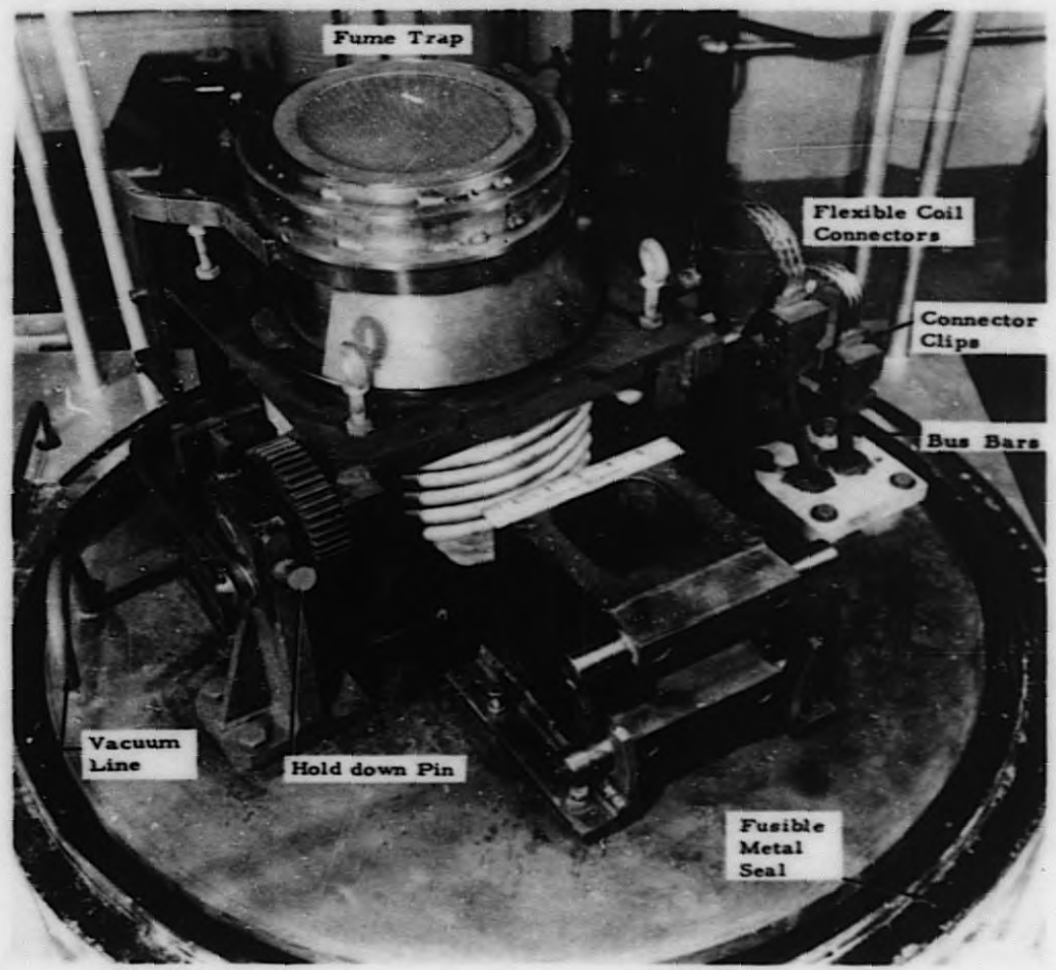

Figure 34

Ingot Remover and Sampler

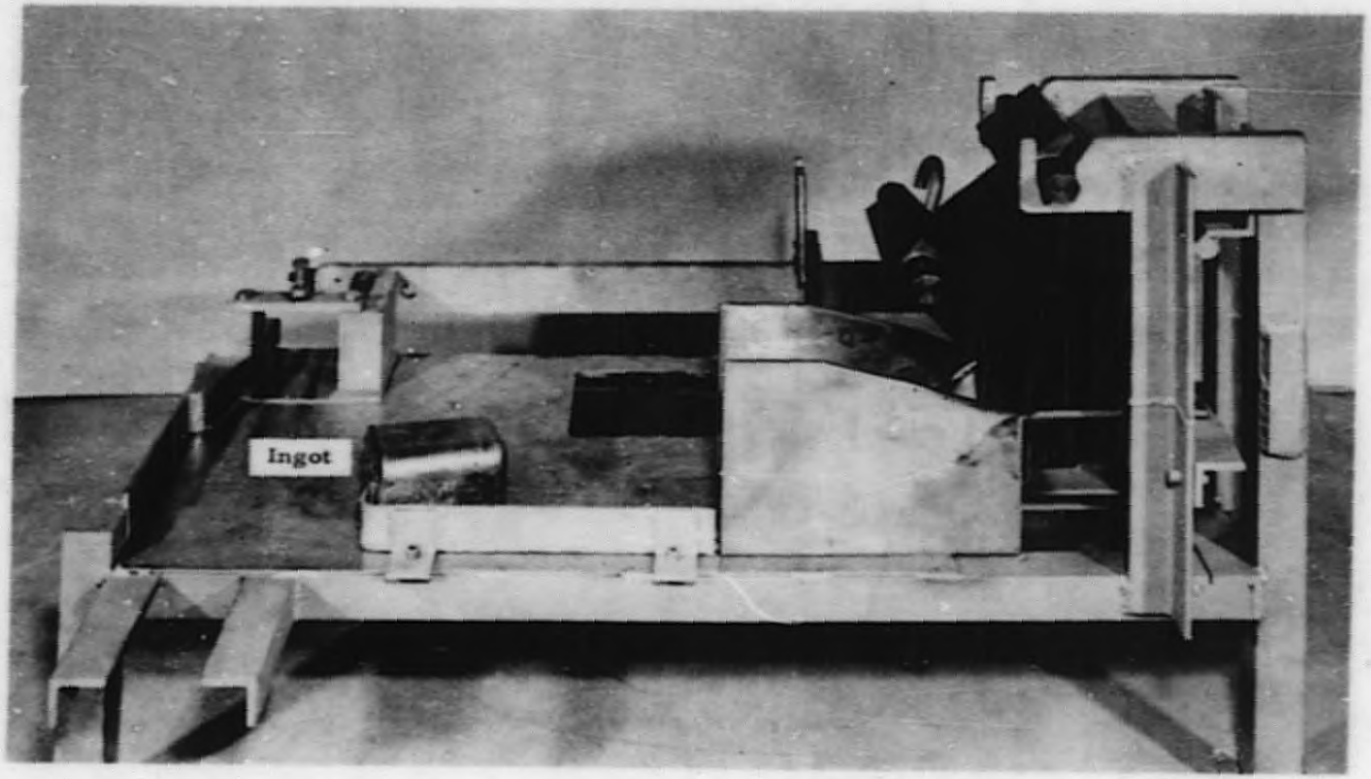

Figure 35

Ingot Remover and Sampler

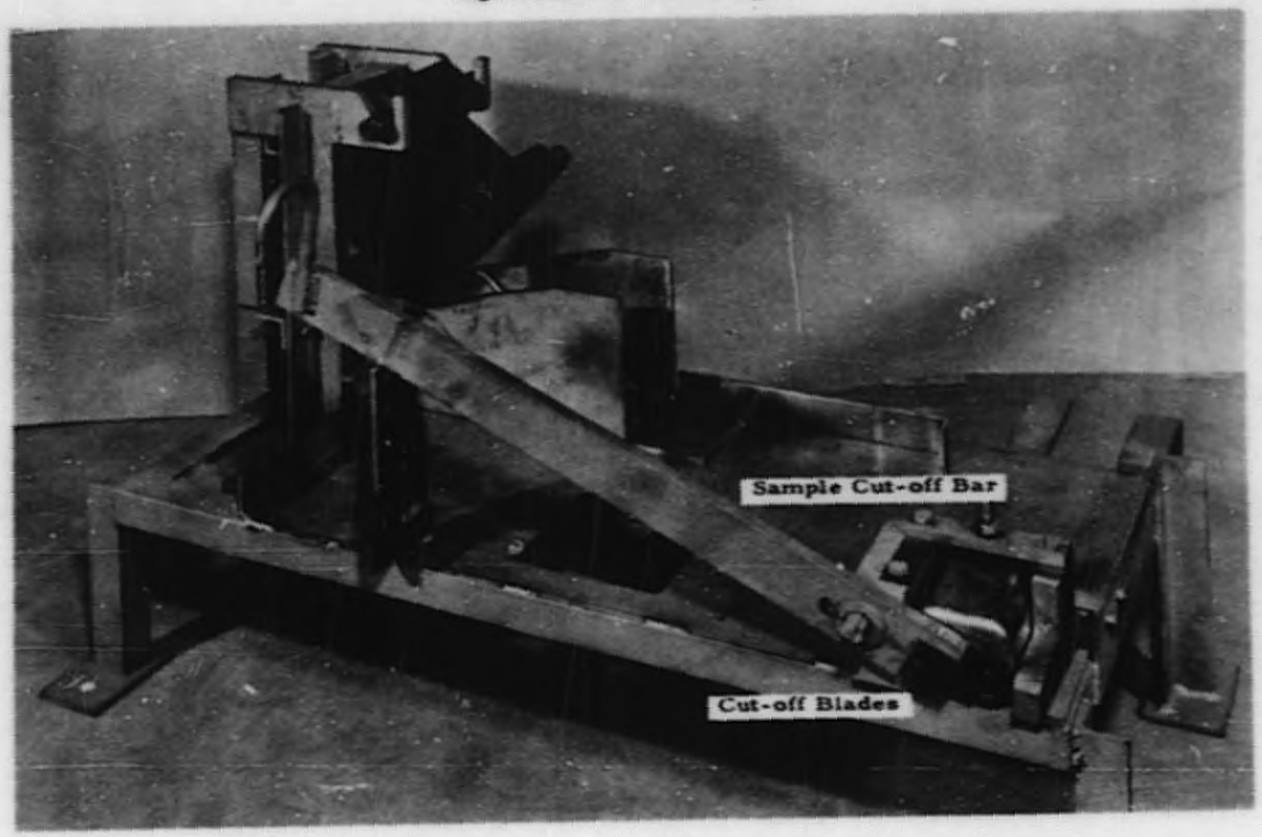

In order to determine the corrosion rate of fissium at 600 C by argon containing nitrogen and less than 10 ppm oxygen and moisture, the tentative atmosphere under which fuel pins will be stored, two additional experiments were performed. The ingot remained unattacked by an exposure of 23 hours to argon containing 1300 ppm (0.13 per cent) nitrogen and by an exposure of 47 hours to argon containing 4.7 per cent nitrogen.

The data of Mallett and Gerds[10] for the reaction of uranium with oxygen-free nitrogen at 600 C for an exposure of 47 hours indicate that about 80 mg nitrogen would react. Their data also show that the presence of an oxide film strongly inhibits nitriding. It appears, therefore, that the oxide film which was formed on casting and cooling the fissium ingot by impurities in the helium atmosphere prevented any attack by nitrogen under these conditions.

4. Control of Volatile Fissium Products
(J. Wolkoff, P. Kelsheimer)

Screening tests of a large number of potentially useful materials for trapping volatilized metals have been essentially completed. Metals volatilized in the slagging process are the fission products, cesium and possibly barium, strontium and cadmium, sodium which adheres to the discharged fuel pins, and magnesium resulting from reaction of uranium and fission products with a magnesia crucible. Materials have been evaluated to date on the basis of retention of vaporized sodium. Out of ten materials that have been found reasonably effective in retaining vaporized alkali metals (see ANL-5633, page 122), three ("Molecular Sieves," activated alumina, and an activated charcoal) have been chosen for further examination in order to limit the experimental work.

Using the method outlined in the last quarterly report (ANL-5633, page 122), the above three materials were tested using larger quantities of sodium (up to 4.2 grams compared with the 1 gram used in the screening tests). "Molecular Sieves" satisfactorily retained 2 grams of sodium (Run 40, Table 27), the maximum quantity tried with this material to date. The activated alumina (Run 42) satisfactorily held 4 grams of sodium, which is equivalent to 0.1 gram per gram of bed or 1.4 g of sodium per cubic inch of bed. With a 4-gram charge, the activated carbon (Run 39) operated satisfactorily at temperatures up to about 750 C, but definite fuming of sodium occurred at the upper temperature of 900 C.

In the screening tests and in the above three runs, a temperature gradient existed across the bed. This gradient will also exist in practice. Temperatures quoted are those near the bottom of the bed. In order to determine the effect of temperature on the capacity and

[10] Mallett, M. W., and Gerds, A. F., J. Electrochem. Soc., 102, 292-6 (1955).

Table 27

TESTS OF GRANULAR BEDS FOR RETAINING VAPORIZED ALKALI METAL

(All runs at atmospheric pressure under argon; bed depth 2")

Run No.	Bed Material	Vaporization Conditions: Max Degas Temp	Na Charged (g)	Crucible Temp (C)	Top of Bed Temp (C)	Cruc Temp when Deposits Noted (C)	Remarks
38 Part 1	AgCl on coconut charcoal[a]	445	1.2	550-900	280-430	550, 650, 750, 880, 900	Only trace amounts of Na detected;[f] visual deposits of AgCl
38 Part 2	AgCl on coconut charcoal[a]	440	none	550-900	265-400	550, 750, 880 900	Control run for Part 1; visual deposits of AgCl containing trace amounts of sodium
39	Activated carbon CXA[b]	615	4.1	550-900	390-620	650, 750, 900	Fuming at 900 C; traces of Na at lower temperatures[f]
40	"Molecular Sieves" 4A[c]	605	2.0	550-900	290-410	750, 840	Trace amounts of Na[f]
41	Glass 7930[d]	550	1.4	550-900	330-470	750, 880	Trace amounts of Na[f]
42	Activated alumina F10[e]	510	4.2	550-925	300-480	650, 880	Trace amounts of Na[f]
43	Activated carbon CXA[b]	670	4.0	550-880	505-910	750, 880	Strong fuming at 880 C; trace amounts up to 750 C[f]

[a] 6/14 mesh coconut charcoal impregnated with AgCl, 0.37 g AgCl/g charcoal

[b] 4/6 mesh, 0.171-in. dia. pellets, activated carbon type CXA, "Columbia" Brand, National Carbon Co.

[c] 1/8-in. dia. pellets, Molecular Sieves type 4A, Linde Air Products Co.

[d] 4/20 mesh glass type 7930, Corning Glass Co., a porous, 96 per cent silica glass

[e] 1/4-8 mesh, activated alumina type F10, Aluminum Co. of America

[f] Trace amount is less than 1 mg of sodium

effeciency of the three selected materials, new equipment is being built and will consist, in part, of a flow system in which the bed temperature, carrier gas rate, and metal concentration in the gas can be varied and closely controlled. A scouting run (Run 43 of Table 27) has been made in the existing equipment to gain preliminary information on operation of beds at essentially uniform temperatures. With the activated charcoal used in Run 43, only traces of sodium came through the bed at 750 C or below, but definite fuming occurred at 880 C. For an activated carbon bed of uniform temperature, the maximum operating temperature is apparently around 750 C.

As a windup of the screening tests, a relatively pure silica material in bead form, a porous glass, was examined. This also proved effective in retaining the sodium. Some fusion of the glass at the bed bottom occurred. The retention mechanism appeared to be a chemical one. The effectiveness of this material contrasts with the ineffectiveness of other high silica materials tested, namely silica gel and diatomaceous earth.

In the previous quarter, testing of silver chloride-impregnated beds was carried out. Although offering the possibility of increased effectiveness through chemical reaction, they appeared to have no advantage over the surface-active materials. In a blank run with the silver-impregnated material (Part 2 of Run 38), deposits of AgCl containing traces of sodium appeared on the bell jar, clearly indicating the bed itself to be the source of sodium in deposits formed at 750 C and below. Therefore, the silver chloride-impregnated beds are considered to be at least as good as the pure surface-active materials. They may have advantages over the latter materials for high temperature use.

5. Uranium Purification by Fractional Crystallization from Liquid Metal Solution
(J. B. Knighton,* A. Chilenskas, V. N. Thelen)

This subject has been previously reported under the heading "Removal of Noble Metals from Uranium" (see ANL-5633, page 125). The work was initially pointed toward the removal of noble metals from a small fraction of fuel material (drag-out) processed by oxidative slagging, which process does not remove the noble metals. However, this work may have broader applications, such as direct processing of discharged fuel of various kinds, and will henceforth be reported under the above heading.

---

*Special Scientific Employee on loan from American Smelting and Refining Co.

In principle, a fractional crystallization process would involve the following sequence of steps:

(1) Dissolution of uranium fuel alloy in a low-melting metal, such as zinc.

(2) Slow cooling to precipitate a uranium intermetallic compound involving the uranium and the metal solvent. It is hoped that fission product elements will remain in solution.

(3) Separation of the solvent metal containing fission products from the uranium intermetallic compound by filtration or some other suitable method.

(4) Recovery of uranium from the intermetallic compound by distillation of the volatile solvent metal.

A schematic of such a process as envisioned for zinc is shown in Figure 36.

FIGURE 36.

PROCESS FOR URANIUM PURIFICATION BY FRACTIONAL CRYSTALLIZATION FROM ZINC.

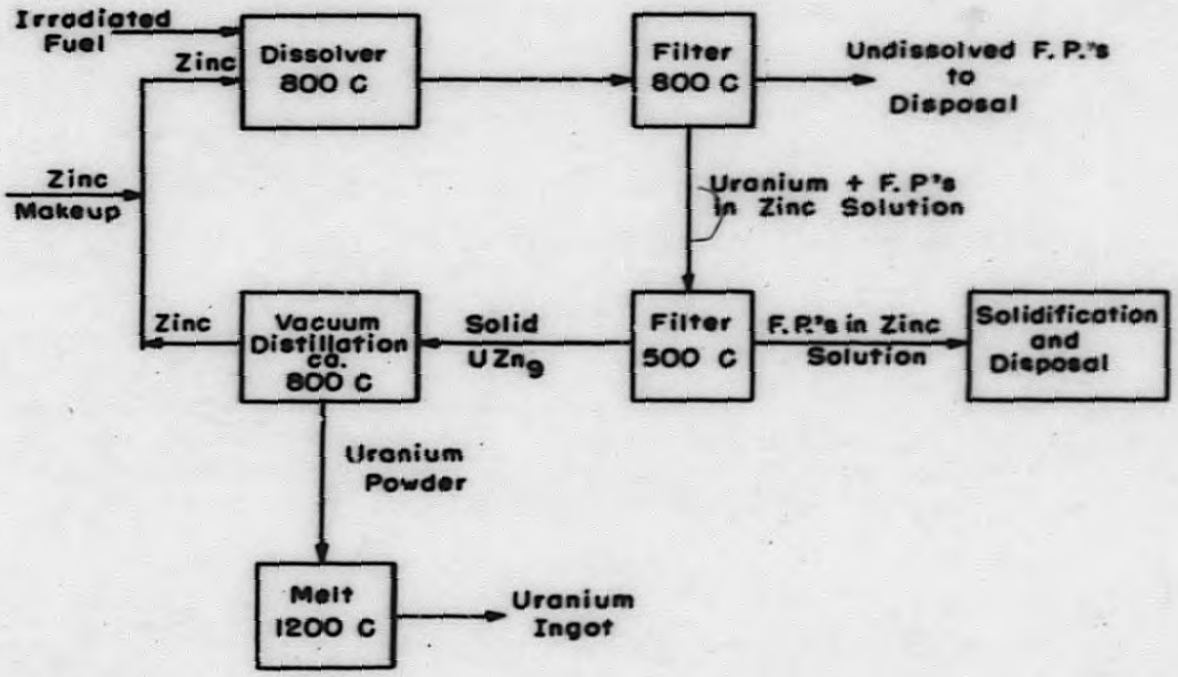

a. Determination of Uranium and Fission Product Element Solubilities in Zinc

Work during this period has been directed mainly toward determining the individual solubilities of uranium and various fission products in zinc. The solubilities of uranium, ruthenium, zirconium, palladium, and rhodium as a function of temperature have been determined (see Figure 37). The solubility of molybdenum shown in this figure was determined for a uranium-saturated zinc solution.

The zinc solutions of the various elements were sampled by drawing the liquid phase through a porous graphite filter plug (33-micron average pore size) into a Vycor tube. The alloys were liquated at 800 C, after which samples were taken at 50 C intervals, the cooling rate being controlled at 50 C/hr.

It is expected that the solubilities of each element will be affected by the presence of other elements. In a particular fission product solubilities are likely to be affected by uranium which is present in considerably higher concentration. This is illustrated in Figure 38, which shows that the solubility of ruthenium is considerably depressed by the presence of uranium at saturation concentrations. At the lower temperatures, where most of the uranium has crystallized as UZn_9, the solubility of ruthenium shifts toward the values expected in the absence of uranium.

The data of Figure 38 were obtained from a run in which a 97 w/o uranium- 3 w/o ruthenium alloy was dissolved in zinc at 800 C. For one-pass, two per cent burn-up fuel, the ruthenium concentration (if the fuel were dissolved in zinc to saturate the zinc with uranium at 800 C) would be very small (0.0114 weight per cent -- see Table 28). The curve in Figure 38 indicates that even in a saturated uranium solution the ruthenium would not become saturated until the melt was cooled to about 500 C. In cooling from 800 C to 500 C, 99+ per cent of the uranium would crystallize as UZn_9. A filtration slightly above 500 C should, therefore, separate the ruthenium from the uranium. In order to verify this contention, a run was made using sufficient ruthenium to simulate one-pass, two per cent burn-up conditions. The results from this run show that most of the ruthenium remained in solution, when 99+ per cent of the uranium had crystallized as UZn_9.

It is informative to list the concentrations of the fission elements which would occur for the dissolution of a two per cent burn-up fuel element in zinc to give 0.5 weight per cent uranium and to compare these with single solute solubilities at 550 C (Table 28). (It is assumed that the uranium is dissolved in the zinc at 800 C with subsequent controlled cooling of the zinc to 550 C to crystallize out 99 per cent of the uranium as UZn_9.) As can be seen from Table 28, the fission product

FIGURE 37.

INDIVIDUAL SOLUBILITIES OF URANIUM AND VARIOUS FISSION PRODUCT ELEMENTS IN LIQUID ZINC AS A FUNCTION OF TEMPERATURE.

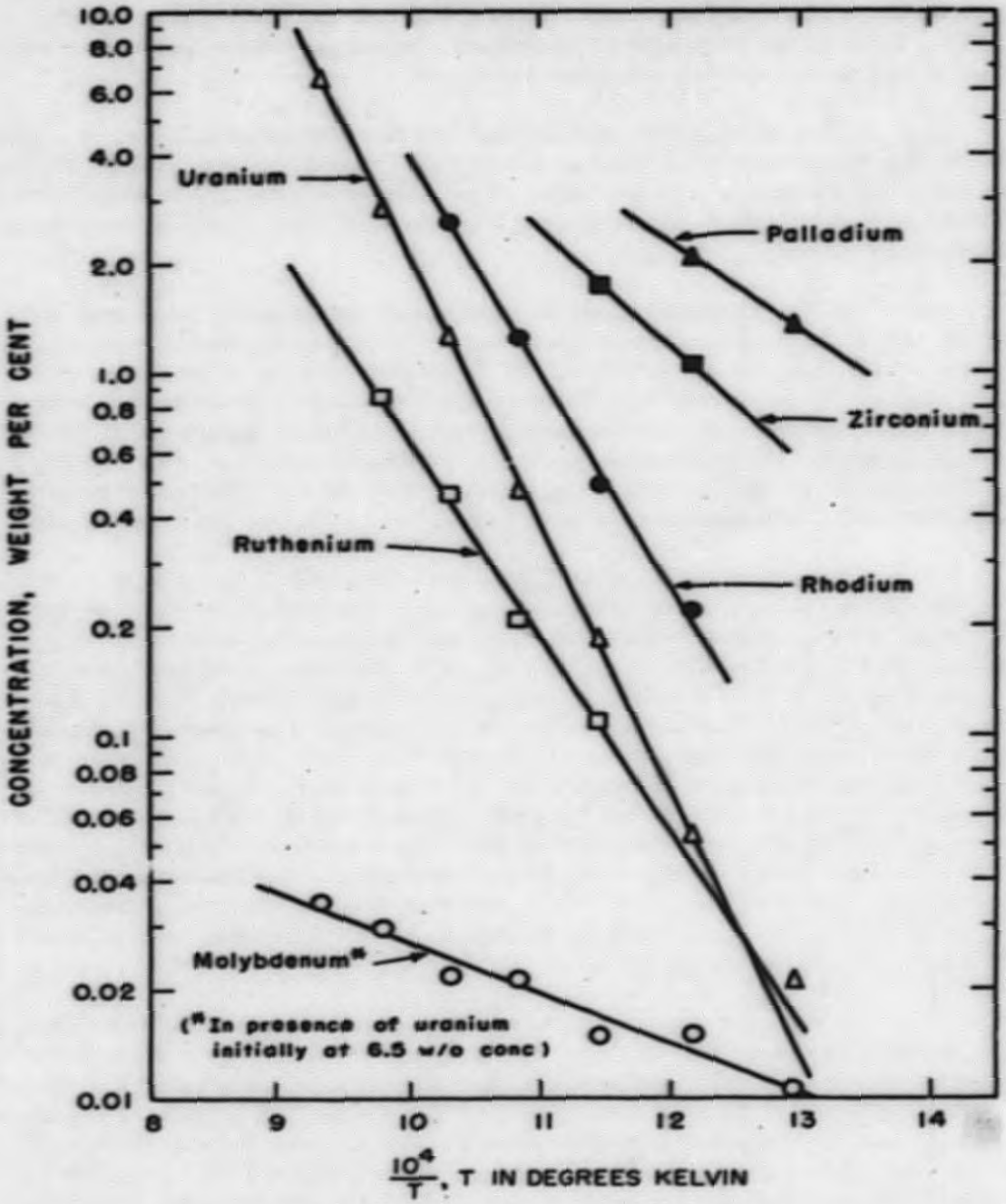

FIGURE 38.

RUTHENIUM AND URANIUM SOLUBILITIES
IN THE SYSTEM URANIUM - RUTHENIUM - ZINC.

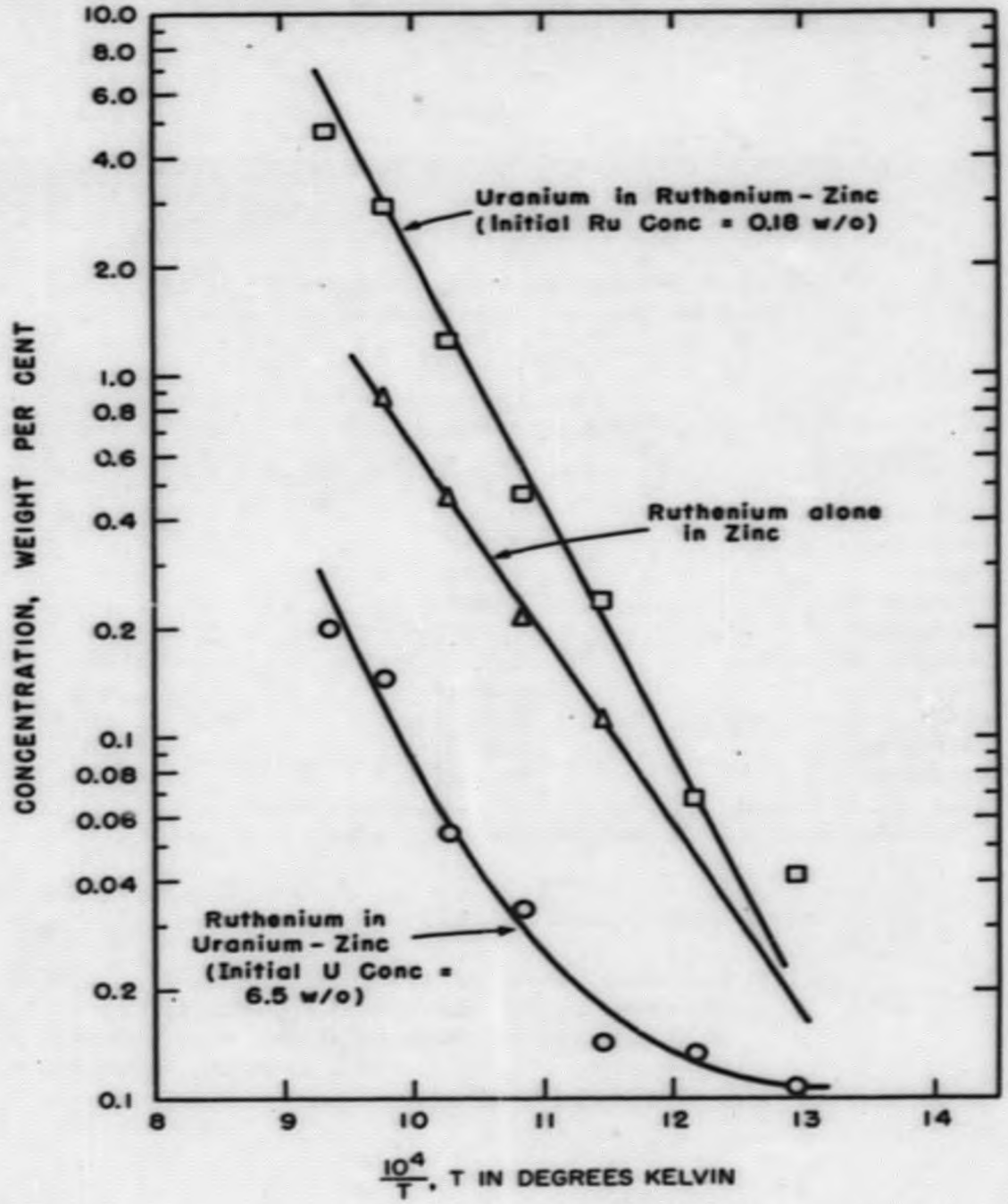

concentrations obtained from single solute solubility studies are considerably higher, with the exception of molybdenum, than the expected fission product concentrations from a dissolution of one-pass two per cent burn-up fuel. There is, therefore, considerable promise that separation of these elements from uranium can be achieved. Runs will be made in the next quarter to measure the separation of fission elements from uranium when these are simultaneously present in zinc solution.

Table 28

FISSION ELEMENT CONCENTRATIONS REALIZED FOR DISSOLUTION OF EBR-II REACTOR FUEL IN ZINC AND COMPARISON WITH AVAILABLE SINGLE SOLUTE SOLUBILITIES

(Fission product concentration are those for one-pass, two per cent burn-up of fuel.)

Element	Fission Product Concentration in Zinc (w/o)	Single Solute Solubility in Zinc at 550 C (w/o)
Cesium	0.0184	-
Total Rare Earth	0.0497	-
Barium	0.0063	-
Strontium	0.0058	-
Niobium	0.0010	-
Zirconium	0.0194	1.06
Ruthenium	0.0114	0.045
Molybdenum	0.0172	0.0135[a]
Palladium	0.0013	2.07
Rhodium	0.0021	0.21

[a]Molybdenum curve determined in presence of uranium.

The work to date can be briefly summarized as follows:

(1) Individual solubilities of uranium and various fission elements in zinc have been determined as a function of temperature. Such solubility data will also be obtained for cerium, cesium, barium, strontium, and plutonium.

(2) The solubility of ruthenium in zinc is depressed by the presence of uranium, but approaches that of ruthenium alone in zinc at low concentrations of uranium.

(3) Ruthenium of one-pass, two per cent burn-up concentration can be held in solution at the anticipated temperature of filtration (500-550 C) for recovery of the uranium.

(4) The solubility of uranium in zinc is not affected by the presence of ruthenium.

The presently anticipated fuel for the EBR-II reactor contains ruthenium and molybdenum as alloying agents. Equilibrium concentrations of these elements are much higher than one-pass concentrations and depend on the percentage of fuel drag-out. The fuel composition resulting for a five per cent drag-out is, for example, designated as five per cent "equilibrium fissium," and has ruthenium and molybdenum concentrations of about 2.5 and 3.3 w/o, respectively. If the entire fuel were processed by the zinc crystallization procedure, sufficient ruthenium removal is possible to maintain any desired equilibrium. Preliminary results have indicated that the separation between ruthenium and uranium (for drag-out material) is enhanced by the addition of magnesium.

b. Process Development

The objectives of this phase of the study are to demonstrate:

(1) The mechanical separation of UZn_9 from the fission elements in zinc solution.

(2) The quantitative recovery of uranium in massive metallic form from crystallized UZn_9.

Recovery of Uranium from UZn_9. The phase diagram for the uranium-zinc system[11] indicates that at 1 atmosphere and 947 C, UZn_9 will decompose to gamma uranium and zinc vapor. Several preliminary experiments were performed to study the separation of the uranium from zinc by vacuum distillation. Distillation of a uranium-zinc alloy charge, under a vacuum of 10^{-3} to 10^{-5} mm mercury and a temperature of about 600 C over a period of four hours, resulted in the formation of a black, powdery residue and grey, needle-like crystals whose total weight corresponded closely to the weight of the uranium in the charge. About 99 per cent of the zinc was recovered as a single zinc biscuit. Further work is continuing in which the conditions necessary to produce metallic uranium from UZn_9 will be established.

[11] Chiotti, P., et al., Uranium-Zinc System, ISC-656 (October 21, 1955)

Filtration of Molten Zinc. As illustrated by the process schematic (Figure 36), it is necessary to effect a clean separation of the molten zinc phase from solids at several points in the process. The efficacy of porous graphite of 33-micron pore size has been demonstrated in the sampling technique used in the solubility studies and suggests the use of porous graphite for filtration. Apparatus is being designed to study this material as a medium for separating molten zinc from crystalline UZn_9 and insoluble residues such as molybdenum.

6. Extraction of Plutonium with Liquid Magnesium

Semi-works equipment studies on the extraction of plutonium from uranium with molten magnesium and the subsequent distillation step have continued. The five-kilogram-scale batch extraction unit was tested using magnesium and uranium-5 w/o chromium alloy. A magnesium distillation unit with a sodium-cooled condenser has been tested and operated satisfactorily. Work has begun on the development and testing of components for a magnesium extraction process.

a. Magnesium Extraction Studies
(I. O. Winsch, K. Olsen)

The large scale batch extraction unit was previously described in ANL-5633, page 128. A schematic of this equipment is again shown in Figure 39. This unit has been put through several tests to determine the efficiency of transferring metals from vessel to vessel by argon pressure. Pressure-equalizing lines which were incorporated into the system between the extraction vessel and the uranium and magnesium receivers have provided excellent control over liquid metal transfer operations. It was observed that only a few seconds are required to transfer the molten magnesium (two to three kilograms) from a vessel at a pressure differential of 5 psi. Heels of about 100 gm of magnesium remained in the vessel from which the transfer was made.

Runs 5 and 6 were made with charges consisting of a uranium-5 w/o chromium alloy and magnesium (Table 29). The materials were transferred in the molten state and without difficulty from the charge vessel to the extraction vessel. The molten metals were agitated in the extraction vessel for a period of one-half hour before separation of the phases. The heels consisted mostly of U-Cr alloy with a thin coating of magnesium (see Table 29).

On cooling, the metal heels remaining in the charge and extraction vessels froze to the transfer lines and prevented removal of the crucible. As a preventive measure, a screw mechanism has been incorporated into the bottom flanges to provide a means of raising and lowering the crucibles within the vessels. Upon completion of a metal transfer, the crucible is lowered to prevent the heel from freezing to the transfer line.

FIGURE 39.

FIVE-KILOGRAM SCALE MAGNESIUM EXTRACTION UNIT. (Schematic)
(Unit is installed in large resistance furnace)

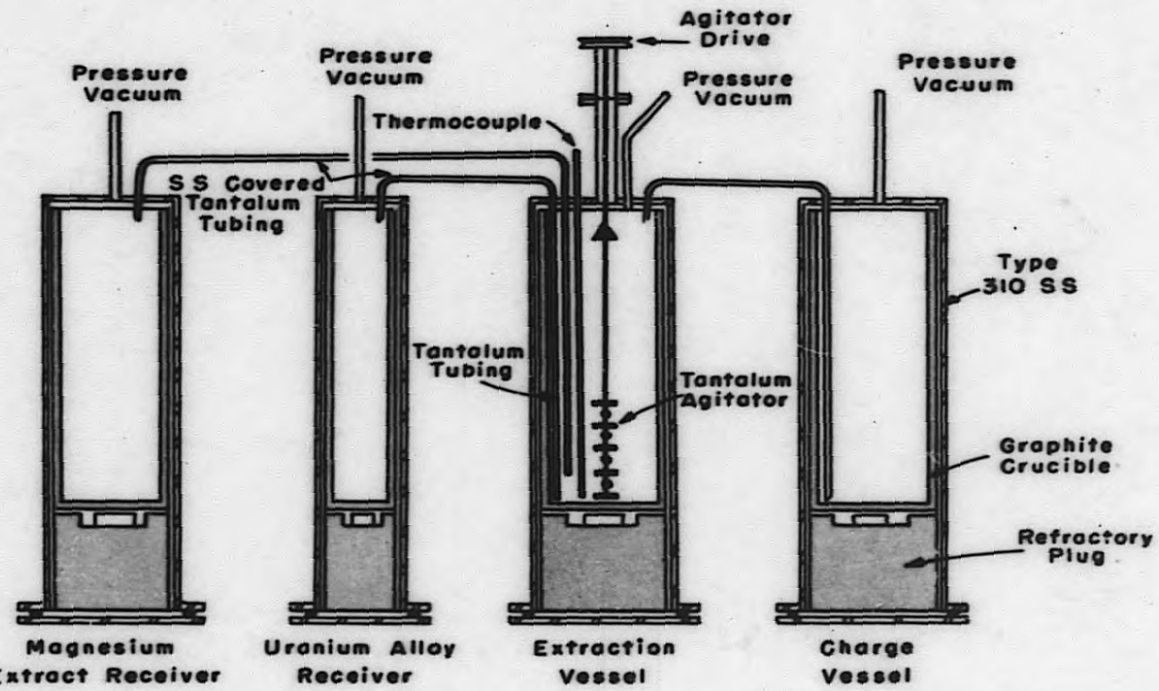

Table 29

SIMULATED MAGNESIUM EXTRACTION

Run No.	U-Cr (kg)	Mg (kg)	Per Cent Metal Transferred to Extraction Vessel		Separated Metal Phases Transferred to Receivers		Per Cent of Charged Metal Transferred to Receivers	
			U-Cr	Mg	U-Cr (kg)	Mg (kg)	U-Cr	Mg
5	4.5	2.5	79	98	1.55[a]	2.16	43.8	87
6	4.1	2.7	71	99.5	2.18[b]	2.53	53.0	94

[a] 0.26 kg of magnesium transferred with U-Cr phase

[b] 0.16 kg of magnesium transferred with U-Cr phase

It has been observed that magnesium would vaporize into and plug the vacuum-pressure lines to the vessels in the extraction tests. In Run 6, baffles were used to cover the tops of the graphite crucibles which are part of each vessel. Excellent results were observed in that only a fine film of magnesium was found in the vacuum-pressure lines. Vapor pressure traps of the type shown in Figure 40 were added to the unit and have proved effective in keeping the lines open.

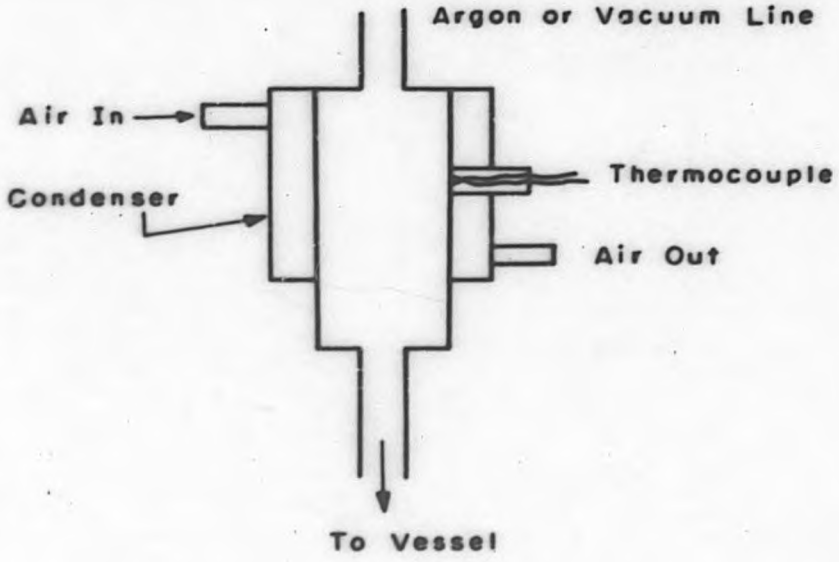

Figure 40

Vapor Pressure Trap

Difficulty has been experienced in removing magnesium ingots and uranium heels from graphite crucibles used in the extraction unit due to penetration of the porous walls of the crucibles. Aluminum oxide and magnesium zirconate-coated graphite crucibles have been tried without success in eliminating this difficulty. "Graphitite" crucibles, which are reported to be impervious to liquid metals at high temperatures, have been ordered and will be tested in the extraction unit.

Plutonium runs are planned for the next quarter.

b. Magnesium Distillation
(I. O. Winsch, K. Olsen, W. Walters)

A sodium-cooled condenser has been incorporated into the magnesium distillation unit, and a cross-sectional view of the unit is shown in Figure 41. Five runs have been completed in the unit, and it now appears that sodium cooling will give a fairly uniform condenser temperature.

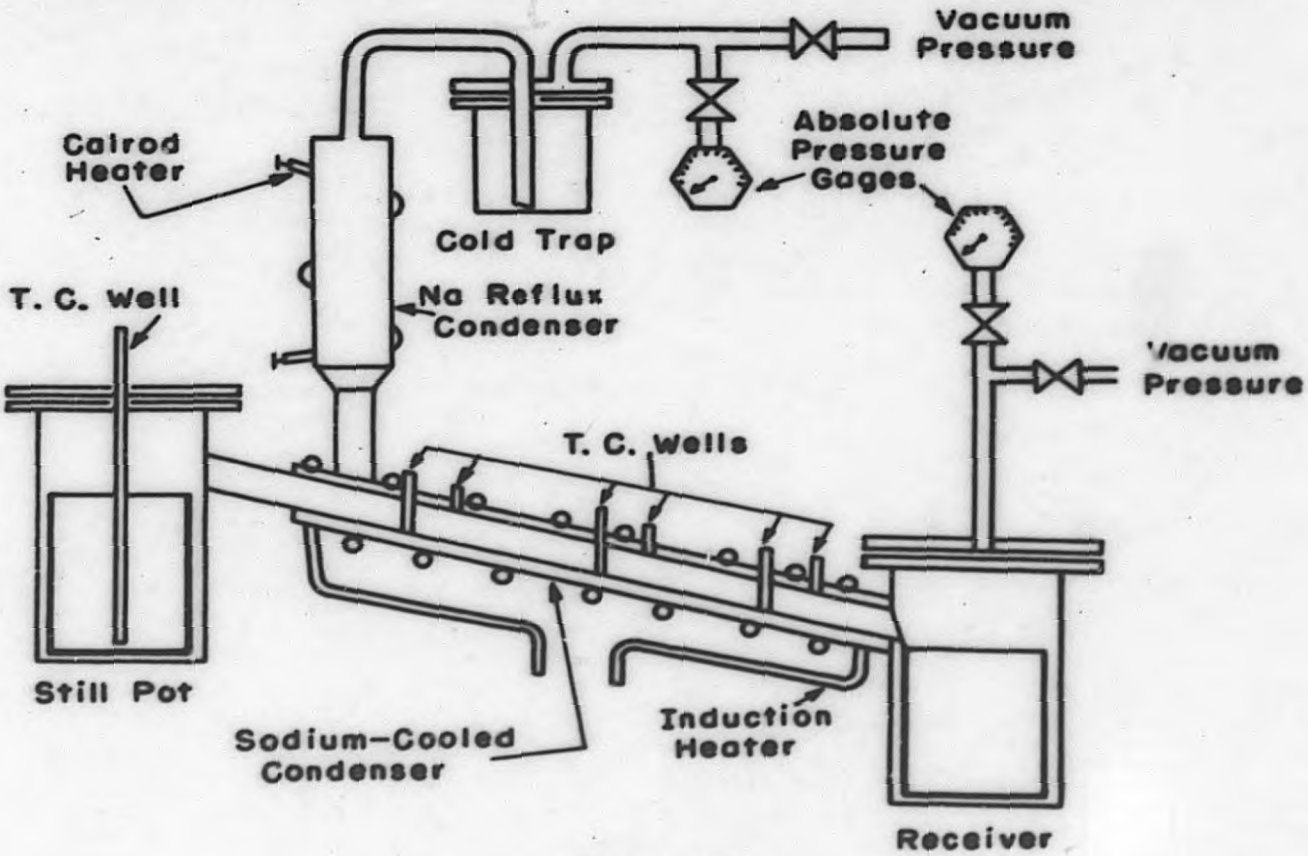

Figure 41

Magnesium Distillation Unit with Sodium-Cooled Condenser

Distillation Run 22 consisted of a charge of 1585 g of magnesium and 2.5 g of plutonium. Baffles were used to reduce entrainment of plutonium and care was taken to prevent running the still pot to dryness. This was accomplished by fixing the still pot thermocouple well about one-half inch above the bottom of the graphite crucible. A rise in the still pot temperature during the course of the distillation run indicated the liquid level was below the tip of the thermocouple well.

A still pot heel of about 300 g resulted. The magnesium distillate was very clean in appearance and an analysis indicated about 0.5 mg of plutonium in the distillate due to entrainment. An analysis of the still pot heel accounted for only 50 per cent of the original plutonium charge. A portion of the graphite crucible was leached with acid and an analysis indicated that only about 0.65 g of plutonium could be accounted for in the entire crucible. Based on an analysis of a sample cut from the bottom of the still pot heel, it would appear that 3.85 g of plutonium was present in the magnesium heel. This indicates the possibility of plutonium segregation in the magnesium. Additional analyses will be made in an attempt to clarify this situation.

c. Development of Components for Magnesium Handling
(G. Bennett, W. Kline, L. Weaver*)

In designing a process for the extraction of plutonium from molten uranium with molten magnesium, the necessity for developing various components to handle molten magnesium has become apparent. The primary aims of the immediate program are the development of the following:

1. a valve for controlling the flow of magnesium,
2. a liquid-level indicator,
3. a satisfactory sampling technique.

In pursuance of this development, data will also be accumulated on pumping methods, flow metering, and corrosion resistance.

Progress in this program may be summarized as follows:

(1) Work on the development of a suitable valve for controlling the flow of magnesium has resulted in the type of "freeze" valve pictured in Figure 42. The chief design features are the use of a smaller diameter at the bottom (one inch as against two inches), and a side exit path for the magnesium at the top of the exit tube. The former makes it possible to effect a seal with a small quantity of magnesium in the valve;

*Special Scientific Employee on loan from International Harvester Co.

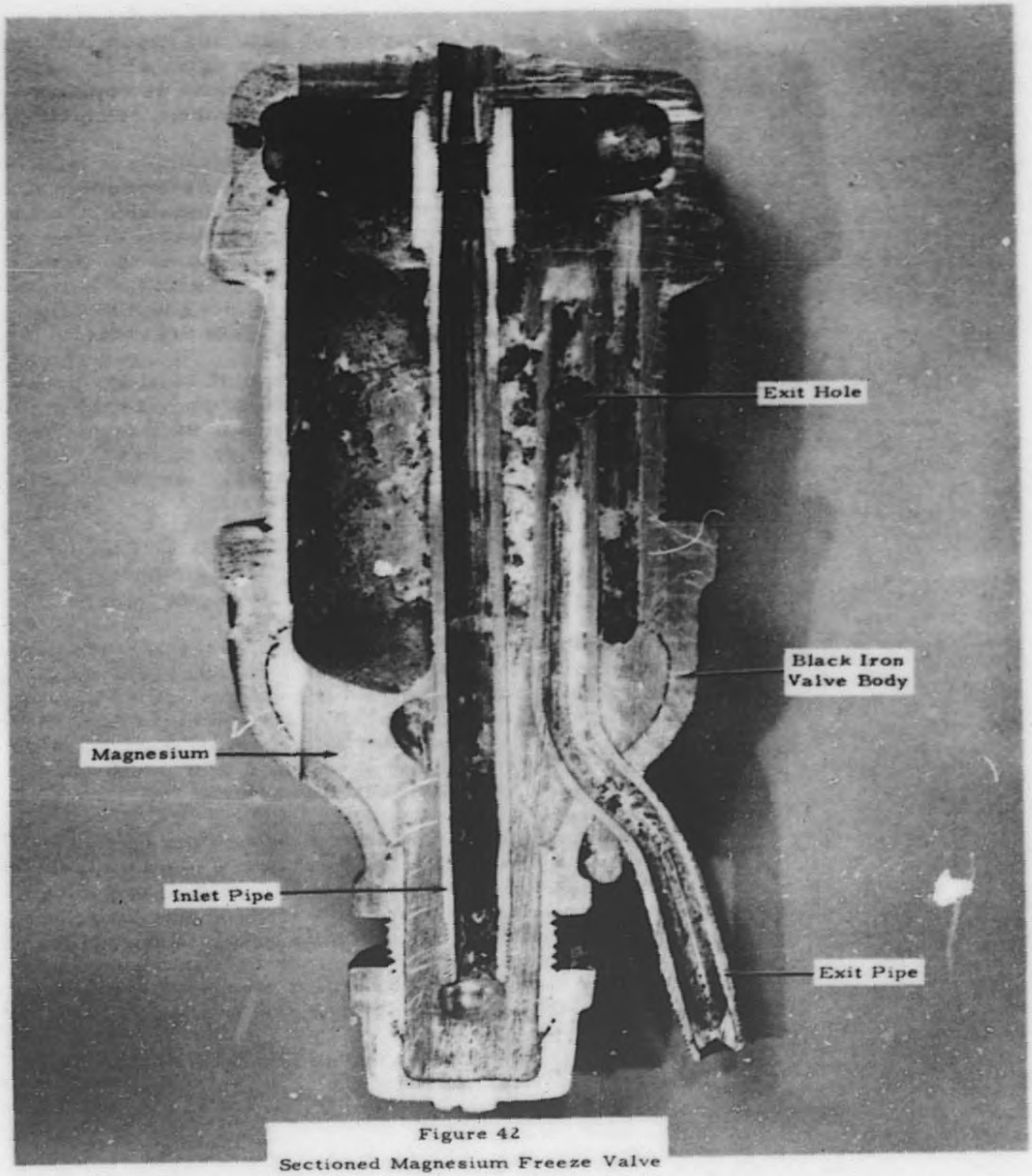

Figure 42
Sectioned Magnesium Freeze Valve

the latter is for the purpose of reducing "blow out" of magnesium by gas passing through a valve after magnesium transfer is completed. The valve is approximately eight inches long and is constructed of black iron.

After initial leak-testing under 50 lb of air pressure, the valve was loaded with magnesium and subjected to a series of 10 alternate melting and freezing cycles in an inert atmosphere. During this operation the temperature varied from 625 to 700 C. The end of a transfer operation was then simulated by purging the valve for 15 seconds with argon under 5-psig pressure.

The valve was then rechecked under 38 lb of air pressure and found to be leakproof. No damage to the welds or pipe walls was discernible. Upon cutting open (see Figure 42), the magnesium seal was found to vary in thickness from 1 1/2 inches to 2 1/4 inches, depending on the position of the freeze cavities.

Further experimental work on this valve will involve investigation of methods of cooling the valve for sealing. Other valve designs are also being considered.

(2) In cooperation with Gerhardt Weiss of the Electronics Division, a method for the determination of the magnesium level inside a tank is being developed. This method involves the use of an induction coil and bridge circuit similar to that used with liquid sodium. The induction coil is raised and lowered in a mild steel or iron pipe extending into the magnesium.

A test tank made from 4-inch pipe with the bottom closed and a 3/4-inch mild steel tube extending from the upper flange to within several inches of the bottom has been constructed and filled with magnesium. The electronics circuit has been able to locate the height of the solid magnesium in the tank to within approximately 1/32 of an inch. The next step will involve testing this circuit with molten magnesium.

(3) Development of sampling techniques will receive emphasis in the next quarter.

7. Inert Gas Purification
(A. Chilenskas, P. Kelsheimer)

a. Nitrogen Removal from Argon

Work has been completed concerning the removal of nitrogen from argon by the use of calcium. As pointed out previously, it is not certain that nitrogen removal by chemical means is necessary, since the nitrogen concentration in the argon can apparently be high enough (5 per cent and perhaps greater) that simple purging with pure argon would be an attractive method of nitrogen control. However, nitrogen removal by hot calcium has been studied to provide for the possibility that lower nitrogen concentrations in the argon blanketing gas may be desirable.

It was shown in the previous quarterly that sodium-activated calcium* at 440 C had approximately the same reactivity towards nitrogen as pure calcium at 650 C; also, that there was negligible reaction between nitrogen and pure calcium at 440 C. It was also shown that sodium-activated calcium continued to react with nitrogen at a decreasing rate until essentially all the calcium was converted to the nitride. However, since the apparatus was of such design that thermal cycling occurred many times and since other investigators[12] have reported that thermal cycling has a beneficial effect upon the amount of conversion of calcium to nitride, four additional experiments were performed in a continuous flow system in which no thermal cycling occurred and in which the efficacy of sodium-activated calcium at 440 C could be compared to that of calcium at 650 C. The results of these tests are shown in Table 30.

Calculations for the four runs based upon the effluent nitrogen analyses for the first 5 hours of operation show that in the activated calcium runs at 440 C, 54 and 47 per cent getter burn-up resulted while getter burnups of 35 and 65 per cent were obtained with calcium at 650 C. These results agree fairly well with the previous work, which indicated that the reactivities of these materials would be approximately the same.

The first ru was continued for a total of nine hours, after which the getter charge was examined. The complete lack of metallic residue was indicative of achievement of a high percentage burn-up and suggests that thermal cycling may be unnecessary for achievement of high burn-ups.

---

*Calcium to which a small lump of metallic sodium is added.

[12] Pawson, R. L., Argon Purification for Metallurgical Operation, AWRE-O-16/54 (April 1954)

Table 30

THE EFFICACY OF SODIUM-ACTIVATED CALCIUM AND CALCIUM FOR THE REMOVAL OF NITROGEN FROM ARGON

Argon-4.7 per cent nitrogen mixture at a flow rate of 335 ml/min passed continuously over calcium getter (30 grams, 46 ml, screened between 10 and 20 US Std. sieves). The argon was purified using a drier and hydrogen-saturated palladium catalyst and is estimated to contain less than 10 ppm oxygen and moisture.

	Per Cent Nitrogen Removal by			
	Na-Activated Ca at 440 C		Ca at 650 C[c]	
Time (hr) \ Run	1[a]	3[b]	2[a]	4[b]
0.5	84.0			
1.0		82.3	61.0	100
1.5	88.5			
2.0		50.2		100
2.5	66.7		39.0	
3.0		53.2		100
3.5				
4.0	76.0		35.0	
4.5		66.4		55.3
5.0	52.7		30.5	
5.5	51.0	53.6		27.6
6.0				
6.5				
7.0	24.3	43.3		

[a]Nitrogen analyses by Orsat-type analyzer. Inlet N_2 analyses 4.70 per cent.

[b]Nitrogen analyses by Mass Spec. Inlet N_2 analyses 4.66 per cent.

[c]Calcium does not react with nitrogen at 440 C.

The results of experiments which are reported here and in previous quarterlies may be summarized as follows:

(1) The reactivity of calcium towards nitrogen was shown to be highly influenced by the presence of metallic sodium (oxide-coated) as the sodium reliably instigated

a vigorous reaction between calcium and nitrogen at about 370 C, whereas pure calcium in an adjacent crucible would not react even when heated to a much higher temperature.

(2) The temperature at which the maximum rate of reaction between calcium and nitrogen occurs was not established; however, it was shown that the reactivity of calcium at 440 C when activated by sodium was about equal to the reactivity of pure calcium at 650 C.

(3) High burn-ups (greater than 65 per cent) were achieved in a flow system for sodium-activated calcium at 440 C and pure calcium at 650 C without thermal cycling. Burn-ups approaching 100 per cent were achieved for sodium-activated calcium at 440 C in which the getter was thermally cycled many times. Specific investigation of the effect of thermal cycling on a given getter charge was not undertaken.

The results of these tests suggest that nitrogen contamination of argon can be effectively removed by a getter of sodium-activated calcium operating at about 440 C as well as by pure calcium at 650 C. The use of a counter-current contactor would permit essentially complete getter burn-up.

b. Oxygen Removal from Argon

The method used for measurement of the oxygen content of argon involves conversion of the oxygen to water and subsequent measurement of the water content. An instrument which has been tested is the General Electric Dew Point Meter and Recorder (see ANL-5494, page 75). This has worked satisfactorily.

Late in the last quarter, a Model W Electrolytic Water Analyzer (Manufacturers Engineering and Equipment Corp., Hatboro, Pa.) was received for testing. In this unit, the water in the gas stream is absorbed and electrolyzed in a cell, and the current which flows in an electrical circuit is a measure of the water content of the gas. This unit has been installed and is ready for testing.

VI. ANALYTICAL RESEARCH

(C. E. Crouthamel, C. Gatrousis)

The need for more effective methods of target analysis has been approached by the application of scintillation and alpha pulse analysis, as has been reported in many previous reports. However, it has been apparent that pulse analysis alone would not be sufficient for many materials. During the past quarter we have turned our attention to paper chromatographic methods which, when coupled with pulse analysis, makes a more sensitive and versatile approach to the varied target and fission product analysis problems.

The final manuscript of the past quarter's work in chromatography is now being reviewed prior to being submitted to the Journal of Inorganic and Nuclear Chemistry for publication. This manuscript ("Ascending Paper Chromatographic Analysis of Irradiated Uranium in a Hydrofluoric Acid Medium") is a compilation of work done at Harwell and Argonne and will be published jointly.

VII. ROUTINE OPERATIONS

(H. G. Swope)

A. Waste Processing Operations

(J. Harast, K. Bremer, D. Raue, J. Pavlik)

The total volume of liquid radioactive wastes processed from October through December, 1956, was 50,000 gallons. Of this amount 46,000 gallons were evaporated, 3500 gallons were flocculated after adjusting the pH to 12 and 500 gallons were absorbed in vermiculite. A summary of the volume and method of processing the wastes for the year, 1956, is shown in Table 31.

B. Gamma-Irradiation Facility

(H. G. Swope, J. Harast, A. Rashinskas, W. Spicer, D. Turner, J. Gates, R. Juvinall, N. Ondracek, L. DeGraff, A. Madsen)

The year 1956 represented the first full year of operation of the gamma-irradiation facility, which uses 12 spent fuel rods in a honeycomb arrangement as an irradiation source.

The total number of samples irradiated during the quarter was 6,148.

On a yearly basis the source was used most by Argonne (7,506 units*), next by the Quartermaster Food and Container Institute (6,266 units). and then by industry (5,284 units).

A new gamma rack was completed and installed in December. The rack provides eight MTR fuel rods arranged radially around the sample urn. The largest cylindrical urn that can be accommodated has an effective inside diameter of 19 1/2 inches and an effective height of 29 1/2 inches -- large enough to contain a quarter of beef. The fuel elements are alternately positioned at the bottom and half way up the side of the urn. This arrangement appreciably flattens the gamma flux so that the variation in flux is about ± 10 per cent. The nominal gamma flux for the large urn is 100,000 rep/hr. An isometric drawing of the new rack is shown in Figure 43.

---

*A unit is 2×10^6 r.

Table 31

SUMMARY OF RADIOACTIVE WASTE PROCESSED DURING THE YEAR, 1956

Gallons of Wastes Treated as Shown

Quarterly Period 1956	Struthers-Wells Evaporator				30-Gallon Concentrator		Flocculation	Filtration		Absorption in Vermiculite	Solvent Washing	Concrete Works	Total Volume Processed Gallons
	Retention Tanks	Decon Soln	Gamma Facility[a]	Misc Aqueous[b]	Evaporator Bottoms	Misc	Retention Tanks	Retention Tanks	D-34 Sludge	Misc Organics	Misc Organics	Misc Aqueous	
Jan- Mar	3,300	14,000	3,520	2,240	770	220	2,450	-	620	240	-	130	27,490
Apr-June	10,100	17,400	5,000	12,200	970	-	4,400	-	3,600	160	-	120	53,950
July-Sept	12,300	18,000	5,300	7,310	1,560	300	13,200	-	-	50	300	-	58,320
Oct-Dec	10,100	19,600	2,760	12,300	1,200	380	3,550	-	-	500	-	-	50,390
Totals	35,800	69,000	16,580	34,050	4,500	900	23,600	-	4,220	950	300	250	190,150

[a]These include water from the carrier when new fuel rods are received and the regenerant solutions from the mixed bed ion-exchange column.

[b]These include not only the small batches of liquid active wastes but also the effluent from the Eimco filter, the residue from flocculation, and water soluble oil-water mixtures from the shops.

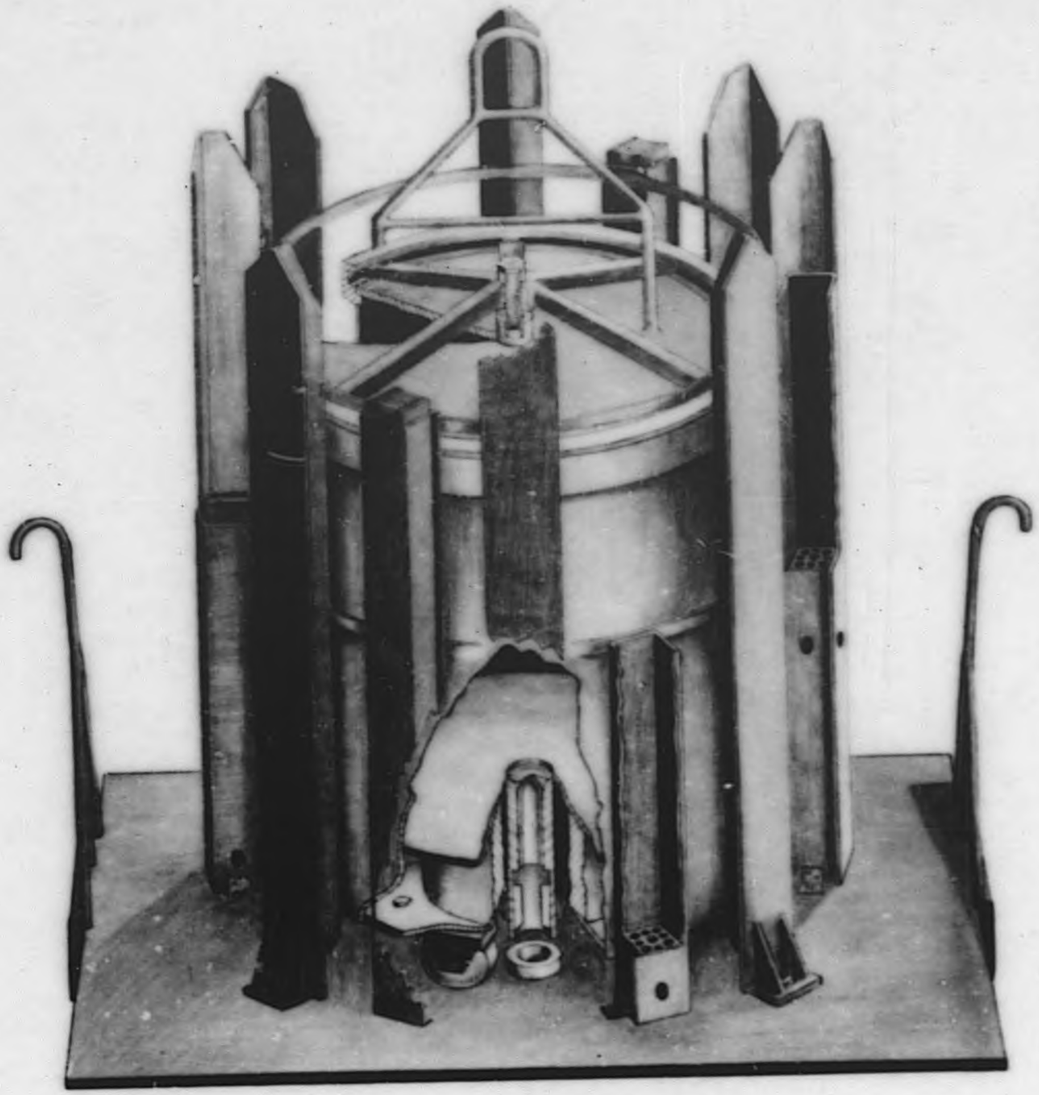

Figure 43

Gamma Irradiation Facility Rack M-2

END